(Draft version January 12, 2021)

Cosmology

Some comments, derivations and notes
on the Lecture material

NOT everything!

by

Michal Jaroszynski
(2020)

Contents

Chapter 1

Introduction

1.1 Paradigms

We take for granted that the Universe is *homogeneous and isotropic* after *averaging over large enough scale*. This approach (I believe) belongs to the mainstream. We do not consider globally nonuniform or anisotropic models.

Isotropy is easier to observe. Comparing the distribution of some class of objects on different parts of the sky one can find their statistical equivalence. The objects have to be far enough (to avoid influence of local inhomogeneity). The samples should be *big enough* for statistical reasons. This implies comparison of samples belonging to big enough solid angles.

The best example of isotropy is the distribution of the photons of cosmic microwave background (CMB). Investigating the temperature distribution on small parts of the sky we can see that it is the same independent of the direction. (To be precise: CMB as seen from Earth has approximately one per cent so called dipole anisotropy, which can be removed by transformation to another frame of reference, moving with appropriate velocity relative to the Earth. Due to the Doppler effect the temperatures of CMB at different points change and the dipole anisotropy can be removed. This also defines a specific *CMB frame of reference*. The temperature fluctuations on the sky in this frame are small: $\delta T/T \sim 10^{-4}$, $\langle T \rangle = 2.73$ K.

Homogeneity If our location in the Universe is not specific (Copernicus principle) other observers (at far away locations) should also notice the isotropy of the Universe. We can see that two regions in space, say A and B which are at the same distance d from us $\Rightarrow$ seen at the same earlier time, but at different directions on the sky, are equivalent. Another observer, also at the distance d from B and another region C can see their equivalence. Repeating this thought experiment one finds any number of equivalent regions of space filling it at the earlier epoch, which implies *statistical uniformity* of the Universe. The regions which are statistically equivalent have sizes ≈ 100 Mpc today and $\approx 100/(1+z)$ Mpc at the epoch of redshift z. (See the definition of z below)

Another argument is based on observations. The figure above shows the maximal radius of correlations in QSO distribution in space as a function of the redshift. When counting QSOs around a given QSO one finds local inhomogeneities in their distribution, but beyond the maximal radius the distribution becomes random and the mean QSO density approaches average for the given epoch. The figure uses *comoving* distances. The physical dimensions at epoch z are $1+z$ times smaller. So the homogeneity scale based on observations is even smaller than the conservative estimate of the previous paragraph.

Hubble's law Relative motion of galaxies and cluster of galaxies with velocities proportional

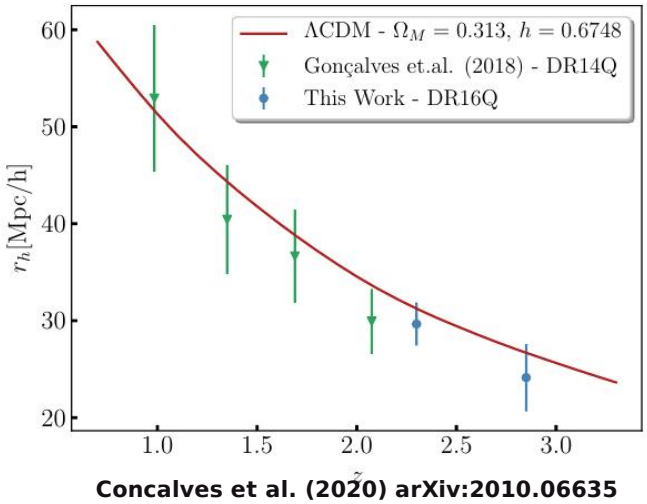

Figure 1.1: The evolution of the maximal inhomogeneity scale expressed in comoving units (see Comoving distance below)

to their distance was observed by Hubble in 1929. If the distribution of objects in space is to remain homogeneous, this is the only possible form of the Universe expansion. (It preserves the ratios of distances between objects, so their distribution in space remains self-similar). Earlier theoretical work of Friedman and Lemaitre on Universe models with constant matter density in space had shown, that in the frame of General Relativity (**GR**) such models cannot be static unless a positive *cosmological constant* of well chosen value were introduced. Lemaitre showed also that in an expanding model the proportionality of the relative velocity to the distance between two matter elements results from the first order Taylor expansion of their relative distance with time. (Higher order terms mix with the terms resulting from the curvature of space and time evolution and there is no reason to consider them). For some the term *Lemaitre - Hubble law* would be more appropriate.

We assume that GR is the valid gravity theory and we do not consider any alternatives. Homogeneity of space implies the possibility of clocks synchronization and the existence of cosmic time. Thus the space-time may be treated as a product of 1D (time) $\bigotimes$ 3D (space). There are only three different types of 3D space which are isotropic and homogeneous. The Cartesian 3D manifold (R^3) is an obvious example: all points are equivalent and all directions at any point are equivalent. This is a 3D flat space, $k = 0$. Now all points on a 2D sphere (S^2) and all directions there are equivalent. 2D sphere is defined as a 2D surface in R^3 given by the equation $x_1^2 + x_2^2 + x_3^2 = R^2$ where x_i are Cartesian coordinates and R is the radius. Similarly one can define a 3D sphere (S^3) in R^4 by $x_1^2 + x_2^2 + x_3^2 + x_4^2 = R^2$. It is hard to visualize, but by analogy with S^2 we may accept that S^3 is also isotropic and homogeneous. This is a 3D space of positive curvature ($k = +1$). The last case is a 3D space defined by $x_4^2 - x_1^2 - x_2^2 - x_3^2 = R^2$. The mathematicians believe it is also isotropic and homogeneous. This is the space of negative curvature ($k = -1$).

We assume that the Universe structure (astronomical objects and their distribution in space) is a result of the **gravitational instability** from tiny primordial fluctuations of the matter density. We also assume that the spectrum of fluctuations was **Gaussian**.

We consider so called models of the **hot** Universe, which means that originally the energy per particle was much higher than its rest energy. (As a consequence we observe CMB and primordial

helium.)

Commentary Approximate or *statistical* uniformity of the Universe may seem to be a too far going idealization. On the other hand we can observe only a part of space, so called observable Universe. (To be precise: we can observe directly only the surface of our past cone. Some scattered radiation may also get into our telescopes from the cone interior, but this is marginal and hard to interpret.) Matter in the Universe was hot and opaque to photons before so called recombination, which sets another limit on the size of the electromagnetically observable part of the Universe. Neutrinos and gravitational waves can (in principle) carry information from larger region but the finite age of the Universe sets another border. Assuming homogeneity we can investigate the whole Universe based on its representative observable part. Without this assumption cosmology becomes cosmography, the description of our surroundings.

1.2 Measurements of the cosmological model parameters

There are few parameters characterizing (defining) a model of the homogeneous Universe. The **Hubble constant** H_0 is basically measured as the ratio of the escape velocity of an object to its distance. (Finding appropriate objects and finding their distances is a difficult observational task, but the method is simple). The average **CMB temperature** measurement ($T_{CMB} = 2.74$ K) is also methodologically simple despite the high cost (e.g. COBE satellite) and detectors complexity. The primordial helium abundance ($Y_p \approx 0.25$) is obtained by spectroscopy of the far away gas clouds. The measurements are difficult but possible. Similarly much lower abundances of deuterium (^2H) or helium -3 (^3He) can be measured. Lithium - 7 (^7Li) is found in atmospheres of low metallicity stars.

Much more difficult is the measurement of the **averaged matter density** in the Universe. While the averaged power emitted by a unit volume ($\approx 2\times 10^8\ L_\odot h/\mathrm{Mpc}^3$) is derivable with decent accuracy, the mass to light ratios M/L for different kind of objects are not known with accuracy allowing sensible estimate of $\langle\rho\rangle$. (The averaged density of matter belonging to stars alone is easier to estimate, based on luminosity measurements.) Measurements of density parameters are based on indirect methods. In short: the values of the cosmological parameters influence the propagation of photons and so the relations between sources internal and observed properties.

The **critical density** of the Universe, $\rho_c \equiv \frac{3H_0^2}{8\pi G} \approx 10^{-29}\rho_{H_2O} \approx 6m_p/\mathrm{m}^3$, where G is the gravity constant, ρ_{H_2O} water density, and m_p is the proton mass, is used as a density unit.

As density parameters of the cosmological models one uses:

$$\Omega_M = \frac{\rho_M}{\rho_c} \qquad \Omega_\Lambda = \frac{\epsilon_\Lambda}{\rho_c c^2} \qquad \Omega_K \equiv 1 - \Omega_M - \Omega_\Lambda$$

where ρ_M is the averaged matter density (baryons plus dark), ϵ_Λ - energy density related to the cosmological constant Λ, and Ω_K characterizes the curvature but is not an independent parameter. It is used to simplify some expressions.

1.3 Distance definitions

The distance measurements in astronomy are based on parallax method or on a measurement of the energy flux from a source of known luminosity. (These are just two examples which have simple analogy in cosmology).

Parallax Θ is the angle of view of the Earth orbit radius (1 AU) as seen from a source at the distance d:

$$\Theta\ [\text{rad}] = \frac{1\ \text{AU}}{d} \qquad \Theta\ [\text{arcsec}] = \frac{1}{d\ [\text{pc}]}$$

Flux of energy F from an isotropic source of luminosity L at distance d reads:

$$F = \frac{L}{4\pi d^2}$$

Using the above equations one can measure the distance, assuming all other quantities are known:

$$d\ [\text{pc}] = \frac{1}{\Theta\ [\text{arcsec}]} \qquad d = \sqrt{\frac{L}{4\pi F}}$$

At large distances the curvature of space and the effects related to light propagation affect distance measurements. We shall see that using methods analogous to parallax and flux measurements in expanding Universe one gets two definitions of the distance which are not identical. Thus there is no unique distance definition in a curved space-time. One can define many quantities which have some intuitive properties of the distance and in the local limit would be distances in common sense. Two quantities which we are discussing are in principle measurable. In Special Relativity one uses times of the light propagation as measures of distances. In cosmology we are not able to measure the time of the emission, so the time of propagation remains unknown and cannot be used to estimate the source distance. (In a Universe model with known parameters we can *calculate* the propagation time from a source of measured redshift but cannot *measure* it.)

We use spherical coordinate system with the observer at its origin. Angular coordinates (θ and ϕ) become coordinates on the sky and χ is a modified radial coordinate. (In case of a flat model it is simply radial coordinate.) We are using *co-moving* coordinates which means that astronomical objects have constant values of coordinates (χ, θ, ϕ) and the Universe expansion is described by the scale factor $a(t)$. The interval differential is given as:

$$ds^2 = c^2dt^2 - dl^2 = c^2dt^2 - a^2(t)\left(d\chi^2 + S^2(\chi)(d\theta^2 + \sin^2\theta d\phi^2)\right)$$

where

$$S(\chi) = \sin\chi \ \ (k=+1), \qquad S(\chi) = \chi \ \ (k=0), \qquad S(\chi) = \sinh\chi \ \ (k=-1)$$

and t is the cosmic time. The coordinates are orthogonal ($\Leftrightarrow$ metric tensor is diagonal), $a(t)$ is an unknown function to be found as a solution to the Einstein equations.

For an object at small distance r from an observer which can also be expressed as $r = a(t)\chi$, where $\chi = \text{const}$ one has:

$$\dot{r} = \dot{a}\chi \equiv \frac{\dot{a}}{a}a\chi = \frac{\dot{a}}{a}r \ \Rightarrow \ v = \frac{\dot{a}}{a}r \ \Rightarrow \ H(t) = \frac{\dot{a}}{a}$$

so the ratio $\dot{a}/a$ plays a role of the Hubble constant which would be measured by astronomers at the time t.

1.3.1 Photon propagation

A ray going through the coordinate origin ($\chi = 0$) propagates radially, so $\theta = const$ and $\phi = const$ along the trajectory, which is implied by the symmetries. Since photons travel with the speed of

light $ds = 0$, and one has:

$$a(t)|d\chi| = cdt \qquad \chi = \int_{t_{em}}^{t_{obs}} \frac{cdt}{a(t)} \qquad \chi(z) = \int_{t(z)}^{t(z=0)} \frac{cdt}{a(t)}$$

The change of $\chi = \chi(z)$ is the same for outgoing and ingoing rays, and depends only on the emission and observation times (t_{em}, t_{obs}). Since objects do not change their coordinates ($\chi = $ const for a given source), we may consider a signal sent later by Δt_{em} which is observed later by Δt_{obs}. That implies:

$$\begin{aligned}
\int_{t_{em}}^{t_{obs}} \frac{cdt}{a(t)} &= \int_{t_{em}+\Delta t_{em}}^{t_{obs}+\Delta t_{obs}} \frac{cdt}{a(t)} \quad \Rightarrow \quad \int_{t_{em}}^{t_{em}+\Delta t_{em}} \frac{cdt}{a(t)} = \int_{t_{obs}}^{t_{obs}+\Delta t_{obs}} \frac{cdt}{a(t)} \quad \Rightarrow \\
\frac{c\Delta t_{em}}{a(t_{em})} &= \frac{c\Delta t_{obs}}{a(t_{obs})} \quad \Rightarrow \quad \frac{a(t_{obs})}{a(t_{em})} = \frac{\Delta t_{obs}}{\Delta t_{em}} = \frac{\nu_{em}}{\nu_{obs}} = \frac{\lambda_{obs}}{\lambda_{em}} = 1+z \quad \Rightarrow \\
1+z &= \frac{a(t_{obs})}{a(t_{em})}
\end{aligned}$$

Since redshifts are measurable, it is desirable to use z as independent variable in integrals as above and other tasks. We use one of the Einstein equations governing the evolution of the Universe to find the z and t relation:

$$\begin{aligned}
\frac{1}{a^2}\left(\frac{da}{dt}\right)^2 &+ \frac{kc^2}{a^2} = \frac{8\pi G}{3c^2}(\epsilon + \epsilon_\Lambda) \\
1+z = \frac{a_0}{a(t)} \quad &\Rightarrow \quad \frac{1}{a}\frac{da}{dt} = -\frac{1}{1+z}\frac{dz}{dt} \\
\frac{1}{(1+z)^2}\left(\frac{dz}{dt}\right)^2 &+ \frac{kc^2}{a_0^2}(1+z)^2 = \frac{8\pi G}{3c^2}(\epsilon + \epsilon_\Lambda)
\end{aligned}$$

We limit ourselves (at least for now) to considerations of *late* Universe, where the relativistic component of matter plays negligible role. (It is safe after the recombination - see later lectures - at $z < 10^3$). That implies $\epsilon(t_0) = \Omega_M \rho_c c^2$, $\epsilon_\Lambda(t_0) = \Omega_\Lambda \rho_c c^2$. Remembering that $H(t) = \dot{a}/a$ and $H_0 = H(t_0)$ we get after substitutions:

$$H_0^2 + \frac{kc^2}{a_0^2} = H_0^2(\Omega_M + \Omega_\Lambda) \quad \Rightarrow \quad \frac{kc^2}{a_0^2} = H_0^2(\Omega_M + \Omega_\Lambda - 1) \quad \Rightarrow \quad a_0 = \frac{c/H_0}{\sqrt{|\Omega_K|}}$$

which gives the present day value of the curvature term ($\Leftrightarrow a_0$) with the values of other parameters. One can also define $\Omega_K = 1 - \Omega_M - \Omega_\Lambda$ so the $z \leftrightarrow t$ relation becomes:

$$\frac{1}{(1+z)^2}\left(\frac{dz}{dt}\right)^2 = H_0^2(\Omega_M(1+z)^3 + \Omega_K(1+z)^2 + \Omega_\Lambda) \equiv H_0^2 h^2(z)$$

We have employed the dependence of cold matter density on the redshift ($\rho = \rho_0(1+z)^3$) and for dark energy ($\epsilon_\Lambda = \epsilon_\Lambda(t_0)(1+z)^0$). Finally we get:

$$\begin{aligned}
H_0\frac{dz}{dt} &= \frac{1}{(1+z)h(z)} \\
t_0 - t(z) &= \frac{1}{H_0}\int_0^z \frac{dz'}{(1+z')h(z')} \qquad t(z) = \frac{1}{H_0}\int_z^\infty \frac{dz'}{(1+z')h(z')} \\
\chi(z) &= \int_0^z \frac{1}{a}\frac{cdt}{dz'}dz' = \frac{c/H_0}{a_0}\int_0^z (1+z')\frac{dz'}{(1+z')h(z')} = \frac{c/H_0}{a_0}\int_0^z \frac{dz'}{h(z')}
\end{aligned}$$

The expression for χ becomes undefined when $|\Omega_K| \to 0$ which implies $a_0 \to \infty$ (flat model). Using Taylor expansion for small $|\Omega_K|$ one gets:

$$a_0 S(\chi(z)) = \frac{c/H_0}{\sqrt{|\Omega_K|}} S\left(\sqrt{|\Omega_K|}\int_0^z \frac{dz'}{h(z')}\right) \underset{|\Omega_K|\to 0}{\to} \frac{c}{H_0}\int_0^z \frac{dz'}{h(z')}$$

One can also notice that in a flat model $S(\chi) = \chi$ so the parameter a_0 reduces with the same factor in the denominator. [1]

[1] In a flat model one has the freedom to choose the present value of the scale factor. It is possible to use $a_0 = c/H_0$, which is of the order of the size of the observable part of the Universe. Some physicists use $a_0 = 1$, as they like $G = 1$, $c = 1$ as well.

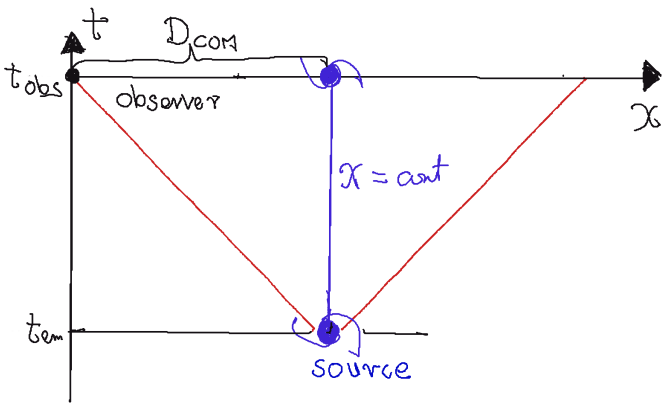

Figure 1.2: Comoving distance to a source

1.3.2 Comoving distance

The picture above shows a present day observer ($t = t_{obs}$) at the origin of space coordinates ($\chi = 0$). Red lines show 2 rays emitted from a source (S-galaxy), one detected by the observer. The blue line shows the source trajectory (χ = const). We introduce the *comoving distance* concept. It is not simply related to any measurement possible on cosmological scale. The comoving distance to the source seen at z_{em} at the time t_{em} is the present day proper distance to the same source (impossible to observe at its today position), so:

$$D_{COM} = a_0\chi_{em} = a_0\int_{t_{em}}^{t_{obs}}\frac{cdt}{a(t)} = \frac{c}{H_0}\int_0^{z_{em}}\frac{dz}{h(z)}$$

Since the expansion of the Universe preserves the ratios of distances between various pairs of objects, knowing all these distances today is enough to find their values at any epoch. (For a pair of objects 1 and 2 their proper distace at epoch z was: $d^{1,2}(z) = D^{1,2}_{COM}/(1+z)$.

It is customary to use comoving distances in many applications. (For instance: when we talk about the scale of galaxy auto-correlations, it is better to use *comoving values*. One knows all distances grow in the expanding Universe but an increase in size expressed in comoving units implies some extra processes - like gravitational instability - going on.)

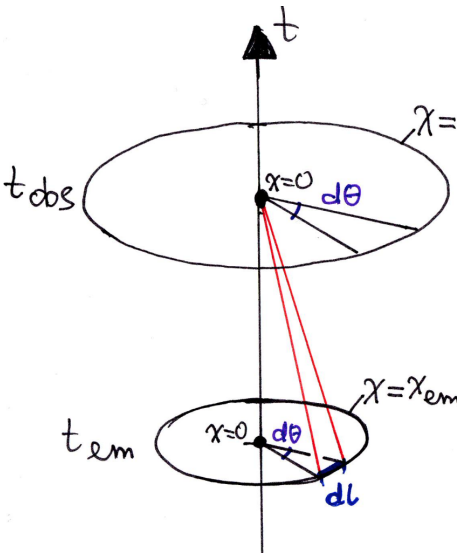

Figure 1.3: Angular diameter distance

1.3.3 Angular diameter distance

Parallax method is based on a relation between the length of a segment perpendicular to the line of sight δl, its angle of view $\delta\theta$ and the distance d: $\delta l = d \times \delta\theta$.

The picture above shows a present day observer ($t = t_{obs}$) at the origin of space coordinates ($\chi = 0$). Two red lines on the observer's past cone surface are two light rays which were sent at $t = t_{em}$ from two points which were δl apart from each other. For simplicity e place both points at the same ϕ on the sky by choosing appropriate orientation of the coordinate system ($\Rightarrow \quad \delta\phi = 0$). Since both rays were emitted at the same time, their source points have the same χ value (isotropy of the Universe $\Rightarrow \quad \delta\chi = 0$). Using the formula for the interval differential one has:

$$\delta l = a(t_{em})S(\chi)\delta\theta = \frac{a(t_0)}{1+z}S(\chi)\delta\theta$$

The proportionality factor between angular and linear sizes can be treated as a distance measure. We define the *angular diameter distance* $R(z)$ as:

$$R(z) = \frac{a_0}{1+z}S(\chi(z))$$

(There are many other symbols used in literature for this quantity, for instance d_{add}.) To get the value of the expression above one needs the values of the cosmological model parameters.

For $k \neq 0$ the expression for $\chi(z)$ is not singular and using the relation for $t = t_0$ ($kc^2/a_0^2 = H_0^2(-\Omega_K)$) we have:

$$R(z) = \frac{a_0}{1+z}S(\chi(z)) = \frac{c/H_0}{\sqrt{|\Omega_K|}(1+z)}S\left(\sqrt{|\Omega_K|}\int_0^z \frac{dz'}{h(z')}\right) \underset{z\to 0}{\to} \frac{c}{H_0}z$$

In the limit of $|\Omega_K| \to 0$ (which corresponds to $a_0 \to \infty$, the radius of curvature increases infinitely, the curvature goes to zero, the model becomes flat) the argument of the $S()$ function goes to zero and the Taylor expansion allows to remove singularity from the denominator, which gives:

$$R(z) = \frac{c/H_0}{(1+z)}\int_0^z \frac{dz'}{h(z')} \underset{z\to 0}{\to} \frac{c}{H_0}z$$

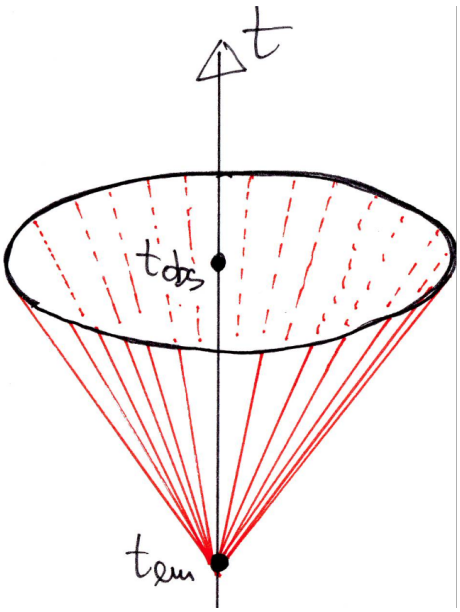

Figure 1.4: Luminosity distance

1.3.4 Luminosity distance

The classic relation $F = L/4\pi d^2$ should be generalized in a curved space-time.

In the picture we have the source at the origin of coordinates ($\chi = 0$). The present time observers ($t = t_{obs}$) are placed on a sphere around the source, at radial coordinate $\chi = \chi_{obs}$. The surface area of the sphere reads $4\pi a^2(t_{obs})S^2(\chi_{obs})$. It may seem that dividing the source luminosity by the surface area occupied by observers we would get the energy flux. The expansion of the Universe implies that the observers are going away from the source which causes another two effects: first each photon is shifted and its energy falls by a factor $1+z$, second the time between arrivals of consecutive photons is expanded by the same factor. Both effects diminish the observed flux of energy:

$$F_{obs} = \frac{L_{em}/(1+z)^2}{4\pi a^2(t_{obs})S^2(\chi_{obs})} \equiv \frac{L_{em}}{4\pi D^2(z)}$$

where

$$D(z) = a_0(1+z)S(\chi(z)) \qquad D(z) = (1+z)^2 R(z)$$

is the *luminosity distance*. (Others may use d_{lum} or similar symbols for this quantity.) The relation between two defined distances is useful in some calculations. For $k \neq 0$ the expression for $\chi(z)$ is not singular and using the relation for $t = t_0$ ($kc^2/a_0^2 = H_0^2(-\Omega_K)$) we have:

$$D(z) = a_0(1+z)S(\chi(z)) = \frac{c/H_0}{\sqrt{|\Omega_K|}}(1+z)S\left(\sqrt{|\Omega_K|}\int_0^z \frac{dz'}{h(z')}\right) \underset{z\to 0}{\to} \frac{c}{H_0}z$$

In the limit of $|\Omega_K| \to 0$ (which corresponds to $a_0 \to \infty$, the radius of curvature increases infinitely, the curvature goes to zero, the model becomes flat) the argument of the $S()$ function goes to zero and the Taylor expansion allows to remove singularity from the denominator, which gives:

$$D(z) = \frac{c}{H_0}(1+z)\int_0^z \frac{dz'}{h(z')} \underset{z\to 0}{\to} \frac{c}{H_0}z$$

1.4 Tests based on $D(z)$ or $R(z)$ measurements

Suppose we know bolometric luminosities of a sample of sources L_i and we measure their redshifts z_i and bolometric fluxes of energy F_i. (L_i may be the same for the whole sample of *standard candles* as in the case of SN Ia). We can define *empirical* values of the luminosity distances to the sources $D_i = \sqrt{L_i/4\pi F_i}$ with uncertainty σ_i resulting mostly from the spread in true values of L_i. On the other hand the value of the luminosity distance to a source at given redshift can be calculated in any cosmological model with known cosmological parameters. That leads to a simple test:

$$\chi^2 = \sum_i \frac{(D_i - D(z_i))^2}{\sigma_i^2}$$

Minimizing χ^2 in $(H_0, \Omega_M, \Omega_\Lambda)$ parameter space allows fitting the model to observations i.e. finding the most likely values of parameters. Investigating the dependence of χ^2 on parameters in the vicinity of their most likely values gives the confidence region for parameters with required confidence.

A similar test would be possible for $R(z)$ provided a sample of objects with defined linear sizes is known. In a sense the measurements of the angular sizes of the hot spots on a CMB sky is a kind of such test. The theory of gravitational instability in a given Universe model gives the distribution of density and temperature fluctuations at the moment of recombination in 3D. Projection onto observer's past cone gives the distribution of hot / cold spot linear sizes as measured at the epoch of recombination. . The angular size of a spot of linear size r is: $\theta = r/R(z_{rec})$, so the 3D linear size distribution translates into 2D distribution of angular sizes, the angular diameter distance to the last scattering surface (corresponding to recombination) $R(z_{rec})$ is the normalizing factor which can be found by fitting the model to observations. Since only one angular diameter distance can be used here, all model parameters cannot be found, but using some other data and fitted $R(z_{rec})$ value one can construct a valid test. [2]

Another example is the measurement of the BAO (baryon acoustic oscillations) scale at different redshift ranges. As explained in the Lecture the BAO scale, the distance traveled by a sound wave since the beginning of the Universe till given epoch, can be calculated theoretically in any model as $s(z)$. BAO scale is also imprinted in auto-correlation function for galaxies, and the corresponding angular scale can be observed for objects at small redshift ranges as $\Theta(z)$. Then the angular diameter distance can be found as $R_i = s(z_i)/\Theta(z_i)$ for several epochs z_i. The comparison of R_i with $R(z_i)$ from the model makes a test.

[2] Using the whole CMB angular anisotropy power spectrum one gets a very strong cosmological test (see future lectures).

Chapter 2

Observations; tests

2.1 Tests using gravitational waves

The direct detection of gravitational waves (GW) is possible at present (2020) at frequencies of several hundred Hz, which corresponds to the final frequencies of merging compact binaries with masses up to hundreds of $M_\odot$.

$$\begin{aligned}
\omega &= \sqrt{\frac{GM}{a^3}} \sim \sqrt{\frac{GM}{(GM/c^2)^3}} = \frac{c^3}{GM_\odot}\frac{M_\odot}{M} = \frac{c^3}{(30\ km/s)^2(1\ AU)}\frac{M_\odot}{M} \\
&= \left(\frac{c}{30\ km/s}\right)^2 \frac{1}{500\ s}\frac{M_\odot}{M} = 2\times 10^5\ rad/sec\ \frac{M_\odot}{M} \\
f &\sim 3\times 10^4\ Hz\frac{M_\odot}{M}
\end{aligned}$$

In the range $30 < M < 300\ [M_\odot]$ we get frequencies in the range 100 - 1000 Hz, detectable with LIGO - VIRGO antennas. The sources emitting detectable GW cannot be too massive, so the power of the sources is limited $\Rightarrow$ they are not observable at distances comparable to c/H_0, typical distance scale in the Universe.

Super-massive black hole binaries (SMBHB) can emit GW of much greater amplitudes, which will be detectable on the in-spiral stage with the help of cosmic interferometer.

2.1.1 Binaries on circular orbits: evolution rate

Masses m_1 and m_2 rotate around their center of mass on the orbits of radii $a_1 = m_2/(m_1+m_2)\ a$ and $a_2 = m_1/(m_1+m_2)\ a$ respectively where $a \equiv a_1 + a_2$ is their distance. We cannot measure the size of the orbit a, but we can measure the orbital angular velocity ω measuring the GW frequency.

We replace a by ω in our equations:

$$\begin{aligned}
\frac{1}{a} &= \left(\frac{\omega^2}{G(m_1+m_2)}\right)^{1/3} \\
\mathcal{M} &\equiv \frac{m_1^{3/5}m_2^{3/5}}{(m_1+m_2)^{1/5}} \\
-\mathcal{E} &= \frac{Gm_1m_2}{2a} = \frac{1}{2}G^{2/3}\left(\frac{m_1^{3/5}m_2^{3/5}}{(m_1+m_2)^{1/5}}\right)^{5/3}\omega^{2/3} \equiv \frac{1}{2}G^{2/3}\mathcal{M}^{5/3}\omega^{2/3} \\
L \equiv -\frac{d\mathcal{E}}{dt} &= \frac{1}{3}G^{2/3}\mathcal{M}^{5/3}\omega^{-1/3}\dot{\omega}
\end{aligned}$$

where we have defined the *chirp mass* $\mathcal{M}$ Comparing the rate of mechanical energy loss to the power emitted in the form of GW one has (see *Calculations*):

$$\begin{aligned}
\frac{1}{3}G^{2/3}\mathcal{M}^{5/3}\omega^{-1/3}\dot{\omega} &= \frac{8G^{7/3}}{5c^5}\mathcal{M}^{10/3}\omega^{10/3} \\
\dot{\omega} &= \frac{24G^{5/3}}{5c^5}\mathcal{M}^{5/3}\omega^{11/3}
\end{aligned}$$

In the case of far away sources their observed frequencies are *red shifted*, $\omega_{obs} = \omega/(1+z)$ where z is the redshift factor, Similarly with time: $dt_{obs} = (1+z)dt$. As a consequence one has:

$$\begin{aligned}
\frac{d\omega_{obs}}{dt_{obs}} &= \frac{1}{(1+z)^2}\frac{d\omega}{dt} = \frac{1}{(1+z)^2}\frac{24G^{5/3}}{5c^5}\mathcal{M}^{5/3}\left((1+z)\omega_{obs}\right)^{11/3} \\
\frac{d\omega_{obs}}{dt_{obs}} &= = \frac{24G^{5/3}}{5c^5}\mathcal{M}^{5/3}(1+z)^{5/3}\omega_{obs}^{11/3}
\end{aligned}$$

Measuring frequency and its rate of change we cannot measure the chirp mass alone, but its product with the redshift $(1+z)\mathcal{M}$. Knowing the redshift from independent measurement, we have:

$$\mathcal{M} = \left(\frac{5}{24}\right)^{3/5}\frac{c^3}{G(1+z)}\omega_{obs}^{-11/5}\left(\frac{d\omega_{obs}}{dt_{obs}}\right)^{3/5}$$

2.1.2 Binaries on circular orbits: GW amplitudes

The luminosity - energy flux relation (see *Calculations*) in cosmology involves the luminosity distance ($D(z)$ here) and is given as:

$$F_{GW}(\theta) = \frac{L}{4\pi D^2(z)}\frac{5}{16}(1+6\cos^2\theta+\cos^4\theta)$$

which shows that GW are not emitted isotropically, but averaging over the sphere we would get the usual relation $\langle F_{GW}\rangle = L/4\pi D^2$. In cosmological context we use $d = D(z)$.

Using expressions from *Calculations* one has for the amplitudes of two GW polarizations:

$$\begin{aligned}
h_+ = \frac{1}{2}(h_{xx}-h_{yy}) &= \frac{2G^{5/3}}{c^4D(z)}\mathcal{M}^{5/3}\omega^{2/3}(1+\cos^2\theta)\cos 2\omega t \\
h_\times = h_{xy} &= \frac{2G^{5/3}}{c^4D(z)}\mathcal{M}^{5/3}\omega^{2/3}(2\cos\theta)\sin 2\omega t
\end{aligned}$$

The angular velocity here is measured in the source frame, so it should be replaced by $(1+z)\omega_{obs}$. The ratio of the two polarization amplitudes defines θ - the position of the observer relative to the orbital motion axis. Finally every source with measured $(z, \omega_{obs}, \dot{\omega}_{obs}, h_+, h_\times)$ gives us an empirical value of D, while a model gives the theoretical $D(z)$. For a sample of sources one can look for a model which fits the data with the best accuracy.

2.1.3 Calculations

We use Field Theory by Landau and Lifschitz, 6th edition, Moscow 1973, Section XIII Gravitational Waves (in Russian) [LL] as main reference.

We consider small perturbations to the metric of the *weak* gravitational field, which means we are far away from compact sources and we assume they are moving slowly, so looking from a large distance we can describe the binary motion using Newtonian dynamics.

We use a standard expansion for the metric components $g_{ik} + h_{ik}$, where h_{ik} are small perturbations. Calculating Riemann and Ricci R_{ik} tensors we limit ourselves to expressions which are linear in h_{ik}. Far from the sources, in empty space the energy - momentum tensor (and so Ricci tensor) both vanish. That implies the wave equation for metric perturbations:

$$R_{ik} = \Box h_{ik} \equiv \left(\Delta - \frac{1}{c^2}\frac{\partial^2}{\partial t^2}\right) h_{ik} \qquad \Rightarrow \qquad \Box h_{ik} = 0$$

where $\Box$ stands for d'Alembert operator, and Δ for Laplace operator.

Far away from the source one treats the propagating perturbation as a plane wave. (In a region much smaller than the distance from the source). We choose z axis as a direction of propagation (against LL, who use x axis). We have

$$\left(\frac{\partial^2}{\partial z^2} - \frac{1}{c^2}\frac{\partial^2}{\partial t^2}\right) h_{ik} = 0 \qquad \Rightarrow \qquad h_{ik} = h_{ik}(t \pm z/c))$$

- as usual for waves - any signal shape propagates with the wave speed ...

In a Cartesian coordinates (x, y, z), far away from the source on z axis, the energy flux of GW along the z axis reads:

$$F_{GW} = \frac{c^3}{16\pi G}\left(\frac{1}{4}\left(\dot{h}_{xx} - \dot{h}_{yy}\right)^2 + \dot{h}_{xy}^2\right)$$

(as shown by LL)

LL show that the interesting components of metric perturbations caused by a non-relativistic motion of sources can be expressed as the second time derivatives of the quadrupole of mass distribution:

$$\begin{aligned} h_{xx} - h_{yy} &= -\frac{2G}{3c^4 d}\left(\ddot{D}_{xx} - \ddot{D}_{yy}\right) \qquad h_{xy} = -\frac{2G}{3c^4 d}\ddot{D}_{xy} \\ D_{\alpha\beta} &= \int \rho\left(3x^\alpha x^\beta - r^2\delta_{\alpha\beta}\right) dV \end{aligned}$$

where d is the distance from the source. (This is the case where neither time-space curvature nor the Universe expansion have any significance and the distance is defined in a unique way, but see below).

Now we limit ourselves to a source which is a binary on circular orbits. Masses m_1 and m_2 move on orbits with the radii $a_1 = m_2/(m_1+m_2)a$ i $a_2 = m_1/(m_1+m_2)a$ around their common

center of mass ($a \equiv a_1 + a_2$) in the (x, y) plane which is perpendicular to the line of sight (LOS) with the angular velocity $\omega = \sqrt{G(m_1 + m_2)/a^3}$. (This is the simplest case to consider). Using Dirac's deltas (δ_D) one can express the mass distribution as:

$$\rho(x, y, z, t) = m_1\delta_D(x - a_1\cos\omega t)\delta_D(y - a_1\sin\omega t)\delta_D(z) + m_2\delta_D(x + a_2\cos\omega t)\delta_D(y + a_2\sin\omega t)\delta_D(z)$$

where the phase of motion has been set arbitrarily, which in a case of circular orbits has no importance. Substituting $\rho(x, y, z, t)$ to the integral expressing quadruple moment we get:

$$\begin{aligned} \frac{1}{2}\left(D_{xx} - D_{yy}\right) &= \frac{1}{2}(m_1a_1^2 + m_2a_2^2)(3\cos^2\omega t - 3\sin^2\omega t) = \frac{3}{2}\frac{m_1m_2}{m_1 + m_2}a^2\cos 2\omega t \\ D_{xy} &= (m_1a_1^2 + m_2a_2^2)(3\cos\omega t\sin\omega t) = \frac{3}{2}\frac{m_1m_2}{m_1 + m_2}a^2\sin 2\omega t \end{aligned}$$

Let us imagine that the orbital plane was rotated by an angle θ around the x axis, so the axis of rotation and LOS are now at the angle θ. Projection of the binary motion into the plane perpendicular to LOS causes a change in mass distribution expression $\sin\omega t \to \cos\theta\sin\omega t$. As a consequence we get:

$$\begin{aligned} \frac{1}{2}\left(D_{xx} - D_{yy}\right) &= = \frac{3}{2}\frac{m_1m_2}{m_1 + m_2}a^2\left(\frac{1}{2}\sin^2\theta + \frac{1}{2}(1 + \cos^2\theta)\cos 2\omega t\right) \\ D_{xy} &= \frac{3}{2}\frac{m_1m_2}{m_1 + m_2}a^2\sin 2\omega t\cos\theta \end{aligned}$$

The energy flux is expressed by the first time derivatives of the metric perturbations and so by the third derivatives of the quadrupole moment. Averaging over the period ($\langle cos^2 2\omega t\rangle = 1/2$, same for the sinus) we get:

$$F_{GW}(\theta) = \frac{G}{8\pi c^5 d^2}\left(\frac{m_1m_2}{m_1 + m_2}\right)^2 a^4\omega^6(1 + 6\cos^2\theta + \cos^4\theta)$$

Replacing the orbit size by the expression containing angular velocity and binary components masses and integrating the energy flux over a sphere of radius d around the source we get:

$$\begin{aligned} F_{GW}(\theta) &= \frac{G^{7/3}}{8\pi c^5 d^2}\mathcal{M}^{10/3}\omega^{10/3}(1 + 6\cos^2\theta + \cos^4\theta) \\ L &= 2\pi d^2\int_0^\pi F_{GW}(\theta)\sin\theta d\theta = \frac{8G^{7/3}}{5c^5}\mathcal{M}^{10/3}\omega^{10/3} \end{aligned}$$

which gives the source GW luminosity.

2.1.4 Numerical values

Let us find some typical values for GW power and amplitudes. We use solar mass as a unit and substitute:

$$GM_\odot = \left(30\frac{km}{s}\right)^2 \times 1AU = \left(30\frac{km}{s}\right)^2 \times c \times 500\ s$$

where the velocity of Earth on its orbit (30 km/s) size of the orbit (1 AU) and the light travel time from the Sun (500 s) are used.

We use dimensionless parameter r which gives the size of the orbit in gravitational radius units ($a = (Gm/c^2) * r$), where $m = m_1 + m_2$. Another dimensionless parameter $s = m_2/m$ sets the binary mass ratio ($q = m_2/m_1 = s/(1-s)$). That leads to the following equalities:

$$\begin{aligned}
\omega^2 &= \frac{Gm}{a^3} = \frac{Gm}{\left(\frac{Gm}{c^2}r\right)^3} = \frac{c^6}{G^2m^2}\, r^{-3} \\
L &= \frac{8G^{7/3}}{5c^5}\mathcal{M}^{10/3}\omega^{10/3} = \frac{8c^5}{5G}\,\frac{s^2(1-s)^2}{r^5} = 5.8\times 10^{52}\ \mathrm{W}\ \frac{s^2(1-s)^2}{r^5} \\
|h_\times| &\approx \frac{2G^{5/3}}{c^4 D(z)}\mathcal{M}^{5/3}\omega^{2/3} = 2\frac{G^{5/3}}{c^4 D(z)}\left(\frac{m_1^{3/5}m_2^{3/5}}{m^{1/5}}\right)^{5/3}\left(\frac{c^3}{Gm}r^{-3/2}\right)^{2/3} \\
&= 2\frac{G}{c^4 D(z)}\, c^2\,\frac{m_1 m_2}{m}\,\frac{1}{r} = 2\frac{Gm}{c^2 D(z)}\,\frac{s(1-s)}{r} \\
&= 2\left(\frac{30km/s}{c}\right)^2\,\frac{1AU}{D(z)}\,\frac{m}{M_\odot}\,\frac{s(1-s)}{r} = 10^{-22}\,\frac{Gpc}{D(z)}\,\frac{m}{M_\odot}\,\frac{s(1-s)}{r}
\end{aligned}$$

The characteristic power $c^5/G = 3.64\times 10^{52}$ W.

2.2 Gravitational lensing

2.2.1 Deflection angle

All gravitational lensing calculations start from the case of a point mass lens. The deflection angle for a ray passing at the encounter parameter b from the lens ($b \gg GM/c^2$ or $b \gg GM/v^2$ where M is the point lens mass, c is the speed of light and v the massive particle velocity considered in a similar problem). In the case of a *fast* particle of mass m passing far from the lens the deflection was calculated by Soldner (1801). In the case of small deflection (guaranteed by the $v^2 \gg GM/b$) one calculates the change in the particle momentum perpendicular to the trajectory assuming motion along a straight line (Born approximation):

$$\Delta\vec{p}_\perp = -\int_{-\infty}^{+\infty} \frac{GMm\vec{b}}{(l^2+b^2)^{3/2}}dt = -\int_{-\infty}^{+\infty} \frac{GMm\vec{b}}{(l^2+b^2)^{3/2}}\frac{dl}{v} = -\frac{2GMm}{vb^2}\vec{b}$$

where l measures the distance along the ray and $\vec{b}$ parametrizes the perpendicular plane. The point lens is at $(\vec{b}, l) = 0$. The particle momentum along the trajectory is $p_{||} = mv$, so the deflection angle calculated by Soldner is:

$$\vec{\alpha} = \frac{\Delta\vec{p}_\perp}{p_{||}} = -\frac{2GM}{v^2}\frac{\vec{b}}{b^2} \to -\frac{2GM}{c^2}\frac{\vec{b}}{b^2} \text{ (Soldner)} \quad \vec{\alpha} = -(1+v^2/c^2)\frac{2GM}{v^2}\frac{\vec{b}}{b^2} \to -\frac{4GM}{c^2}\frac{\vec{b}}{b^2} \text{ (Einstein)}$$

In General Relativity (GR) it is not enough to make $v = c$ substitution in the Soldner formula. Instead one has to use the geodesic equation.

In the so called weak field approximation, applicable when the matter occupies a limited region in space, which is *asymptotically flat*, the metric has the form:[1]

$$ds^2 = \left(1 + \frac{2}{c^2}\Phi\right) d(ct)^2 - \left(1 - \frac{2}{c^2}\Phi\right)\left(db_1^2 + db_2^2 + dl^2\right)$$

where Φ is the Newtonian potential, ct plays the role of the time coordinate, and $(\vec{b}, l)$ are Cartesian space coordinates, l directed along the particle trajectory. The geodesic equation reads:

$$\begin{aligned}
u^a &= \frac{(1,0,0,v/c)}{\sqrt{1-v^2/c^2}} \equiv (\gamma, 0, 0, \gamma v/c) \qquad ds = \sqrt{1-v^2/c^2}\,d(ct) \\
\frac{d\vec{u}^\perp}{ds} &= -\frac{1}{2}\left(u^0u^0\nabla_\perp g_{00} + u^lu^l\nabla_\perp g_{ll}\right) = -\frac{1}{c^2}(\gamma^2(1+v^2/c^2)\nabla_\perp\Phi \\
\gamma\frac{d\vec{u}^\perp}{d(ct)} &= -\gamma^2(1+v^2/c^2)\nabla_\perp\left(\frac{\Phi}{c^2}\right) \\
\Delta\vec{u}^\perp &= -\frac{\gamma(1+v^2/c^2)}{v}\int \nabla_\perp\Phi dl \qquad \vec{\alpha} = \frac{\Delta u^\perp}{\gamma v} = -\frac{1+v^2/c^2}{v^2}\int \nabla_\perp\Phi dl \to -\frac{2}{c^2}\int \nabla_\perp\Phi dl
\end{aligned}$$

Thus the GR result for photons gives twice larger deflection angle as compared to the Soldner result and for slow particles it agrees with the Newtonian approach. At the beginning (1911?) Einstein thought Soldner formula to be correct, but then (1915) he derived his own formula. The measurement of the ray deflection during the solar eclipse (1919) was one of the classic tests of

[1] It is discussed elsewhere in these Lectures

GR, proving that Einstein formula was correct and that GR was a better approximation to the gravity theory than the Newtonian one.

The integral above represents the projection of the 3D potential gradient into 2D. One may think of a 2D potential:

$$\psi(\vec{b}) \stackrel{def}{=} \frac{2}{c^2}\int_{-\infty}^{+\infty}(\Phi(\vec{b},l)-\Phi(\vec{b}_1,l))dl = \frac{4}{c^2}\int_0^{\infty}(\Phi(\vec{b},l)-\Phi(\vec{b}_1,l))dl = \frac{4GM}{c^2}\ \ln\left(\frac{|\vec{b}|}{|\vec{b}_1|}\right)$$

where the last form is for a point mass. To avoid an apparent divergence of the integral, we calculate the difference between the results of the integration along two parallel lines crossing the lens plane at the positions $\vec{b}$ and $\vec{b}1$, respectively, $\vec{b}_1$ being some arbitrary reference position. (Potentials are usually defined up to a constant).

$$\psi(\vec{b}) = \frac{4GM}{c^2}\ \ln|\vec{b}| + \text{const} \qquad \vec{\alpha} = -\nabla_{\vec{b}}\psi(\vec{b})$$

In our derivations we implicitly assume that the point lens is at the origin of the coordinate system. For a lens at a position $\vec{b}_L$ and a ray passing at $\vec{b}$ the replacement of $|\vec{b}|$ into $|\vec{b}-\vec{b}_L|$ would generalize our formulae.

2.2.2 Time delay

We consider two parallel rays passing the lens plane at $\vec{b}$ and some reference position $\vec{b}_1$. We use Born approximation neglecting the influence of the deflections on the trajectories, which would introduce corrections of the higher order.

$$\begin{aligned}
ds &= 0 \ \Rightarrow\ cdt = \left(1-\frac{2}{c^2}\Phi\right)dl \\
ct(\vec{b})-ct(\vec{b}_1) &= \int_{-\infty}^{+\infty}\left(1-\frac{2}{c^2}\Phi(\vec{b},l)\right)dl - \int_{-\infty}^{+\infty}\left(1-\frac{2}{c^2}\Phi(\vec{b}_1,l)\right)dl \\
&= -\frac{2}{c^2}\int_{-\infty}^{+\infty}(\Phi(\vec{b},l)-\Phi(\vec{b}_1,l))dl \quad\equiv\quad -\psi(\vec{b}) = c\Delta t_{grav}(\vec{b}) \\
&\Rightarrow\ \vec{\alpha} = -\nabla_{\vec{b}}\psi(\vec{b}) = +\nabla_{\vec{b}}c\Delta t_{grav}(\vec{b})
\end{aligned}$$

We name the effect *gravitational time delay* $c\Delta t_{grav}$. The relation between the relative time delay and the deflection angle is not surprising: the rays propagate perpendicularly to the wave fronts, which are constant phase surfaces, or equivalently, surfaces of the same propagation time. The form of the above equations suggests that the time delay is longer for rays passing closer to the potential Φ minimum. Thus after passing through matter distribution the originally flat wave front becomes concave (as seen from not yet passed positions) which introduces convergence of the originally parallel light bundles.

Example. The most obvious and simple example would be the point mass lens, but its applications are not interesting, at least on cosmological scales. Time delays are measured for QSOs with multiple images, where galaxies serve as gravitational lenses. The true mass distribution in galaxies is rather complicated but the spherical galaxy halo with flat rotation curve is a good starting point.

For maximal simplicity we ignore the shape of the rotation curve near the center and do not limit the size of the system. Thus we have an infinite mass distribution with flat rotation curve

called *singular isothermal sphere* (SIS). Rays passing at a distance b from the sphere center are deflected by the mass inside an infinite cylinder of radius b with the base perpendicular to the propagation direction (not the finite sphere of the same radius!). To calculate the mass in the cylinder we project the 3D density $\rho(r)$ into a plane obtaining 2D surface mass density $\Sigma(b)$. By integration we get mass inside a cylinder $M_{cyl}(b)$ and using the Einstein formula we obtain the deflection angle. Its relation to the gravitational time delay allows calculation of the latter. We also limit the cylinder radius to some value b_{max}. Such an approach is a crude approximation to the more realistic case of a finite SIS sphere. Close to the center this approximation is acceptable, but at b_{max} it overestimates the deflection angle by a factor $\pi/2$.

$$
\begin{aligned}
M_{sph}(r) &= \frac{v^2 r}{G} \;\Rightarrow\; \frac{dM_{sph}}{dr} = \frac{v^2}{G} = 4\pi r^2 \rho(r) \;\Rightarrow\; \rho(r) = \frac{v^2}{4\pi G r^2} \\
\Sigma(b) &= \int_{-\infty}^{+\infty} \rho(\sqrt{b^2+l^2})dl = \frac{v^2}{4Gb} \\
M_{cyl}(b) &= \int_0^b 2\pi b' \Sigma(b')db' = \frac{\pi v^2 b}{2G} \;\Rightarrow \\
|\alpha(b)| &= \frac{4GM_{cyl}(b)}{c^2 b} = \begin{cases} 2\pi\frac{v^2}{c^2} \approx 1.29'' \; (v/300 \text{ km/s})^2 & \text{if } b \le b_{max} \\ 2\pi\frac{v^2}{c^2}\frac{b_{max}}{b} & \text{if } b > b_{max} \end{cases} \\
c\Delta t_{grav} &= \begin{cases} -2\pi\frac{v^2}{c^2} b & \text{if } b \le b_{max} \\ -2\pi\frac{v^2}{c^2}(b_{max} + \ln(b/b_{max})) & \text{if } b > b_{max} \end{cases}
\end{aligned}
$$

Since $1'' \times 1$ kpc $= 1000$ AU a ray passing 1 kpc closer to a SIS with the rotation velocity of ~ 300 km/s is delayed ~ 6 days more; 5 kpc difference in rays distances makes ~ 1 month relative delay. Days - months are typical for multiple image QSOs.

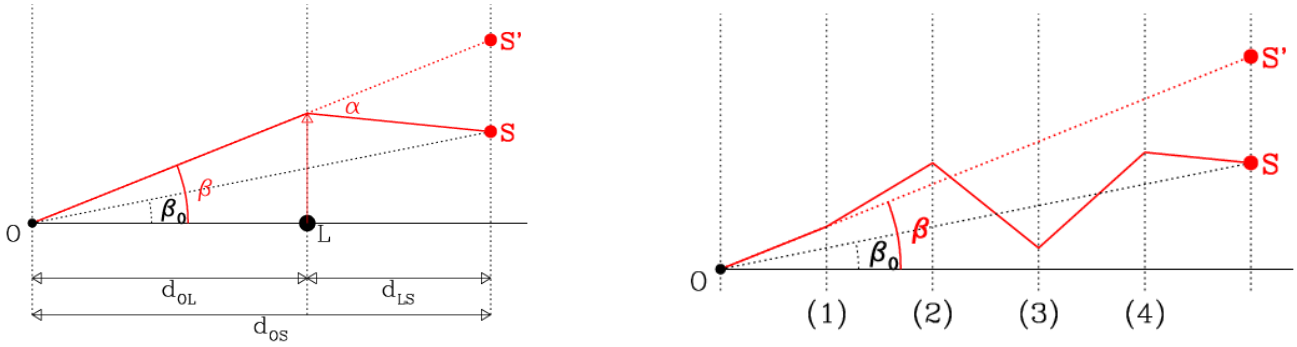

Figure 2.1: Ray paths for a single (left) and multiple (right) deflections

2.2.3 Lens equation

Here we are not interested in the deflection angle itself but in its influence on the ray trajectory; in particular what is the the position on the sky $\vec{\beta}_0$ of the source seen on the sky (after the deflection on the way) at $\vec{\beta}$. Using the graph on the left above and making some algebra we get the *lens equation*:

$$\vec{\beta}_0 = \vec{\beta} + \frac{d_{LS}}{d_{OS}}\vec{\alpha}$$

where d_{IJ} denote the distances as on the graph. Using the graph on the right we get the similar formula for multiple deflections:

$$\vec{\beta}_0 = \vec{\beta} + \sum_i \frac{d_{LS}(i)}{d_{OS}}\,\delta\vec{\alpha}(i)$$

d_{OS} is the distance between the observer and the source plane (as before) while $d_{LS}(i)$ denote the distances between the i-th deflecting layer as numbered on the graph and the source plane, $\delta\vec{\alpha}(i)$ is the deflection angle in the i-th layer.

Now we shall generalize our findings. Suppose we measure the length along the line of sight (LOS) from the observer to a source using l and l_S is the distance to the source. The Cartesian coordinates $(b'_1, b'_2, l) \equiv (\vec{b}', l)$ parametrize the the space. Everything which has any influence on rays propagating near LOS belongs to its close vicinity at positions with $|\vec{b}'| \ll l_s$ but formally we consider matter distribution in the whole space. (In reality photons taking part in Galactic microlensing pass at few AU from stellar mass lenses, while the sources lie at several kiloparsecs, some eight orders of magnitude larger. Similarly multiple QSO images are seen at kiloparsecs distances from centers of galaxies causing the phenomena, while the sources are at gigaparsecs distances, larger by five orders of magnitude.)

Anticipating cosmological applications, we consider the deflection of rays by the fluctuations in matter density $\delta\rho$ only. Since $\langle\delta\rho\rangle = 0$ the fluctuations far away from LOS cancel out (screening) and again only close vicinity of LOS plays any role, so we can formally integrate over $d_2 b$ to infinity without risking singularities.

For convenience we now replace our coordinates by the transformation $\vec{b}' = \vec{\beta}' * l$. We may think of a volume element of a density $\delta\rho$ as a point lens of mass $\delta m = \delta\rho l^2 d_2\beta' dl$ (which can be negative or positive). We use Born approximation again assuming photons move along their unperturbed trajectory, which is $\vec{b}_{ray} = \vec{\beta} * l$ in our parametrization. Now the multiple deflection

lens equation can be written as:

$$\begin{aligned}\vec{\beta}_0 &= \vec{\beta} - \int l^2 d_2\beta' \int_0^{l_S} dl\ \frac{4G\delta\rho(\vec{\beta}', l)}{c^2} \times \frac{\vec{\beta} l - \vec{\beta}' l}{|\vec{\beta} l - \vec{\beta}' l|^2} \times \frac{l_s - l}{l_s} \\ &= \vec{\beta} - \int d_2\beta' \int_0^{l_S} dl\ \frac{4G\delta\rho(\vec{\beta}', l)}{c^2} \times \frac{\vec{\beta} - \vec{\beta}'}{|\vec{\beta} - \vec{\beta}'|^2} \times \frac{l(l_s - l)}{l_s}\end{aligned}$$

where we assume that a fluctuation at $(\vec{\beta}', l)$ deflects the ray at a distance l from the observer. Inspecting the expression under the integral which depends on $\vec{\beta}$, we notice that it is equal to the gradient of $\ln|\vec{\beta} - \vec{\beta}'|$. By mathematical transformations one has:

$$\begin{aligned}\nabla_{\vec{\beta}} \ln|\vec{\beta} - \vec{\beta}'| &= \frac{\vec{\beta} - \vec{\beta}'}{|\vec{\beta} - \vec{\beta}'|^2} \quad \Rightarrow \\ \psi(\vec{\beta}) &\stackrel{def}{=} \int d_2\beta' \int_0^{l_S} dl\ \frac{4G\delta\rho(\vec{\beta}', l)}{c^2} \times \ln|\vec{\beta} - \vec{\beta}'| \times \frac{l(l_s - l)}{l_s} \quad \Rightarrow \\ \vec{\beta}_0 &= \vec{\beta} - \nabla_{\vec{\beta}}\, \psi(\vec{\beta})\end{aligned}$$

It is not explicitly shown, but again the potential is defined up to an additive constant, and introducing some reference position on the sky $\vec{\beta}_1$ and calculating $\psi(\vec{\beta}) - \psi(\vec{\beta}_1)$ one would avoid divergency. (When $|\vec{\beta}'| \to \infty$, the difference in logarithms under the integral would behave like $\sim |\vec{\beta} - \vec{\beta}_1|/|\vec{\beta}'|$. The surface area of a ring on the sky between $|\vec{\beta}'|$ and $|\vec{\beta}'| + d|\vec{\beta}'|$ is $\sim |\vec{\beta}'|$. The product of the two above factors is asymptotically constant. The averaged density fluctuation on a ring of radius $|\vec{\beta}'|$ goes to zero - question how fast. We **assume** that fast enough to make the integral finite. (In fact the same divergence problem applies to the lens equation: again the ring area is proportional to $|\vec{\beta}'|$ and the vector under the integral is inversely proportional to it, so one has to use the **assumption**.)

One does not have to use ψ itself but only its derivatives $\psi_{,a}$, $\psi_{,ab}$ which are correctly (?) defined. The indices $a, b \in \{1, 2\}$ and denote two Cartesian coordinates on a small part of the sky, β_1 and β_2. The second order derivatives are safe: now there is average density on a ring divided by its radius under the integral

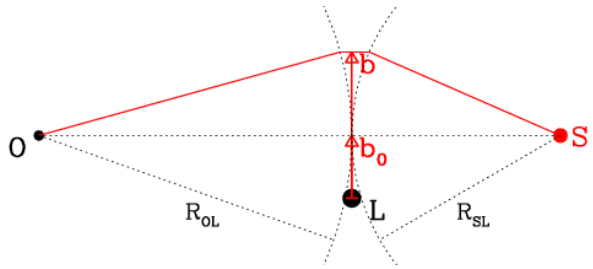

Figure 2.2: Geometric time delay

2.2.4 Fermat principle

In the figure above the ray from the source (S) to the observer (O) is drawn schematically. The spherical wave-front of the radius R_{SL} outgoing from the source is on the right, the wave-front ingoing to the observer, with radius R_{OL} is on the left relative to the lens plane. The lens (L) is some mass concentration near the lens plane of the size much smaller than R_{SL} or R_{OL}. The actual ray (red poly-line from S to O, crossing the lens plane at $\vec{b}$) is longer than the straight line passing at $\vec{b}_0$), by the length of the horizontal section between the wave fronts, which causes the *geometrical time delay*. In the lowest order one has:

$$c\Delta t_{geom} = \frac{1}{2}\frac{(\vec{b}-\vec{b}_0)^2}{R_{OL}} + \frac{1}{2}\frac{(\vec{b}-\vec{b}_0)^2}{R_{SL}} = \frac{1}{2}\frac{(\vec{b}-\vec{b}_0)^2}{D} \qquad D = \frac{R_{OL}R_{SL}}{R_{OL}+R_{SL}}$$

In the flat space the radii of curvature of the wave fronts are just the distances between S-L and L-S ($R_{OL} = d_{OL}$, $R_{SL} = d_{LS}$ in previous notation). In cosmology these equalities do not hold, but

$$\frac{1}{D} = \frac{1}{R_{OL}} + \frac{1}{R_{SL}} = \frac{d_{OS}}{d_{OL}d_{LS}}$$

is still valid. (See Sec. 2.2.8) Using angular coordinates one has:

$$c\Delta t(\vec{\beta}) = c\Delta t_{geom}(\vec{\beta}) + c\Delta t_{grav}(\vec{\beta}) = \frac{1}{2}\frac{d_{OL}^2(\vec{\beta}-\vec{\beta}_0)^2}{D} - \psi(d_{OL}\vec{\beta})$$

According to the Fermat principle rays propagate along paths of extremal length, so

$$\nabla_{\vec{\beta}} c\Delta t(\vec{\beta}) = 0 \Rightarrow \frac{d_{OL}^2}{\frac{d_{OL}d_{LS}}{d_{OS}}}(\vec{\beta}-\vec{\beta}_0) - d_{OL}\vec{\alpha} = 0 \;\Rightarrow\; \vec{\beta}_0 = \vec{\beta} + \frac{d_{LS}}{d_{OS}}\vec{\alpha}$$

As one can see the lens equation results from the Fermat principle.

2.2.5 Example: double imaged QSO modeled using a SIS lens

As an illustration we calculate the relative time delay for two images of a distant point source (e.g. QSO) seen through a SIS lens. (SIS is a zeroth order approximation to mass distribution in a galaxy with dark matter halo.)

Because SIS serves as a lens the deflection angles are equal: $|\alpha'| = |\alpha''|$. This implies equal geometric time delays for both images. The gravitational time delay depends on the distance of a

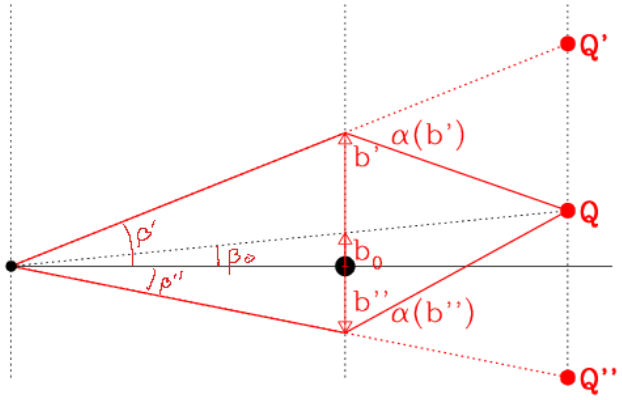

Figure 2.3: Double QSO images due to SIS lens

ray from the SIS center. Using Fig.2.3 and equations in Sec.2.2.2 we find that in the case illustrated one would have:

$$\begin{aligned} c\Delta t_{grav} &= |\alpha| \times (|b'| - |b''|) = |\alpha| \times d_{OL}(|\beta'| - |\beta''|) \\ |Q'Q''| &= d_{OS}(|\beta'| + |\beta''|) = d_{LS}(|\alpha| + |\alpha|) \\ c\Delta t_{grav} &= \frac{1}{2}\frac{d_{OS}}{d_{LS}}(|\beta'| + |\beta''|) \times d_{OL}(|\beta'| - |\beta''|) = \frac{d_{OS}d_{OL}}{2d_{LS}}\left||\beta'|^2 - |\beta''|^2\right| \\ c\Delta t_{obs} &= (1 + z_L)\, c\Delta t_{grav} \end{aligned}$$

where z_L is the lens redshift. Time delays are calculated in the lens frame (gravitational for obvious reason, geometric because the corresponding section of the poly-line in Fig. 2.2 is also in this location), so they become $1 + z_L$ times longer when measured by the observer.

In a case when the rotation velocity in of the lens (or, more frequently the velocity dispersion) is measured, the deflection angle $|\alpha|$ can be calculated. Measuring time delay and positions of the images relative to the lens center one can estimate d_{OL}. If only the position of images are known the combination of distances $d_{OS}d_{OL}/d_{LS}$ can be estimated. In both cases the result is proportional to c/H_0 times a function weakly dependent on other cosmological parameters, so effectively this is a method of measuring the Hubble constant.

2.2.6 Deformation matrix and the Kaiser - Squires algorithm

The influence of the lensing on the shape and size of images are described by the deformation matrix:

$$A_{ab} \equiv \frac{\partial \beta_0^a}{\partial \beta^b} = \delta_{ab} - \psi_{,ab}$$

which can be calculated using previous equations. If $\det ||A_{ab}|| > 0$ in the whole considered region, we say that the lensing is *weak*, $\vec{\beta}_0 \leftrightarrow \vec{\beta}$ is a one to one relation and each point of a source can have only one image. If the opposite is true, multiple images are possible. In a customary matrix notation one has:

$$A = \left|\left| \begin{array}{cc} 1 - \kappa - \gamma_1 & -\gamma_2 \\ -\gamma_2 & 1 - \kappa + \gamma 1 \end{array} \right|\right|$$

where $\kappa = (\psi_{,11} + \psi_{,22})/2$ is called *convergence* and $\gamma_1 = (\psi_{,11} - \psi_{,22})/2$, $\gamma_2 = \psi_{,12} = \psi_{,21}$ are the *shear* components.

In the following we do not use ψ itself, but only its derivatives which are well defined. We use Fourier transforms of various variables denoting them by the same symbols with tilde, and $\vec{k}$ in the Fourier space corresponds to $\vec{\beta}$.

$$\begin{aligned}
\tilde{\kappa} &= \frac{1}{2}(ik_1\tilde{\psi}_{,1} + ik_2\tilde{\psi}_{,2}) \\
\tilde{\gamma_1} &= \frac{1}{2}(ik_1\tilde{\psi}_{,1} - ik_2\tilde{\psi}_{,2}) \quad \Rightarrow \quad \tilde{\kappa} = \frac{k_1^2 - k_2^2}{k_1^2 + k_2^2}\tilde{\gamma}_1 + \frac{2k_1k_2}{k_1^2 + k_2^2}\tilde{\gamma}_2 \\
\tilde{\gamma_2} &= \frac{1}{2}(ik_1\tilde{\psi}_{,2} + ik_2\tilde{\psi}_{,1})
\end{aligned}$$

we obtain the shear - convergence relation. Assuming γ_a are measured ($\Rightarrow$ $\tilde{\gamma}_a$ are known) by using back Fourier transformation one can obtain κ. This is the idea of the Kaiser - Squires algorithm. Fourier transformations lead to:

$$\begin{aligned}
\kappa(\vec{\beta}) &= \kappa_0 + \frac{1}{\pi}\int d_2\beta' \mathcal{D}^*(\vec{\beta} - \vec{\beta}')(\gamma_1(\vec{\beta}') + i\gamma_1(\vec{\beta}')) \\
\mathcal{D}(\beta) &= \frac{\beta_1^2 - \beta_2^2 + 2i\beta_1\beta_2}{|\vec{\beta}|^4}
\end{aligned}$$

(More about the shear measurements and its implications - see the Lectures).

We go back to the expressions for the potential ψ. According to the definition of κ it is proportional to the 2D Laplacian of ψ. Using the Gauss theorem in 2D we have

$$\nabla_{\vec{\beta}} \cdot \frac{\vec{\beta} - \vec{\beta}'}{|\vec{\beta} - \vec{\beta}'|^2} = 2\pi\delta(\vec{\beta} - \vec{\beta}') \quad \Rightarrow \quad \kappa(\vec{\beta}) = \int_0^{l_S} \frac{4\pi G\delta\rho(\vec{\beta}, l)}{c^2} \frac{l(l_s - l)}{l_S} dl$$

Thus the convergence $\kappa(\vec{\beta})$ is related to the integral of matter density fluctuations (weighted by some combination of distances) along LOS. If we observe surroundings of a galaxy cluster, we may assume that the main input to the integral comes from the matter belonging to this object. In this case one has:

$$\kappa(\vec{\beta}) = \frac{4\pi G D\Sigma(\vec{\beta})}{c^2} \quad \text{where} \quad D = \frac{l_{cluster}(l_S - l_{cluster})}{l_S} = \frac{d_{OL}d_{LS}}{d_{OS}}$$

We use Σ for the surface mass density. Characteristic distance D is expressed as a combination of observer-lens, lens-source, and observer-source distances, using the actual and more general symbols.

2.2.7 Cosmological generalizations

The lens equation is based on the equalities (compare Fig. 2.1, left panel) $|SS'| = |d_{LS}\alpha| = |d_{OS}(\beta - \beta_0)|$, which shows that we are dealing wit angular diameter distances. The observer-lens and observer-source distances are just angular diameter distances as defined before. The lens-source distance requires some extra thought. As seen on the graph above, the length δl measured in the source plane can be expressed as the product of an angle α measured by an observer on the lens and the distance from the lens to source d_{LS}. The radial coordinate of the source in our

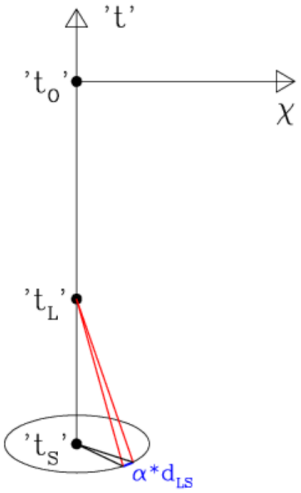

Figure 2.4: Angular diameter distance to the source measured by an observer on the lens

coordinate system is χ_{LS}, so:

$$\begin{aligned} \delta l &= a(t_L)S(\chi_{LS})\alpha = \frac{a_0}{1+z_S}S(\chi_{LS})\alpha \quad \Rightarrow \\ d_{LS} &= \frac{a_0}{1+z_S}S(\chi_{LS}) \quad \text{where} \\ \chi_{LS} &= \frac{c/H_0}{a_0}\int_{z_L}^{z_S}\frac{dz}{h(z)} \end{aligned}$$

We use the same symbols as used in the derivation of angular diameter distance. While the coordinate distances are additive ($\chi_{OS} = \chi_{OL} + \chi_{LS}$) the angular diameter distances are not ($d_{OS} \neq d_{OL} + d_{LS}$). When considering lens equation in a cosmological model one has to replace distances defined in a flat static space by angular diameter distances defined above and previously. Another corrections are necessary when considering so called *time delays* (see below?). The convergence in cosmological context is given by:

$$\kappa = \int_0^{z_S}\frac{4\pi G\delta\rho(z)}{c^2}\cdot\frac{d_{OL}d_{LS}}{d_{OS}}\underbrace{\frac{c/H_0}{(1+z)h(z)}dz}_{dl} = \frac{4\pi G a_0 c/H_0}{c^2}\int_0^{z_S}\delta\rho(z)\cdot\frac{S(\chi_{OL})S(\chi_{LS})}{S(\chi_{OS})}\frac{dz}{(1+z)^2h(z)}$$

where the integration is along LOS. In a flat model further simplifications are possible:

$$\begin{aligned} \delta\rho(z) &= \frac{\delta\rho}{\langle\rho(z)\rangle}\cdot\langle\rho(z)\rangle = \delta(z)\cdot\Omega_M\cdot\frac{3H_0^2}{8\pi G}\cdot(1+z)^3 \\ \kappa(z_S) &= \frac{3}{2}\Omega_M\int_0^{z_S}\delta(z)\cdot\frac{\chi_{OL}\chi_{LS}}{\chi_{OS}}\frac{(1+z)dz}{h(z)} \end{aligned}$$

The last form of the formula for κ is apparently dimensionless since all dimensional factors shorten out.

Suppose we observe many far away galaxies from a small redshift interval $z \in \{z_S - \Delta z/2, z_S + \Delta z/2\}$. Measuring ellipticies of individual objects and finding average ellipticies on small portions

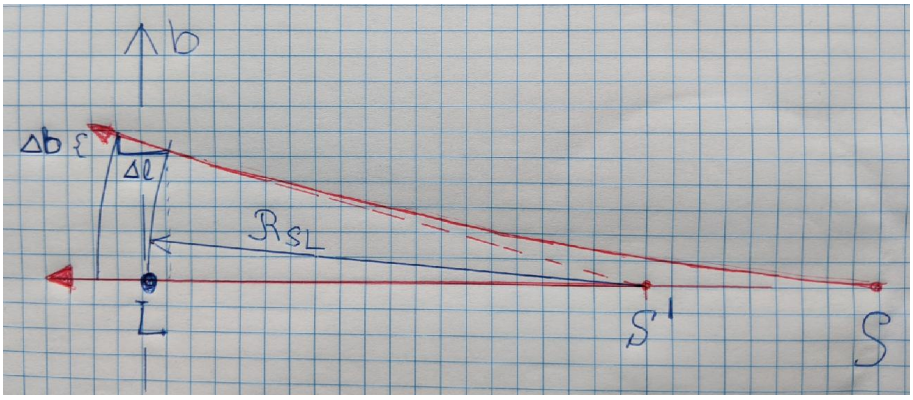

Figure 2.5: Radius of curvature of the wave outgoing from the source¿

of the sky one can estimate shear and calculate resulting $\kappa(z_S)$ using Kaiser-Squires algorithm. When repeated for several z_S one deals with *cosmic tomography*: $\kappa(z_1)$ says something about matter distribution up to z_1. The difference $\kappa(z_2) - \kappa(z_1)$ depends on matter distribution between these redshifts so we get information layer by layer.

2.2.8 Curvature radii of the wave fronts

In Fig. 2.5 two rays are drawn schematically. They are emitted from the source at angle $\Delta\alpha$ and travel toward the lens plane. The distance between the rays changes according to:

$$b(t) = a(t)S(\chi(t))\Delta\alpha \qquad \chi(t) = \int_{t_S}^{t} \frac{cdt}{a(t)}$$

where we use the same symbols as usual and previous equations. Drawing tangential lines to both rays we imagine that they propagate from a source at S', which defines the radius of curvature of the wave fronts near the lens. Using Tales theorem and expressing various quantities in (t, χ) coordinates one has:

$$\begin{aligned}
\frac{\Delta b}{\Delta l} &= \frac{b}{\mathcal{R}_{SL}} \\
\Delta b &= (\dot{a}S(\chi) + aC(\chi)\dot{\chi})c\Delta t\Delta\alpha \qquad \Delta l = a\Delta\chi = c\Delta t \\
\frac{1}{\mathcal{R}_{SL}} &= \frac{\dot{a}}{a}(t_L) + \frac{C(\chi_{LS})}{a(t_L)S(\chi_{LS})} \\
C(\chi) &= \cos\chi \quad \text{if } k=+1, \qquad 1 \quad \text{if } k=0, \qquad \cosh\chi \quad \text{if } k=-1
\end{aligned}$$

For a wave ingoing to the observer the relations are basically the same, but: the earlier ($\Rightarrow$ larger) wavefront corresponds to smaller t and larger χ, so the expression for $\mathcal{R}_{OL}$ remain similar up to the sign:

$$\begin{aligned}
\frac{1}{\mathcal{R}_{OL}} + \frac{1}{\mathcal{R}_{SL}} &= -\frac{\dot{a}}{a} + \frac{C(\chi_{OL})}{a_L S(\chi_{OL})} + \frac{\dot{a}}{a} + \frac{C(\chi_{LS})}{a_L S(\chi_{LS})} = \frac{C(\chi_{OL})S(\chi_{LS}) + S(\chi_{OL})C(\chi_L S)}{a_L S(\chi_{OL})S(\chi_{LS})} \\
&\equiv \frac{S(\chi_{OL}+\chi_{LS})}{a_L S(\chi_{OL})S(\chi_{LS})} \equiv \frac{a_S S(\chi_{OS})}{a_L S(\chi_{OL})a_S S(\chi_{LS})} \equiv \frac{d_{OS}}{d_{OL}d_{LS}} \equiv \frac{1}{D}
\end{aligned}$$

Chapter 3

Physical foundations

3.1 Cosmology and General Relativity

3.1.1 The metric

We limit ourselves to a case of uniform and isotropic space. Uniformity (all positions are equivalent, all observers are equivalent) implies the possibility of introducing *cosmic time* t i.e. synchronizing the clocks of all observers. The interval has the form:

$$ds^2 = c^2dt^2 - dl^2$$

where dl is the length interval in 3D space. There are only three possible metrics in 3D uniform and isotropic space (Mathematics!). For astronomical applications it is convenient to use a spherical coordinate system with the observer at the origin and angles corresponding to the positions on the observer's sky. In an expanding space it is also convenient to use comoving coordinates, where all objects have constant coordinate values and distances change in proportion to a scale factor. We choose the following form:

$$\begin{aligned} dl^2 &= a^2(t)\left(d\chi^2 + S^2(\chi)\left(d\theta^2 + \sin^2\theta\phi^2\right)\right) \\ S(\chi) &= \sin\chi \quad \text{if } k=+1, \qquad \chi \quad \text{if } k=0, \qquad \sinh\chi \quad \text{if } k=-1 \end{aligned}$$

where $a(t)$ is a scale factor depending on time, to be found as a solution to Einstein equations (next sections), χ plays the role of a radial coordinate, θ and ϕ are angular coordinates on the sky, k enumerates the possible geometry of space: S^3 (3D sphere, *closed model* $k=+1$), R^3 (3D flat space, *flat model* $k=0$), H^3 (3D hyperbolic (my name) space, *open model*, $k=-1$). The metric components are:

$$g_{tt} = c^2 \qquad g_{\chi\chi} = -a^2(t) \qquad g_{\theta\theta} = -a^2(t)S^2(\chi) \qquad g_{\phi\phi} = -a^2(t)S^2(\chi)\sin^2\theta$$

and all other vanish. The metric is diagonal so the coordinate system is orthogonal.

3.1.2 Covariant derivative

In a flat space with Cartesian coordinates the calculation of a derivative of a vector is simple and it is enough to calculate derivatives of all its components. We denote a unit vectors along the i-th Cartesian coordinate $\vec{e}_i$ an then for any vector $\vec{V}$ one has $\vec{V} = V^i\vec{e}_i$, where V^i are the vector

components and there is a summation over repeating indices. The derivative of $\vec{V}$ along another vector $\vec{U}$ is given as

$$\nabla_{\vec{U}}\vec{V} = U^j\nabla_j(V^i\vec{e}_i) = U^j V^i_{,j}\vec{e}_i \quad \text{and in this case:} \quad \nabla_j\vec{e}_i = 0$$

In other coordinate systems it is more complicated. Again we use some base vectors $\vec{e}_i$ which are not necessary unit vectors. One of the choices would be the requirement that the length differential can be expressed as:

$$dl^2 = \vec{e}_i\cdot\vec{e}_j\ dx^i dx^j \quad \Leftrightarrow \quad g_{ij} = \vec{e}_i\cdot\vec{e}_j$$

where x^i are the coordinates (not necessary Cartesian) and g_{ij} is the metric tensor. As a 2D example we use polar coordinates (r,ϕ) on the plane. We define base vectors according to the requirement above and use their Cartesian coordinates in calculations:

$$\begin{aligned}
\vec{e}_r &= (\cos\phi,\sin\phi) \quad \vec{e}_\phi = (-r\sin\phi, r\cos\phi) \quad dl^2 = \vec{e}_r\cdot\vec{e}_r\ dr^2 + \vec{e}_\phi\cdot\vec{e}_\phi\ d\phi^2\\
\nabla_r\vec{e}_r &= 0 \quad \nabla_r\vec{e}_\phi = (-\sin\phi,\cos\phi) = \frac{1}{r}\vec{e}_\phi\\
\nabla_\phi\vec{e}_r &= (-\sin\phi,\cos\phi) = \frac{1}{r}\vec{e}_\phi \quad \nabla_\phi\vec{e}_\phi = (-r\cos\phi,-r\sin\phi) = -r\vec{e}_r\\
\nabla_a\vec{e}_b &\equiv \Gamma^k_{ab}\vec{e}_k \quad \Gamma_{ab|c} = \Gamma^k_{ab}g_{ck} \quad \Gamma^\phi_{r\phi} = \frac{1}{r} \quad \Gamma^\phi_{\phi r} = \frac{1}{r} \quad \Gamma^r_{\phi\phi} = -r \quad \text{other vanish}
\end{aligned}$$

We have defined so called *Christoffel* symbols Γ^c_{ab} (and $\Gamma_{ab|c}$) which are coefficients to express derivative of a base vector as a sum of other base vectors. We find an equality $\Gamma^\phi_{r\phi} = \Gamma^\phi_{\phi r}$. It is not a chance, in fact $\Gamma^c_{ab} = \Gamma^c_{ba}$ is a rule. Calculating the derivative of $g_{ab} = \vec{e}_a\vec{e}_b$ and other metric components and using the symmetry of Christoffel symbols one has:

$$\begin{aligned}
\nabla_a g_{bc} &= g_{bc,a} = \Gamma^k_{ab}\vec{e}_k\vec{e}_c + \Gamma^k_{ac}\vec{e}_k\vec{e}_b = \Gamma^k_{ab}g_{kc} + \Gamma^k_{ac}g_{kb} \quad (+)\\
\nabla_b g_{ac} &= g_{ac,b} = \Gamma^k_{ab}\vec{e}_k\vec{e}_c + \Gamma^k_{bc}\vec{e}_k\vec{e}_a = \Gamma^k_{ab}g_{kc} + \Gamma^k_{bc}g_{ka} \quad (+)\\
\nabla_c g_{ab} &= g_{ab,c} = \Gamma^k_{ac}\vec{e}_k\vec{e}_b + \Gamma^k_{bc}\vec{e}_k\vec{e}_a = \Gamma^k_{ac}g_{kb} + \Gamma^k_{bc}g_{ka} \quad (-)\\
\frac{1}{2}(g_{bc,a} + g_{ac,b} - g_{ab,c}) &= \Gamma^k_{ab}\ g_{kc} \quad \Rightarrow \quad \Gamma^c_{ab} = \frac{1}{2}(g_{bk,a} + g_{ak,b} - g_{ab,k})g^{ck}
\end{aligned}$$

Finally we get the formula for Christoffel symbols. In general it may require long calculations, but in orthogonal coordinates it simplifies a lot. In the simple cases like polar coordinates it is easy to guess.

As an example we calculate the centripetal acceleration of a point mass moving on circular orbit of radius r with angular velocity ω:

$$\begin{aligned}
\vec{v} &= \dot{r}\vec{e}_r + \dot{\phi}\vec{e}\phi = \omega\vec{e}_\phi\\
\frac{d\vec{v}}{dt} &= \left(\dot{r}\nabla_r + \dot{\phi}\nabla_\phi\right)\vec{v} = \omega\nabla_\phi(\omega\vec{e}_\phi) = \omega^2\Gamma^r_{\phi\phi}\vec{e}_r = -\omega^2 r\ \vec{e}_r
\end{aligned}$$

We have obtained the standard result.

In general, we would like to know the components of the derivative of a vector. We calculate the derivative of $A^j\vec{e}_j$ along coordinate numbered b and project the result onto vector $g^{ak}\vec{e}_k$:

$$\begin{aligned}
g^{ak}\vec{e}_k\ \nabla_b\left(A^j\vec{e}_j\right) &= g^{ak}\vec{e}_k\ \left(A^j_{,b}\vec{e}_j + A^j\Gamma^l_{bj}\vec{e}_l\right) = g^{ak}g_{kj}A^j_{,b} + g^{ak}g_{kl}A^j\Gamma^l_{bj}\\
&= \delta^a_j A^j_{,b} + \delta^a_l A^j\Gamma^l_{bj} = A^a_{,b} + \Gamma^a_{bc}A^c
\end{aligned}$$

or in short:

$$\nabla_b A^a = A^a_{,b} + \Gamma^a_{bc} A^c \qquad \nabla_b (A^j A_j) = A_j A^j, b + A^j A_{j,b} \quad \Rightarrow \quad \nabla_b A_a = A_{a,b} - \Gamma^c_{ab} A_c$$

The formulae above define the covariant derivative of a vector. For tensors one would have

$$\nabla_c \, T^{ab} = T^{ab}_{,c} + \Gamma^a_{cj} T^{jb} + \Gamma^b_{cj} T^{aj}$$

and similarly for higher dimension tensors.

Another example: covariant derivative of a uniform field $\vec{B} = B\vec{e}_x$ calculated in polar coordinates. (B is a constant, so $\vec{B}$ given in Cartesian coordinates is apparently constant.) The calculation is a bit more complicated as compared to centripetal acceleration but elementary:

$$\begin{aligned}
B^x &= B \qquad B^y = 0 \qquad B^r = \frac{\partial r}{\partial x} B^x + \frac{\partial r}{\partial y} B^y = B\cos\phi \qquad B^\phi = \frac{\partial \phi}{\partial x} B^x + \frac{\partial \phi}{\partial y} B^y = -B\frac{\sin\phi}{r} \\
\nabla_r B^r &= B^r_{,r} + \Gamma^r{}_{r\alpha} B^\alpha = 0 + 0 = 0 \\
\nabla_r B^\phi &= B^\phi_{,r} + \Gamma^\phi{}_{r\alpha} B^\alpha = +B\frac{\sin\phi}{r^2} + \Gamma^\phi{}_{r\alpha} B^\alpha = +B\frac{\sin\phi}{r^2} - B\frac{\sin\phi}{r^2} = 0 \\
\nabla_\phi B^r &= B^r_{,\phi} + \Gamma^r{}_{\phi\alpha} B^\alpha = -B\sin\phi - r\left(-B\frac{\sin\phi}{r}\right) = 0 \\
\nabla_\phi B^\phi &= B^\phi_{,\phi} + \Gamma^\phi{}_{\phi\alpha} B^\alpha = -B\frac{\cos\phi}{r} + \frac{1}{r} B\cos\phi = 0
\end{aligned}$$

As one can see the covariant derivatives calculated in polar coordinates all vanish, as expected. The nonvanishing partial derivatives of the vector polar components are compensated by derivatives of base vectors in polar system (expressed via Christoffel symbols).

3.1.3 Geodesic line

A trajectory in a system of coordinates $\{x^a\}$ can be described as $x^a(\lambda)$, where λ is a parameter. Using the length along the trajectory as a parameter ($d\lambda^2 = g_{ab} dx^a dx^b$) we have a unit vector tangential to the trajectory:

$$\vec{n} = \frac{dx^a}{d\lambda} \, \vec{e}_a \qquad n^a = \frac{dx^a}{d\lambda} \qquad \vec{n} \cdot \vec{n} = g_{ab} \frac{dx^a}{d\lambda} \frac{dx^b}{d\lambda} = 1$$

In a flat space vectors tangential to a straight line in any point are parallel to each other. Requirement that two vectors tangential to a curve in two points close to each other in any space be parallel to each other is a similar condition. Curves fulfilling the requirement are geodesic lines which generalize the concept of a straight line.

The mathematical condition is that the covariant derivative of the tangent vector along the tangent vector should vanish. It leads to:

$$\begin{aligned}
\frac{d}{d\lambda} &= \frac{dx^a}{d\lambda} \nabla_a \equiv n^a \nabla_a \\
0 &= n^b \nabla_b n^a = \frac{dx^b}{d\lambda} \left(\partial_b \frac{dx^a}{d\lambda} + \Gamma^a_{bc} \frac{dx^c}{d\lambda} \right) = \frac{dx^b}{d\lambda} \partial_b \left(\frac{dx^a}{d\lambda} \right) + \Gamma^a_{bc} \frac{dx^b}{d\lambda} \frac{dx^c}{d\lambda} \\
0 &= \frac{d^2 x^a}{d\lambda^2} + \Gamma^a_{bc} \frac{dx^b}{d\lambda} \frac{dx^c}{d\lambda}
\end{aligned}$$

which is the geodesic equation.

3.1.4 Riemann and Ricci tensors

The order of covariant derivatives (as opposed to partial derivatives) may affect the result. Below we check this:

$$\begin{aligned}
\nabla_c\nabla_d A^a &= \nabla_c(\nabla_d A^a) = \partial_c(\nabla_d A^a) + \Gamma^a_{cj}(\nabla_d A^j) - \Gamma^j_{cd}(\nabla_j A^a) \\
&= A^a_{,dc} + \Gamma^a_{dj,c}A^j + \Gamma^a_{dj}A^j_{,c} + \Gamma^a_{cj}(A^j_{,d} + \Gamma^j_{dk}A^k) - \Gamma^j_{cd}(\nabla_j A^a) \\
&= A^a_{,dc} + \Gamma^a_{dj,c}A^j + \Gamma^a_{dj}A^j_{,c} + \Gamma^a_{cj}A^j_{,d} + \Gamma^a_{cj}\Gamma^j_{dk}A^k - \Gamma^j_{cd}(\nabla_j A^a) \quad |+ \\
\nabla_d\nabla_c A^a &= \nabla_d(\nabla_c A^a) \\
&= A^a_{,cd} + \Gamma^a_{cj,d}A^j + \Gamma^a_{cj}A^j_{,d} + \Gamma^a_{dj}A^j_{,c} + \Gamma^a_{dj}\Gamma^j_{ck}A^k - \Gamma^j_{dc}(\nabla_j A^a) \quad |- \\
(\nabla_c\nabla_d - \nabla_d\nabla_c)A^a &= \left(\Gamma^a_{db,c} - \Gamma^a_{cb,d} + \Gamma^a_{cj}\Gamma^j_{db} - \Gamma^a_{dj}\Gamma^j_{cb}\right)A^b \equiv R^a_{bcd}A^b
\end{aligned}$$

where R^a_{bcd} is the **Riemann tensor**, given by the formal definition.

To get some geometrical intuition we ask what would be the result of the so called *parallel transport* of a vector around a closed poly-line made of caustics segments. The requirement that a vector A^a should remain parallel to itself after a little move along a geodesic with a tangent vector $\vec{n}$ is $\nabla_{\vec{n}}A^a = 0$ or:

$$\begin{aligned}
\frac{dx^c}{d\lambda}\nabla_c A^a &= 0 \;\Rightarrow\; \frac{dx^c}{d\lambda}A^a_{,c} = -\Gamma^a_{cb}A^b\frac{dx^c}{d\lambda} \;\Rightarrow \\
\Delta A^a &= \oint_{\partial S} A^a_{,c}dx^c = -\oint_{\partial S}\Gamma^a_{cb}A^b dx^c \\
&= -\int_S \left((\Gamma^a_{cb}A^b),d - (\Gamma^a_{db}A^b),c\right)dx^c dx^d
\end{aligned}$$

where we have used the Stokes theorem. When differentiating under the integral we use the condition of parallel transport again and we replace partial derivatives of A^b by expressions containing Christoffel symbols which gives:

$$\Delta A^a = -\int_S \left(\Gamma^a_{cb,d} - \Gamma^a_{db,c} - \Gamma^a_{cj}\Gamma^j_{db} + \Gamma^a_{cj}\Gamma^j_{db}\right)A^b dx^c dx^d = +\int_S R^a_{bcd}A^b dx^c dx^d$$

Thus the effect of a parallel transport of a vector around a closed curve can be expressed as the integral over the surface surrounded by the curve of the product of the vector and the Riemann tensor.

Suppose the closed contour is an infinitesimal geodesic triangle. Vectors v^c and w^d are tangent to the two triangle sides at the same vertex. The lengths of the sides are proportional to the lengths of the respective vectors. (The third side is just a geodesic line joining the other vertexes.) The parallel transport of A^a around the triangle changes it by:

$$\Delta A^a = R^a{}_{bcd}A^b v^c w^d$$

The Riemann tensor has many symmetries. They are easier to discuss with the form $R_{abij} \equiv g_{ac}R^c{}_{bij}$. The parallel transport does not change the length of a transported vector but only its direction. Thus the first two indices of the Riemann tensor correspond to the rotation of the vector, so we expect asymmetry in this pair. The vectors v^c and w^d define the surface area of the triangle, their order defines the orientation of the figure so again we expect asymmetry in second pair of the indices. These asymmetries and the symmetry when we exchange the first pair of indices with

the second can be directly checked using the definition of $R^a{}_{bcd}$. Still another identity (with the permutation of three indices) also can be proved with the definition. We show the identities:

$$R_{abij} = +R_{ijab} = -R_{baij} = -R_{abji} = +R_{baji}$$

$$R_{aijk} + R_{ajki} + R_{akij} = 0$$

In general a fourth order tensor in 4D can have $4^4 = 256$ independent components. Asymmetries in the pairs of indices would leave only 6x6 indepemdent values. Symmetry of exchanging the pairs with each other makes the 6x6 object symmetric, so there are only 21 independent components and finally the last identity lowers it to 20. Thus the Riemann tensor in 4D has 20 independent components. By checking the definition one obtains *Bianchi identity*:

$$\nabla_i R^a{}_{bjk} + \nabla_j R^a{}_{bki} + \nabla_k R^a{}_{bij} = 0$$

The Riemann tensor contains the whole local information about the space-time curvature. Algebraic classification of its form gives several classes, but we are not going to pursue this topic.

The **Ricci tensor** R_{ab} is defined as a "trace" of the Riemann tensor and the **curvature scalar** R as a trace of the Ricci tensor:

$$R_{ab} = R^i{}_{aib} \qquad R^a{}_b = g^{ai} R_{ib} \qquad R = R^i{}_i$$

Using Bianchi identity one can show that

$$\nabla_a R^a{}_b = \frac{1}{2} \nabla_b R \quad \Leftrightarrow \quad \nabla_a \left(R^a{}_b - \frac{1}{2} R \delta^a{}_b \right) = 0$$

(The expression in parenthesis is the LHS of the Einstein equations see Sec. 3.1.6.)

3.1.5 Geodesic deviation

The term *geodesic deviation* in the simplest case has to do with the relative acceleration of test particles moving on two geodesic lines. (In general case of abstract curved spaces it may not be the case). In Newtonian dynamics free particles move along straight trajectories without any acceleration, so the relative acceleration of two of them is zero. Now imagine two test particles starting at the pole of a 2D sphere and moving with the same constant velocity v along meridians with small difference in "geographic" longitude $\delta\phi$. Let the radius of the sphere be R and θ measures the angle from the pole. The distance between particles δr and its time derivatives are:

$$\begin{aligned} \delta r &= R \sin\theta \delta\phi \qquad \theta = \frac{vt}{R} \\ \frac{d\delta r}{dt} &= v \cos\theta \delta\phi \\ \frac{d^2\delta r}{dt^2} &= -\frac{v^2}{R} \sin\theta \delta\phi \end{aligned}$$

From the 3D perspective we recover the formula for centripetal acceleration and the projection of its difference onto the sphere surface. From the 2D perspective (of observes living in a curved space-time) we see the relative acceleration of two free particles.

In Newtonian dynamics the relative acceleration of particles moving close to each other may be caused by gravitational tidal forces. In GR gravity is described "by the geometry of space-time" and there are no gravity forces, fields etc. We shall now calculate the eefect in GR.

Points $x^a(\lambda,\eta)$ belong to a 2D surface. For a given η the line $x^a(\lambda,\eta=\text{const})$ is a geodesic line. We define:

$$n^a = \frac{\partial x^a}{\partial \lambda} \qquad v^a = \frac{\partial x^a}{\partial \eta}$$

where n^a is a vector tangential to the geodesic going through the point x^a and v^a measures the distance to another geodesic. (It is safe to think of it as infinitesimally close). For the covariant derivatives in this case one has:

$$\underline{n^i\nabla_i v^a} = \frac{\partial^2 x^a}{\partial\eta\partial\lambda} + \Gamma^a_{ij} n^i v^j = \frac{\partial^2 x^a}{\partial\lambda\partial\eta} + \Gamma^a_{ij} v^i n^j = \underline{v^i\nabla_i n^a}$$

an identity. Now we calculate the second derivative of v^a along the geodesic, which plays the role of the relative acceleration. We use underlines in places where we apply the identity

$$\begin{aligned}
n^i\nabla_i n^j\nabla_j v^a =& n^i\nabla_i(\underline{n^j\nabla_j v^a}) = n^i\nabla_i(\underline{v^j\nabla_j n^a}) \\
=& \underline{n^i\nabla_i(v^j)}\nabla_j n^a + n^i v^j\nabla_i\nabla_j n^a \\
=& \underline{v^i\nabla_i(n^j)}\nabla_j n^a + n^i v^j\nabla_i\nabla_j n^a \\
=& v^i\nabla_i(\underbrace{n^j\nabla_j n^a}_{0}) - v^i n^j\nabla_i\nabla_j n^a + n^i v^j\nabla_i\nabla_j n^a \\
=& 0 + v^i n^j(\nabla_i\nabla_j - \nabla_j\nabla_i)n^a \\
n^i\nabla_i n^j\nabla_j v^a =& R^a_{bij} n^b v^i n^j
\end{aligned}$$

which is the geodesic deviation equation.

In the most obvious application geodesics belong to particles moving slowly (due to small perturbations?) in the frame of our comoving coordinates. Then $n^a = u^a \approx \delta^a_0$ where u^a is the four-velocity. Since our result is due to a geometric effect of a curved space-time, in GR we may interpret it as the action of gravity and name it (relative) gravitational acceleration g^a:

$$g^a = R^a{}_{bij}\delta^b_0 v^i \delta^j_0 = R^a{}_{0i0} v^i$$

where v^i gives the direction and distance to the other particle which relative acceleration is measured.

In our case of isotropic and uniform metric with orthogonal coordinates we may examine three acceleration components using $v^i = \Delta x^\alpha \delta^i_\alpha$ where Δx^α is a small number and $\alpha \in \{\chi,\theta,\phi\}$. Examining the components of the Riemann tensor we get the components of acceleration:

$$\Delta g^\chi = R^\chi{}_{0\chi0}\Delta\chi \qquad \Delta g^\theta = R^\theta{}_{0\theta0}\Delta\theta \qquad \Delta g^\phi = R^\phi{}_{0\phi0}\Delta\phi$$

We use Δg^α to stress that we consider relative acceleration between test particles at an infinitesimal distance. $R^\beta{}_{0\alpha0} \neq 0$ only if $\alpha=\beta$, so each component of acceleration is defined by only one component of the Riemann tensor. Using finite diffrences wa get the divergence of the acceleration vector

$$\begin{aligned}
\sum \frac{\Delta g^\alpha}{\Delta x^\alpha} &= R^\chi{}_{0\chi0} + R^\theta{}_{0\theta0} + R^\phi{}_{0\phi0} \equiv R_{00} \\
&= -3\frac{\ddot{a}}{a} \quad \text{in our metric} \\
&= +\frac{4\pi G}{c^2}(\epsilon + 3P) \quad \text{our metric and Einstein equations}
\end{aligned}$$

where R_{00} stands for a component of the Ricci tensor introduced with the Einstein equations in Sec. 3.1.6.

3.1.6 Einstein equations

The Ricci tensor components are obtained as sums of some Riemann tensor components (not all take part):

$$R_{ab} = R^{i}{}_{aib} \qquad R_{ab} = R_{ba}$$

which is symmetric due to the Riemann tensor $R_{abij} = R_{ijab}$ symmetry. The scalar of curvature:

$$R = g^{ab} R_{ab}$$

In theoretical physics the field equations may follow the introduction of action S. In GR it contains the gravity and matter parts:

$$S = S_g + S_m = \int \left(\frac{c^4}{16\pi G} R + \mathcal{L}_m \right) \sqrt{-g} d_4 x$$

which is a 4D volume integral on the whole space-time, R is the curvature scalar and $\mathcal{L}$ - matter Lagrangian density. Applying variational principle, $\delta S = 0$ one arrives after complicated calculations, which we are not following, at:

$$R_{ab} - \frac{1}{2} g_{ab} R = \frac{8\pi G}{c^4} T_{ab}$$

which are the Einstein equations. The symbols in the LHS are already defined, T_{ab} is the energy-momentum tensor. In the simplest case (ideal fluid) it describes the distribution of the energy density, pressure and velocity of matter. The Einstein equations are general, though, and it is a'priori not known what can be the geometry of space-time and which matter distribution would match it. The physical space-time should locally allow for the Special Relativity, so in each point there should exist a tangent flat space equivalent to Minkowski space-time.

There is no general solution to the Einstein equations. The known *exact solutions* have been obtained with postulated high symmetry of the space-time (homogenity, isotropy, spherical symmetry, cylindrical symmetry, staticity, stationarity and other which may have no obvious interpretation). The equations are nonlinear, contain components of the metric tensor, its first, and second partial derivatives combined. On the other hand it is possible (since 2000, say) to start from a simple matter distribution in an almost flat space (e.g. two compact bodies orbitting their center of mass radiating GW) and follow their evolution up to the final stages using *numerical relativity*.

In cosmology we are happy to use homogenoues and isotropic models (in zeroth order approximation), which implies a simple form of the metric and a simple set of equations. The next order approximation - the small perturbations to the metric and matter distribution - do not pose either fundamental GR problems, nor the numerical problems from the point of view of finding algorithms, but are demanding very high data volume and computational resources.

3.1.7 Friedman space-time: calcuation details

Here, up to the introduction of Friedman equations, we use a variable $x_0 \equiv ct$, so for any scalar X one has $\partial X / \partial(ct) = \dot{X}$. Our coordinate system consists now of $(x^0, \chi, \theta, \phi)$. Writing down formulae explicitly:

$$ds^2 = (dx^0)^2 - a^2(x^0) \left(d\chi^2 + S^2(\chi) \left(d\theta^2 + \sin^2\theta d\phi^2 \right) \right)$$

$$\vec{e}_0 = (1,0,0,0) \quad \vec{e}_\chi = (0,a,0,0) \quad \vec{e}_\theta = (0,0,aS(\chi),0) \quad \vec{e}_\phi = (0,0,0,aS(\chi)\sin\theta)$$

where

$$\begin{aligned} S(\chi) &= \sin\chi & C(\chi) &= \cos\chi & k &= +1 \\ S(\chi) &= \chi & C(\chi) &= 1 & k &= 0 \\ S(\chi) &= \sinh\chi & C(\chi) &= \cosh\chi & k &= -1 \end{aligned}$$

The Christoffel symbols are defined by derivatives of metric components. Only three of them depend on any variable, so $\Gamma_{ab|c}$ must contain a pair of χ, θ, or ϕ subscripts. Since metric is diagonal, $\Gamma^c{}_{ab}$ also posses this property. So we have:

$$\begin{aligned} \Gamma^0_{\chi\chi} &= a\dot{a} \quad \Gamma^\chi_{0\chi} = \frac{\dot{a}}{a} \\ \Gamma^0_{\theta\theta} &= a\dot{a}S^2 \quad \Gamma^\theta_{0\theta} = \frac{\dot{a}}{a} \quad \Gamma^\chi_{\theta\theta} = -SC \quad \Gamma^\theta_{\chi\theta} = \frac{C}{S} \\ \Gamma^0_{\phi\phi} &= a\dot{a}S^2\sin^2\theta \quad \Gamma^\phi_{0\phi} = \frac{\dot{a}}{a} \quad \Gamma^\chi_{\phi\phi} = -SC\sin^2\theta \\ \Gamma^\phi_{\chi\phi} &= \frac{C}{S} \quad \Gamma^\theta_{\phi\phi} = -\sin\theta\cos\theta \quad \Gamma^\phi_{\theta\phi} = \frac{\cos\theta}{\sin\theta} \end{aligned}$$

and other vanish. Using the definition we calculate the Riemann tensor components which we need for the calculation of the Ricci tensor. We omit the repeating results. The components of the Ricci tensor with mixed indices have the same dimensions ($1/\text{length}^2$) so we use them as well:

$$\begin{aligned} R^\chi{}_{0\chi0} &= R^\theta{}_{0\theta0} = R^\phi{}_{0\phi0} = -\frac{\ddot{a}}{a} \quad R_{00} = -3\frac{\ddot{a}}{a} \quad R^0{}_0 = -3\frac{\ddot{a}}{a} \\ R^0{}_{\chi0\chi} &= a\ddot{a} \quad R^\theta{}_{\chi\theta\chi} = \dot{a}^2 + k \quad R^\phi{}_{\chi\phi\chi} = \dot{a}^2 + k \\ R_{\chi\chi} &= R^i{}_{\chi i\chi} = a\ddot{a} + 2\dot{a}^2 + 2k \quad R^\chi{}_\chi = -\frac{\ddot{a}}{a} - 2\frac{\dot{a}^2}{a} - 2\frac{k}{a^2} \\ R^\theta{}_\theta &= R^\phi{}_\phi = R^\chi{}_\chi \\ R &= R^i{}_i = -6\left(\frac{\ddot{a}}{a} + \frac{\dot{a}^2}{a^2} + \frac{k}{a^2}\right) \end{aligned}$$

The LHS of the Einstein equations (a.k.a. as the Einstein tensor) read:

$$\begin{aligned} R^0{}_0 - \frac{1}{2}R\delta^0_0 &= 3\frac{\dot{a}^2}{a^2} + 3\frac{k}{a^2} \\ R^\chi{}_\chi - \frac{1}{2}R\delta^\chi_\chi &= 2\frac{\ddot{a}}{a} + \frac{\dot{a}^2}{a^2} + \frac{k}{a^2} \\ R^\theta{}_\theta - \frac{1}{2}R\delta^\theta_\theta &= 2\frac{\ddot{a}}{a} + \frac{\dot{a}^2}{a^2} + \frac{k}{a^2} \\ R^\phi{}_\phi - \frac{1}{2}R\delta^\phi_\phi &= 2\frac{\ddot{a}}{a} + \frac{\dot{a}^2}{a^2} + \frac{k}{a^2} \end{aligned}$$

Other components vanish automatically.

Energy-momentum tensor The space is filled with an ideal gas of energy density ϵ, pressure P and four-velocity u^a. (Since it is *ideal* there is no friction or stress, which would require more terms.) The tensor has the form:

$$T^a_b = (\epsilon + P)u^a u_b - P\delta^a_b \tag{3.1}$$

$T^0_{\ 0}$ is the energy density (including internal energy), $T^0_{\ \alpha}$ is the energy flux (α being one of spatial coordinates), and $T^\alpha_{\ \beta}$ stand for the pressure, including the dynamical pressure. In a comoving coordinate system ($u^a = \delta^a_{\ 0}$) the tensor has a simlified form $T^0_{\ 0} = \epsilon$, $T^\chi_{\ \chi} = T^\theta_{\ \theta} = T^\phi_{\ \phi} = -P$. We return to the cosmic time as an independent variable, so we multiply the equations by c^2 factor. the dot stands for time derivative now ($\dot{a} = da/dt$). The Einstein equations take the form:

$$\begin{aligned} 3\frac{\dot{a}^2}{a^2} + 3\frac{kc^2}{a^2} &= +\frac{8\pi G}{c^2}\epsilon \\ 2\frac{\ddot{a}}{a} + \frac{\dot{a}^2}{a^2} + \frac{kc^2}{a^2} &= -\frac{8\pi G}{c^2}P \end{aligned}$$

The other equations on the diagonal of the Einstein tensor are identical to the second one and off-diagonal are trivial (of the $0 = 0$ kind). Little manipulation gives the standard form:

$$\begin{aligned} \frac{\dot{a}^2}{a^2} + \frac{kc^2}{a^2} &= +\frac{8\pi G}{3c^2}\epsilon \\ \frac{\ddot{a}}{a} &= -\frac{4\pi G}{3c^2}(\epsilon + 3P) \end{aligned}$$

Cosmological constant In general the equations with the so called *cosmological term* have the form

$$R^a_b - \frac{1}{2}R\delta^a_b = \frac{8\pi G}{c^4}T^a_b + \Lambda\delta^a_b$$

or:

$$\begin{aligned} \frac{\dot{a}^2}{a^2} + \frac{kc^2}{a^2} &= +\frac{8\pi G}{3c^2}\epsilon + \frac{1}{3}\Lambda c^2 \\ \frac{\ddot{a}}{a} &= -\frac{4\pi G}{3c^2}(\epsilon + 3P) + \frac{1}{3}\Lambda c^2 \end{aligned}$$

where Λ is the cosmological constant. Assuming that the cosmological term represents a vacuum field with the energy density $\epsilon_\Lambda = +\frac{c^4}{8\pi G}\Lambda$ and the pressure $P_\Lambda = -\frac{c^4}{8\pi G}\Lambda$ one gets:

$$\begin{aligned} \frac{\dot{a}^2}{a^2} + \frac{kc^2}{a^2} &= +\frac{8\pi G}{3c^2}(\epsilon_M + \epsilon_\Lambda) \\ \frac{\ddot{a}}{a} &= -\frac{4\pi G}{3c^2}(\epsilon_M + 3P_M + \epsilon_\Lambda + 3P_\Lambda) \\ &= -\frac{4\pi G}{3c^4}(\epsilon_M + 3P_M - 2\epsilon_\Lambda) \end{aligned}$$

where the subscript $_M$ stands for "matter". If $P_M = 0$ and $\epsilon_\Lambda > \frac{1}{2}\epsilon_M$ we have a positive RHS of the second equation corresponding to an accelerated expansion of the Universe. (Nobel 2011 for an observational confirmation of this fact.)

3.1.8 History: the static Universe of Einstein

The cosmological term was introduced by Einstein to allow static solution his equations for a uniform and isotropic metric. At the time (circa 1915) the expansion of the Universe was not known, so the static model was plausible.

Static means time derivatives in the EE should vanish automatically. We are also assuming that matter is cold ($\rightarrow \epsilon = \rho c^2 \;\; P = 0$), which is observed in the present epoch. Thus the EE with Lambda read:

$$\begin{aligned} \frac{kc^2}{a^2} &= + \frac{8\pi G}{3}\rho + \frac{1}{3}\Lambda c^2 \\ 0 &= - \frac{4\pi G}{3}\rho + \frac{1}{3}\Lambda c^2 \end{aligned}$$

These are two equations with unknowns $\{k, a, \rho, \Lambda\}$ Eliminating ρ one gets

$$\frac{kc^2}{a^2} = \Lambda c^2 \quad \Rightarrow \quad k = +1 \quad \Lambda = \frac{1}{a^2}$$

which means that the static model is closed (i.e. 3D space is a 3D sphere). The cosmological constant and the radius of curvature are simply related. Postulating $a = c/H_0$ would give $\rho = H_0^2/4\pi G = \rho_c/1.5$ in today's notation.

3.2 Weak field limit

We are going to check whether GR becomes the Newtonian dynamics in the limit of small velocities and weak fields. We expect only small (first order) differences of the metric tensor as compared to Minkowski form. Thus the Christoffel symbols are small quantities of the firs order or higher. Four-velocity and the geodesic equation take form:

$$\begin{aligned} u^a &= \left(1, \frac{\delta\vec{v}}{c}\right) \qquad \frac{|\delta\vec{v}|}{c} \ll 1 \\ \frac{d}{dct}&\left(\frac{\delta v^\alpha}{c}\right) + \Gamma^\alpha_{\;bc} u^b u^c = 0 \end{aligned}$$

where $\alpha \in \{x, y, z\}$ and $cdt \approx ds$. Since Γ^α_{bc} are small quantities only u^0 (which is not small) in places of u^b, u^c can make first expressions. Thus:

$$\begin{aligned} \Gamma^\alpha_{\;00} \approx g^{\alpha\alpha}\Gamma_{00|\alpha} &= (-1) * (-\frac{1}{2} g_{00,\alpha}) \\ \frac{1}{c^2}\frac{d\delta v^\alpha}{dt} &+ \frac{1}{2} g_{00,\alpha} = 0 \\ \frac{d\delta v^\alpha}{dt} = -\nabla_\alpha \delta\phi \;\; &\Rightarrow \quad g_{00} = 1 + 2\frac{\delta\phi}{c^2} \end{aligned}$$

We have found the form of g_{00} in the weak field approximation, where $\delta\phi$ is the Newtonian potential. Other components of the metric do not apper here and it is not so easy to find them.

We are checking the implications of postulating the followin form of the metric:

$$g_{00} = 1 + 2\delta\psi \qquad g_{xx} = g_{yy} = g_{zz} = -1 + 2\delta\psi$$

where $|\delta\psi| \ll 1$ is a function and other metric components vanish. Metric is diagonal, so only the Christoffel symbols with at least two identical indices do not vanish automatically:

$$\begin{aligned} &\Gamma^0_{\;00} = + \dot{\delta\psi} \quad \Gamma^\alpha_{\;00} = +\delta\psi_{,\alpha} \quad \Gamma^0_{\;0\alpha} = +\delta\psi_{,\alpha} \\ &\Gamma^\alpha_{\;\alpha 0} = - \dot{\delta\psi} \quad \Gamma^0_{\;\alpha\alpha} = -\dot{\delta\psi} \\ &\Gamma^\alpha_{\;\alpha\alpha} = - \delta\psi_{,\alpha} \quad \Gamma^\alpha_{\;\alpha\beta} = -\delta\psi_{,\beta} \quad \Gamma^\beta_{\;\alpha\alpha} = +\delta\psi_{,\beta} \end{aligned}$$

(Assuming $\alpha \neq \beta$ in the above notation.) Products of two Christoffel symbols are of the second or higher order so we neglect them. For the interesting Riemann and Ricci tensors components we get:

$$\begin{aligned}
R^{\alpha}{}_{0\alpha 0} &= +\Gamma^{\alpha}{}_{00,\alpha} - \Gamma^{\alpha}{}_{0\alpha,0} = \delta\psi_{,\alpha\alpha} + \delta\ddot{\psi} \\
R_{00} &= +\triangle\delta\psi + 3\delta\ddot{\psi} = +R^{0}{}_{0} \\
R^{0}{}_{\alpha 0\alpha} &= -R^{\alpha}{}_{0\alpha 0} = -\delta\psi_{,\alpha\alpha} - \delta\ddot{\psi} \\
R^{\beta}{}_{\alpha\beta\alpha} &= +\Gamma^{\beta}{}_{\alpha\alpha,\beta} - \Gamma^{\beta}{}_{\alpha\beta,\alpha} = +\delta\psi_{,\beta\beta} + \delta\psi_{,\alpha\alpha} \\
R_{\alpha\alpha} &= +\triangle\delta\psi - \delta\ddot{\psi} = -R^{\alpha}{}_{\alpha} \\
R &= -2\triangle\delta\psi + 6\delta\ddot{\psi}
\end{aligned}$$

and for the Einstein tensor:

$$R^{0}{}_{0} - \frac{1}{2}R\delta^{0}{}_{0} = +2\triangle\delta\psi \qquad R^{\alpha}{}_{\alpha} - \frac{1}{2}R\delta^{\alpha}{}_{\alpha} = -2\delta\ddot{\psi}$$

In our approach we assume the LHS of the Einstein equations, expressed as derivatives of the potential $\delta\psi \equiv \phi/c^2$ are "small". By the same argument matter density is also small, and multiplied by velocity gives terms of higher order. We also assume that the pressure is negligible ($\delta P = 0$). The Einstein equations have the following form and consequences:

$$\begin{aligned}
T^{0}{}_{0} &= \delta\rho c^2 \qquad T^{\alpha}{}_{\alpha} = 0 \\
R^{0}{}_{0} &= \frac{8\pi G}{c^4}T^{0}{}_{0} \qquad \frac{2}{c^2}\triangle\delta\phi = \frac{8\pi G}{c^2}\delta\rho \\
R^{\alpha}{}_{\alpha} &= \frac{8\pi G}{c^4}T^{\alpha}{}_{\alpha} \qquad \frac{2}{c^2}\delta\ddot{\phi} = 0 \\
\triangle\delta\phi &= 4\pi G\delta\rho \qquad \delta\ddot{\phi} = 0
\end{aligned}$$

We have obtained the Poisson equation for the gravitational potential. The other equation (vanishing of the second time derivative of the potential) results from our approximations: low velocities imply slow changes of the potential (due to the slow changes in matter distribution) which means that the time derivatives are much smaller than the spatial derivatives, so the former are neglected. (At any time the potential is given by the density distribution through the Poisson equation. It changes due to the evolution of the matter distribution, its time derivatives are not used to define its future state.)

We may also use a different argument for the form of energy-momentum tensor, assuming the coordinate system is comoving to the zeroth order. Then the off-diagonal energy momentum components are of the higher order but the pressure perturbation can be of the same order as the energy density perturbation. Calculations give the following results. In Sec. 3.1.5 we have introduced relative gravitational acceleration (here symbol $\delta\vec{g}$). We get a generalization of the Poisson equation in the case of (possibly) relativistic fluid:

$$\begin{aligned}
R_{00} &= \frac{8\pi G}{c^4}\left(T_{00} - \frac{1}{2}Tg_{00}\right) \\
T &= T^{0}{}_{0} + T^{x}{}_{x} + T^{y}{}_{y} + T^{z}{}_{z} = \delta\epsilon - 3\delta P \\
R_{00} &= \frac{8\pi G}{c^4}\left(\delta\epsilon - \frac{1}{2}(\delta\epsilon - 3\delta P)\right) \\
\triangle\phi &= -\nabla\cdot\delta\vec{g} = \frac{4\pi G}{c^2}(\delta\epsilon + 3\delta P)
\end{aligned}$$

Chapter 4

Gravitational instability of cosmological models

4.1 Equations of hydrodynamics

In the Euler's approach we have a static coordinate system $(t, \vec{r})$ and all quantities describing matter, its motion, acting forces etc depend on these variables. The forces act on matter, not on the place it is located in, so the time derivative should follow the matter element and it is called the matter derivative:

$$\frac{D}{dt} \equiv \frac{\partial}{\partial t} + \vec{v} \cdot \nabla \tag{4.1}$$

where $\vec{v}$ is the matter velocity. The density ρ, the pressure P and the velocity $\vec{v}$ describe matter (also named "gas", "fluid"). Gravitational field is described by its potential Φ

In the Euler's description the equations of hydrodynamics have the form:

$$\begin{aligned}
\frac{D\vec{v}}{dt} &= -\frac{\nabla P}{\rho} - \nabla\Phi \quad \text{(Euler)} \\
\frac{D\rho}{dt} &= -\rho\nabla\cdot\vec{v} \qquad \text{(continuity)} \\
\nabla^2\Phi &= 4\pi G\rho \qquad \text{(Poisson)} \\
P &= P(\rho) \qquad \text{(eq. of state)}
\end{aligned}$$

The Euler equation is the equation of motion for the fluid element. The continuity equation (the mass conservation equation) says that the changes in matter density are caused by the influx/outflux of matter. Poisson equation is the Newtonian equation defining the gravitational potential. Equation of state closes the system of equations. We neglect effects of energy transport, so the entropy remains constant for each fluid element and its evolution is an adiabatic transformation. Thus the temperature depends on the density and is not a separate variable.

We consider small perturbations to the fluid parameters and gravitational potential. We neglect energy transport (as before) so we deal with adiabatic perturbations:

$$\begin{aligned}
\rho &= \rho_0 + \delta\rho \equiv \rho_0(1+\delta) \\
\vec{v} &= \vec{v}_0 + \delta\vec{v} \equiv \frac{\dot{a}}{a}\vec{r} + \delta\vec{v} \\
\Phi &= \Phi_0 + \delta\Phi \\
P &= P_0 + \delta P \equiv P_0 + c_S^2\delta\rho \equiv P_0 + \rho_0 c_S^2\delta
\end{aligned}$$

The velocity is described as the *Hubble flow* ($\frac{\dot{a}}{a}\vec{r}$) plus the peculiar velocity $\delta\vec{v}$. After calculating the perturbations of the equations and preserving only the first order termas we see that in this approximation the peculiar velocity does not enter the matter derivative:

$$\frac{D}{Dt} = \frac{\partial}{\partial t} + \vec{v}\cdot\nabla_{\vec{r}} \approx \frac{\partial}{\partial t} + \frac{\dot{a}}{a}\vec{r}\cdot\nabla_{\vec{r}} = \frac{d}{dt}$$

where we introduce d/dt the time derivative in a frame moving with the Hubble flow. Using this definition one has for the continuity equation:

$$\begin{aligned}
\left(\frac{\partial}{\partial t} + \frac{\dot{a}}{a}r^j\nabla_j\right)\delta\rho &= -\,\delta\rho\nabla\left(\frac{\dot{a}}{a}\vec{r}\right) - \rho_0\nabla\delta\vec{v} \\
\frac{1}{\rho_0}\frac{d}{dt}\delta\rho &= -\,3\frac{\dot{a}}{a}\frac{\delta\rho}{\rho_0} - \nabla\delta\vec{v} \\
\frac{1}{\rho_0}\frac{d}{dt}(\rho_0\delta) + 3\frac{\dot{a}}{a}\delta &= -\,\nabla\delta\vec{v} \\
\frac{d}{dt}\delta &= -\nabla\delta\vec{v}
\end{aligned}$$

where we have defined $\delta \equiv \delta\rho/\rho$ the relative density perturbation. Similar approach to the Euler equation:

$$\begin{aligned}
\left(\frac{\partial}{\partial t} + \frac{\dot{a}}{a}r^j\nabla_j\right)\delta v^i + \delta v^j\nabla_j\left(\frac{\dot{a}}{a}r^i\right) &= -\,\frac{\nabla_i\delta P}{\rho_0} - \nabla_i\delta\Phi \\
\left(\frac{\partial}{\partial t} + \frac{\dot{a}}{a}r^j\nabla_j\right)\delta v^i + \frac{\dot{a}}{a}\delta v^i &= -\,\frac{\nabla_i\delta P}{\rho_0} - \nabla_i\delta\Phi
\end{aligned}$$

We calculate the divergence of both sides:

$$\begin{aligned}
\partial t(\nabla\delta\vec{v}) + \frac{\dot{a}}{a}\delta_i^j\nabla_j\delta v^i + \frac{\dot{a}}{a}r^j\nabla_j(\nabla\delta\vec{v}) + \frac{\dot{a}}{a}\nabla\delta\vec{v} &= \\
-\,\frac{\nabla^2\delta P}{\rho_0} - \nabla^2\delta\Phi& \\
\frac{d}{dt}(\nabla\delta\vec{v}) + 2\frac{\dot{a}}{a}\nabla\delta\vec{v} &= -\,c_S^2\nabla^2\delta - \nabla^2\delta\Phi
\end{aligned}$$

Using the continuity equation we eliminate the velocity divergence:

$$\begin{aligned}
\frac{d}{dt}\left(-\frac{d}{dt}\delta\right) + 2\frac{\dot{a}}{a}\left(-\frac{d}{dt}\delta\right) &= -\,c_S^2\nabla^2\delta - 4\pi G\rho_0\delta \\
\ddot{\delta} + 2\frac{\dot{a}}{a}\dot{\delta} &= +\,c_S^2\nabla^2\delta + 4\pi G\rho_0\delta
\end{aligned}$$

For a plane wave perturbation (a single Fourier component) we have:

$$\delta = \delta_{\vec{k}}\ \exp(i\vec{k}\vec{x}) \qquad \vec{r} = a\vec{x} \qquad \lambda = \frac{2\pi a}{|\vec{k}|}$$

$$\ddot{\delta} + 2\frac{\dot{a}}{a}\dot{\delta} + \left(\frac{k^2c_S^2}{a^2} - 4\pi G\rho_0\right)\delta = 0$$

The equation is written down in a frame comoving with the unperturbed fluid or, as we have called it, in the Hubble's frame. we are using coordinates $(t, \vec{x})$ $(\vec{r} = a\vec{x})$.

4.2 Relativistic hydrodynamics

In the early Universe the rest mass of matter is not dominating. The internal energy and pressure do have influence on gravitational and inertial mass. This modifies the equations of motion.

In Sec. 3.1.4 we have shown (or at least argue) that the divergence of the LHS of the Einstein equations is zero, which implies the same for the RHS i.e $\nabla_b T^{ab} = 0$. The matter derivative in relativistic mechanics has the form of $D/Ds \equiv u^b \nabla_b$. Calculating the divergence of the energy-momentum tensor we get:

$$T^{ab} = (\epsilon + P)u^a u^b - P g^{ab} \qquad \nabla_b T^{ab} = 0$$
$$u^a \frac{D}{Ds}(\epsilon + P) + u^a(\epsilon + P)\nabla_b u^b + (\epsilon + P)a^a - \nabla^a P = 0$$

where $a^a \equiv u^b \nabla_b u^a$ is the acceleration. (Fluid may be accelerated by pressure gradients; it does not move along a geodesic.) Since four-velocity u^a is normalized ($u_a u^a = 1$) its derivative must be orthogonal ($u_a a^a = 0$). Multiplying the above equation by u_a we have:

$$\frac{D}{Ds}\epsilon + (\epsilon + P)\nabla_b u^b = 0$$

which is the energy conservation equation. (Projecting the equation into a hypersurface orthogonal to the four-velocity one would obtain the equation of motion (acceleration proportional to minus pressure gradient, $(\epsilon + P)/c^2$ playing the role of the density of inertial mass).

Now we go back to the 3D notation in a local frame. In a small region, of a size Δr say, the expansion of the Universe generates relative motions with velocities $\sim H_0 \Delta r \ll c$. We treat the peculiar velocities $\delta v \ll c$, caused by gravitational instability as a perturbation of the first order. Thus, to the first order, the relativistic effects in kinematics do not show, so we may use the following equations for velocity:

$$\vec{v} = \frac{\dot{a}}{a}\vec{r} + \delta\vec{v} \qquad \nabla \cdot \vec{v} = 3\frac{\dot{a}}{a} + \nabla \cdot \delta\vec{v}$$

The assumption that peculiar velocities are of the first order corresponds to the condition $|\nabla \cdot \delta\vec{v}| \ll 3\dot{a}/a$. We use $d/dt \equiv \partial/\partial t + (\dot{a}/a)r^i \nabla_i$. The linearized energy equation is given in the first row. Then we check the value of the time derivative of the relative energy density perturbation $\delta\epsilon/(\epsilon + P)$ showing its relation to the peculiar velocity divergence.

$$\frac{d}{dt}\delta\epsilon + 3\frac{\dot{a}}{a}(\delta\epsilon + \delta P) + (\epsilon + P)\nabla\delta\vec{v} = 0 \qquad \text{en.eq.}$$
$$\frac{d}{dt}\left(\frac{\delta\epsilon}{\epsilon + P}\right) = \frac{1}{\epsilon + P}\frac{d}{dt}\delta\epsilon - \frac{\delta\epsilon}{(\epsilon + P)^2}(1 + c_S^2/c^2)\frac{d\epsilon}{dt} \qquad (\text{but: } \delta P = c_S^2/c^2 * \delta\epsilon)$$
$$= \frac{1}{\epsilon + P}\frac{d}{dt}\delta\epsilon - \frac{\delta\epsilon + \delta P}{(\epsilon + P)^2}(-3\frac{\dot{a}}{a}(\epsilon + P))$$
$$= \frac{1}{\epsilon + P}\frac{d}{dt}\delta\epsilon + 3\frac{\dot{a}}{a}\frac{\delta\epsilon + \delta P}{\epsilon + P} \equiv \frac{1}{\epsilon + P}\left(\frac{d}{dt}\delta\epsilon + 3\frac{\dot{a}}{a}(\delta\epsilon + \delta P)\right)$$
$$\frac{d}{dt}\left(\frac{\delta\epsilon}{\epsilon + P}\right) = -\nabla\delta\vec{v}$$

In our approach we use nonrelativistic kinematics and relativistic thermodynamics. Our equation of motion has the former form, but we replace the Newtonian potential gradient with "gravitational acceleration" ($-\nabla_i \delta\Phi \to \delta g_i$) as in the problem of geodesic deviation (Sec. 3.1.5) and the mass density by the entalpy density ($\rho \to (\epsilon + P)/c^2$):

$$\left(\frac{\partial}{\partial t} + \frac{\dot{a}}{a} r^j \nabla_j\right) \delta v^i + \frac{\dot{a}}{a} \delta v^i = -\frac{c^2 \nabla_i \delta P}{\epsilon + P} + \delta g^i$$

Calculating the divergence of the above equation one gets:

$$\begin{aligned}
\partial t(\nabla \delta\vec{v}) + \frac{\dot{a}}{a}\delta_i^j \nabla_j \delta v^i + \frac{\dot{a}}{a} r^j \nabla_j (\nabla \delta\vec{v}) + \frac{\dot{a}}{a} \nabla \delta\vec{v} &= -\frac{c^2 \nabla^2 \delta P}{\epsilon_0 + P_0} + \nabla \cdot \delta\vec{g} \\
\left(\frac{\partial}{\partial t} + \frac{\dot{a}}{a} r^j \nabla_j\right) (\nabla \delta\vec{v}) + 2\frac{\dot{a}}{a} \nabla \delta\vec{v} &= -c_S^2 \nabla^2 \frac{\delta\epsilon}{\epsilon + P} - \frac{4\pi G}{c^2}(\delta\epsilon + 3\delta P) \\
\frac{d}{dt}(\nabla \delta\vec{v}) + 2\frac{\dot{a}}{a} \nabla \delta\vec{v} &= -c_S^2 \nabla^2 \frac{\delta\epsilon}{\epsilon + P} - \frac{4\pi G}{c^2}(\delta\epsilon + 3\delta P)
\end{aligned}$$

Where we have applied the result of geodesic deviation equation. The perturbations are assumed to be adiabatic so $\delta P = c_s^2 \delta\epsilon / c^2$. Substituting time derivative of the relative energy density perturbation δ in place of velocity divergence one gets finally:

$$\frac{d}{dt}\left(-\frac{d\delta}{dt}\right) + 2\frac{\dot{a}}{a}\left(-\frac{d\delta}{dt}\right) = -c_S^2 \nabla^2 \delta - 4\pi G \rho_0 \frac{\epsilon + P}{\epsilon}(1 + 3c_S^2/c^2)\delta$$

For a plane wave perturbation (a single Fourier component defined by the wave number $\vec{k}$; $\lambda = 2\pi a/k$) one has:

$$\ddot{\delta} + 2\frac{\dot{a}}{a}\dot{\delta} + \left[\frac{k^2 c_S^2}{a^2} - 4\pi G \rho_0 (1 + w)(1 + 3c_S^2/c^2)\right] \delta = 0$$

where $w \equiv P/\epsilon$ is introduced for compactness. We recover the equation describing the evolution of small density perturbations in an expanding Universe model from previous section (sec. 4.1) up to corrections resulting from possibly relativistic equation of state.

4.3 Growth of the adiabatic density perturbations

In the early epochs ($t \ll t_{eq}$) the relativistic component of matter dominates ("eq" stands for "matter radiation equality") so $w = 1/3$ and $c_S^2 = c^2/3$. For a plane wave perturbation we get

$$\begin{aligned}
\delta \equiv & \delta\epsilon/(\epsilon + P) \\
\ddot{\delta} + & 2\frac{\dot{a}}{a}\dot{\delta} + \left[\frac{k^2 c_S^2}{a^2} - \frac{32\pi G}{3c^2}\epsilon\right] \delta = 0 \\
\epsilon = & \frac{3c^2}{32\pi G t^2} \qquad \text{(early: } t \ll t_{eq}\text{)} \\
a(t) \propto & \; t^{1/2} \qquad \text{(early: } t \ll t_{eq}\text{)} \\
\lambda(t) = & \frac{2\pi a(t)}{k} \\
\Rightarrow \; & \ddot{\delta} + \frac{1}{t}\dot{\delta} + \left[\frac{c_S^2}{a^2}\left(\frac{2\pi a}{\lambda}\right)^2 - \frac{1}{t^2}\right] \delta = 0
\end{aligned}$$

We see that for $\lambda \gg 2\pi c_S t$ the second term in parenthesis dominates and we have:

$$\begin{aligned} \ddot{\delta} &+ \frac{1}{t}\dot{\delta} - \frac{1}{t^2}\delta = 0 \\ \Rightarrow \quad \delta &\propto t^1 \propto a^2 \quad \text{or} \quad \delta \propto t^{-1} \propto a^{-2} \end{aligned}$$

so on *super-horizon* scales we have one power-law growing mode and another fading away. Our approximtions break when relativistic component no longer dominates. Since averaged matter energy density today is $\sim 10^4$ times larger than the energy density of relic photons, they had roughly the same value at $1+z_{eq} \approx 10^4$. (There are also corresponding t_{eq} and a_{eq}.) Later on, at $1+z_{rec} \approx 1100$ the recombination took place and baryons decoupled from photons. After the recombination one can treat matter (baryons and dark) as cold gas with vanishing/negligible pressure ($P = 0$, $c_S = 0$). (This is an approximation valid except for the smallest scales corresponding to masses $M < 10^6\ M_\odot$.)

According to the present day measurements the density parameters of the Universe are $\Omega_M \approx 0.3$, $\Omega_\Lambda \approx 0.7$, and $|\Omega_K| < 10^{-4}$. This implies that in the not so much distant past the matter density was (as would be measured by past observers) close to critical:

$$\begin{aligned} \frac{\rho_M(z)}{\rho_c(z)} &= \frac{\frac{3H_0^2}{8\pi G}\Omega_M(1+z)^3}{\frac{3H_0^2}{8\pi G}\left(\Omega_M(1+z)^3 + \Omega_K(1+z)^2 + \Omega_\Lambda\right)} \approx 1 - \frac{\Omega_K}{\Omega_M(1+z)} - \frac{\Omega_\Lambda}{\Omega_M(1+z)^3} \\ \Rightarrow \quad \rho_M &\approx \frac{1}{6\pi G t^2} \qquad a \propto t^{2/3} \\ \ddot{\delta} &+ \frac{4}{3}\frac{1}{t}\dot{\delta} - \frac{2}{3}\frac{1}{t^2}\delta = 0 \\ \Rightarrow \quad \delta &\propto t^{2/3} \propto a \quad \text{or} \quad \delta \propto t^{-1} \propto a^{-3/2} \end{aligned}$$

Our results show that superhorizon perturbations in the early Universe (at $t < t_{eq}$ or until they become subhhorizon) grow in proportion to a^2 and after the recombination as a^1, practically regardles of scale. In between there is a period not so easy to describe. Our treatment uses one component fluid to describe matter content of the Universe. This is an adequate description of the radiation coupled with plasma up to recombination if the dark matter is missing and for the mixture of baryons and dark matter after. For subhorizon perturbations before recombination one needs another approach taking into account different behavior of cold, not coupled to anything dark matter, which should be described as the second fluid. (see below).

To get some intuition we shall integrate our equation numerically. Since we start at large redshift ($z \sim 10^{10}$) all variables cover many orders of magnitude. We are replacing time with the logarithm of scale factor as an independent variable:

$$\begin{aligned} \frac{d}{dt} &= \dot{a}\frac{d}{da} \equiv \frac{\dot{a}}{a}\frac{d}{d\ln a} \\ \frac{d^2}{dt^2} &= \frac{\dot{a}}{a}\frac{d}{d\ln a}\ \frac{\dot{a}}{a}\frac{d}{d\ln a} = \frac{\dot{a}^2}{a^2}\frac{d^2}{(d\ln a)^2} + \left(\frac{\ddot{a}}{a} - \frac{\dot{a}^2}{a^2}\right)\frac{d}{d\ln a} \end{aligned}$$

Substituting:

$$\frac{\dot{a}^2}{a^2}\delta'' + \left(\frac{\ddot{a}}{a} + \frac{\dot{a}^2}{a^2}\right)\delta' + \left[\frac{k^2 c_S^2}{a^2} - 4\pi G\rho(1+w)(1+3c_S^2/c^2)\right]\delta = 0 \tag{4.2}$$

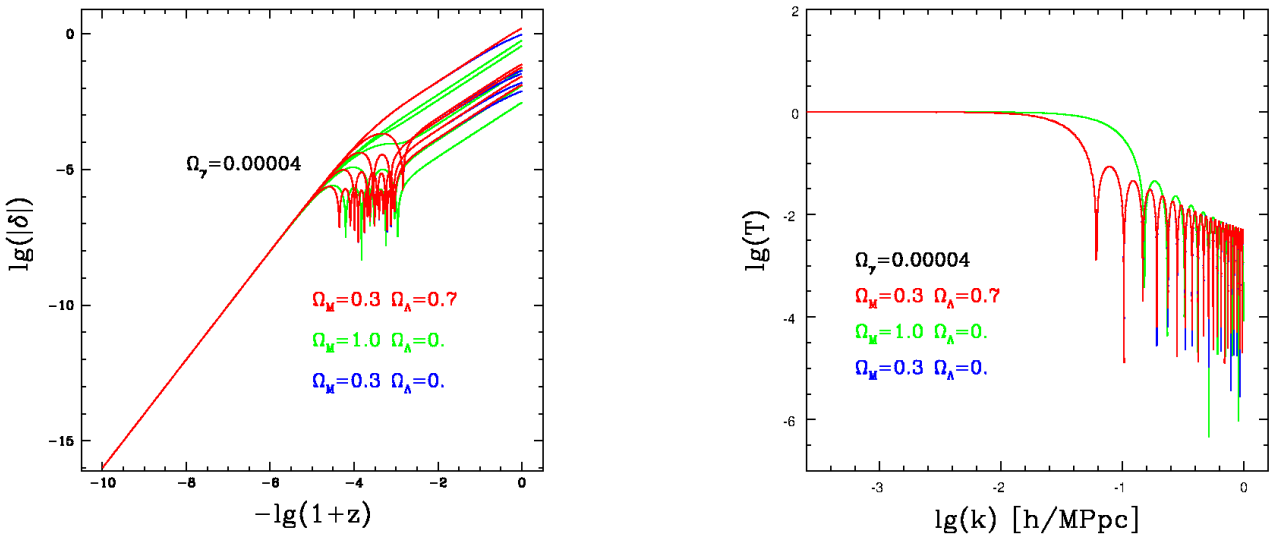

Figure 4.1: Growth of perturbations in single fluid approximation. Left: examples of numerical solutions. Right: transmission factor for the same models

where by prime we denote derivatives with respect to $\ln a$. After transformations we get:

$$\delta''+\left(1+\frac{\ddot{a}a}{\dot{a}^2}\right)\delta'+\frac{a^2}{\dot{a}^2}\left[\frac{k^2c_S^2}{a^2}-4\pi G\rho(1+w)(1+3c_S^2/c^2)\right]\delta=0$$
$$\delta''+w_1\delta'+w_0\delta=0$$

where w_1, w_0 are the coefficients denoting more complicated expressions used in the preceding form of the equation.

An approximate solution for the growing mode of instability is proportional to the function:

$$f=\frac{a^2}{a+a_{eq}}$$

which has the right behavior asymptotically ($f\propto a^2$ for $a\ll a_{eq}$ and $f\propto a^1$ for $a\gg a_{eq}$). It also changes by many orders of magnitude. We look for an exact solution to our equation in the form $\delta=Af$, where A is an unknown function:

$$\begin{aligned}\delta&=Af\\ \delta'&=A'f+Af'\\ \delta''&=A''f+2A'f'+Af''\end{aligned}$$

Substituting and transforming:

$$(fA''+2f'A'+f''A)+w_1(fA'+f'A)+w_0fA=0$$
$$A''+\left(w_1+2\frac{f'}{f}\right)A'+\left(w_0+w_1\frac{f'}{f}+\frac{f''}{f}\right)A=0$$

we get the equation for A. The initial conditions at $a\ll a_{eq}$ are:

$$A_{\rm init}=1\qquad A'_{\rm init}=0$$

where we have assumed that f properly describes the rate of growth of perturbations δ at an early stage of the process. In Fig. 4.1 we present examples of the solutions to our equations for three different cosmological models and for few different wavelengths. We start calculations at the same redshift and assume the same initial amplitude for all wave-lengts and all models. As can be seen, the subhorizon fluctuations undergo oscillations for some time prior to recombination. The shorter the wave-length, the earlier the oscillations begin. Because of plotting technique the red is overplotted on other colors. The red monotonic curve, corresponding to "always" superhorizon mode, hides under green and blue ones. After the recombination we see the same rate of growth for all curves; their level depends on the phase of oscillation of a given perturbation at the moment of recombination. Thus at the recombination the amplitude of perturbations in not a monotonic function of their wave-length. For the longest (always superhorizon) perturbations their amplitude at the recombination is approximatelly the same, but for shorter waves it becomes smaller and shows modulation (see below about the *transmission factor*).

4.4 Condition for instability; Jeans mass

Considering the growth of the perturbations in athe early Universe, we have already used the argument that the expression inside the square brackets in the perturbation evolution equation must be negative for the existence of a growing mode. Our numerical experience shows the oscillatory behaviour of the perturbations when the condition is not met. It is customary to name the characteristic wave-length, which is an approximate border between nongrowing and possibly growing solutions to perturbation equation after Jeans. Thus at the beginning, for $t \leq t_{eq}$, when we may assume the relativistic equation of state $\epsilon = \frac{1}{3}P$ is valid, we get:

$$[...] < 0 \quad \Rightarrow \quad \lambda > 2\pi c_S t \quad \text{or} \quad \lambda_J = 2\pi c_S t$$

where λ_J is the Jeans wavelength. The related wave number is $k_J = 2\pi a/\lambda_J$. Of course both parameters depend on time.

It is also customary to use *Jeans mass* as the parameter giving the minimal "mass of perturbation" which may be unstable. By mass we understand the mass of cold matter (baryons + dark) inside the region of the size of Jeans length:

$$M_J = \rho_M \lambda_J^3$$

Since matter density changes as $\rho_M \propto 1/a^3$ and at $t < t_{eq}$ $\lambda_J \propto t \propto a^2$, we get $M_J \propto a^3 \propto t^{3/2}$ at this epoch.

We shall make few estimates to learn the typical Jeans mass values. We assume that the relativistic equation of state was valid until t_{eq},. During anihillations of various particles (most recently electron - positron pairs at $T \approx 10^9$ K and $t \approx 1$ s) the relation $\epsilon \propto 1/t^2$ does not hold exactly, but since the last such process took place at $t \ll t_{eq}$ it can have only little (if any) influence on our result. More interesting are neutrinos. They have small rest energy, probably < 0.2 eV. If this is a valid estimate, it corresponds to the temperature ~ 2000 K, less than $T = (1 + z_{eq}) \times 3$ K $\approx 3 \times 10^4$ K. Thus at t_{eq} neutrinos were relativistic, but their temperature was by a factor $(4/11)^{1/3}$ lower than for photons. Because the number of neutrinos and antineutrinos is 6, they have 1 polarization state (photons 2) and they are fermions, their total energy density is

$$\epsilon_\nu = 6 * \frac{1}{2} * \frac{7}{8} * \left(\frac{4}{11}\right)^{4/3} \epsilon_\gamma = 0.681 \; \epsilon_\gamma$$

The dimensionless density parameter for photons today is $\Omega_\gamma \approx 0.00004$ as seen on Fig. 4.1. This gives photon energy density as of today. Multiplying by $(1+z_{eq})^4$ factor and by 1.68 (to account for neutrinos) we get the relativistic energy density at t_{eq}, which is independently given by its dependence on time:

$$\begin{aligned} 1.68 * \Omega_\gamma * \frac{3H_0^2}{8\pi G} c^2 (1+z_{eq})^4 &= \frac{3c^2}{32\pi G t_{eq}^2} \\ 4 * 1.68 * \Omega_\gamma (1+z_{eq})^4 {H_0}^2 &= \frac{1}{t_{eq}^2} \\ t_{eq} = \frac{1}{\sqrt{6.72\Omega_\gamma}} \frac{1}{(1+z_{eq})^2} \frac{1}{H_0} = 6.1 \times 10^{-7} \frac{1}{H_0} &= 8.5 \times 10^3 \text{ y} \\ \lambda_J(t_{eq}) = 2\pi \sqrt{\frac{1}{3}} c t_{eq} &\approx 10 \text{ kpc} \end{aligned}$$

For the Jeans mass one gets:

$$\begin{aligned} M_J(t_{eq}) &= \Omega_M \frac{3H_0^2}{8\pi G} (1+z_{eq})^3 * \left(2\pi \sqrt{\frac{1}{3}} c t_{eq} \right)^3 \\ &= \frac{\pi^2}{\sqrt{3}} \frac{\Omega_M}{(6.72\Omega_\gamma)^{3/2}} \frac{1}{(1+z_{eq})^3} \frac{c^2 * (c/H_0)}{G} \approx 3.2 \times 10^{16}\ M_\odot \end{aligned}$$

At recombination the Universe is nonrelativistic and has critical density as we have already argued. Earlier (at $t \le t_{eq}$) the matter was relativistic. Since $t_{eq} \ll t_{rec}$ (not everybody would agree?) we may neglect this early period as having little influence on the epoch of recombination. We again use energy density dependence on time but for nonrelativistic case.

$$\begin{aligned} \Omega_M * \frac{3H_0^2}{8\pi G} (1+z_{rec})^3 &= \frac{1}{6\pi G t_{rec}^2} \\ \frac{9}{4} \Omega_M (1+z_{rec})^3 {H_0}^2 &= \frac{1}{t_{rec}^2} \\ t_{rec} = \frac{2/3}{\sqrt{\Omega_M (1+z_{rec})^3}} \frac{1}{H_0} = 3.3 \times 10^{-5} \frac{1}{H_0} &= 467 \times 10^3 \text{ y} \end{aligned}$$

Since there are $\sim 10^9$ photons per baryon, the radiation pressure is always dominating (assuming dark matter to be cold) and the (rest) energy density of matter dominates at $t \ge t_{eq}$. One has:

$$\begin{aligned} P_\gamma &= \frac{1}{3} \Omega_\gamma \frac{3{H_0}^2}{8\pi G} c^2 (1+z)^4 \qquad \rho_M = \Omega_M \frac{3{H_0}^2}{8\pi G} (1+z)^3 \\ {c_S}^2 &= \frac{dP_\gamma/dz}{d\rho_M/dz} = \frac{4}{9} c^2 \frac{\Omega_\gamma}{\Omega_M} (1+z) \qquad c_S(t_{rec}) \approx 0.25\ c \\ \lambda_J(t_{rec}) &= 2\pi c_S(t_{rec}) t_{rec} \approx 225 \text{ kpc} \\ M_J(t_{rec}) &= \Omega_M \frac{3H_0^2}{8\pi G} (1+z_{rec})^3 {\lambda_J}^3(t_{rec}) \approx 1.3 \times 10^{18}\ M_\odot \end{aligned}$$

Using the perturbation evolution equation directly one would get the following formula for the

Jeans wave-vector and wave-length:

$$k_{\rm J} = \frac{a}{c_S}\sqrt{4\pi G\rho(1+w)(1+3c_S^2/c^2)}$$
$$\lambda_{\rm J} = \frac{2\pi a}{k} = \frac{2\pi c_S}{\sqrt{4\pi G\rho(1+w)(1+3c_S^2/c^2)}}$$

Particles of *dark matter* practically do not interact with anything (including themselves), so they should be treated as a collisionless gas. Condition of instability is obtained after considering perturbations to their distribution function $f(\vec{x},\vec{v})$. The result is very similar to the result for an ideal gas but the sound velocity is replaced by the "harmonic" velocity square average:

$$\lambda_{\rm J} = \frac{2\pi b}{\sqrt{4\pi G\rho(1+w)(1+3b^2/c^2)}}$$
$$\frac{1}{b^2} \equiv \frac{\int \frac{f(\vec{v})}{v^2} d_3v}{\int f(\vec{v}) d_3v} = \frac{\int f(v) dv}{\int f(v) v^2 dv}$$

For "cold" dark matter $b \ll c$ and the Jeans wave-length is small and does not influence instability on scales of galaxies and larger. For "warm" dark matter it may play a role. An example are neutrinos, which were still relativistic at *equality* ($b = c$) but do have nonvanishing rest mass and become non-relativistic later on. The influence of neutrinos on the gravitational instability in the Universe depands on their rest energy. For $m_\nu c^2 \approx 15$ eV their density would be close to critical ($\Omega_\nu \approx 1$) and they might be the only constituent of dark matter (history: 1980-90). The "rule of thumb" gives the estimate of the comoving Jeans length:

$$\lambda_J^{(\nu)} = a_0 \int_0^t \frac{v_\nu dt}{a(t)}$$

This value increases monotonically but slowes down when neutrinos become nonrelativistic. In the case of dominating neutrinos $\lambda_J^{(\nu)}$ reaches value of ~ 30 Mpc. The diffusion of neutrinos from regions of high density to regions of low density smooths out perturbations on small scales up to 30 Mpc as measured today and the first object to form would br on the *super-cluster* scale. This implies so called "top-down" scenario of the structure formation, where the smaller objects form by fragmentation of larger ones (history: mainly Zeldovich and coworkers). Top-down scenario produces wrong spectrum of perturbations which implies wrong (not observed) spectrum of CMB anisotropy. Small admixture of massive neutrinos ($m_\nu c^2 \sim 0.2$ eV, $\Omega_\nu \sim 0.02$) is still considered and plays a secondary role in the scenario of structure formation (see below when it exists).

4.5 Two fluid instability

Since dark matter exists and practically does not interact with baryonic matter the present content of the Universe consists of at least two fluids. Thus the equations for two fluids are independent with the exception of the term related to gravity.

We are using term "baryons" for baryonic gas filling the Universe after the recombination which was ionized and coupled to photons before. There are $\sim 10^9$ of photons per baryon so the radiation pressure always dominates and plasma pressure can be neglected. The pressure to energy density

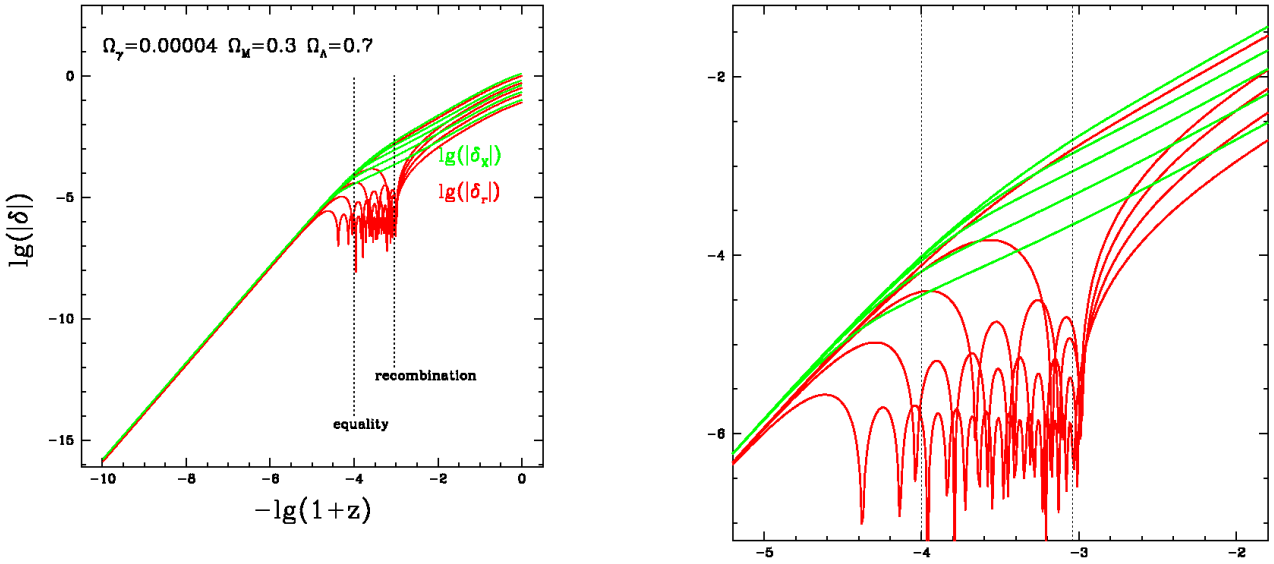

Figure 4.2: Growth of perturbations in two fluid approximation. Left: examples of numerical solutions. Right: zoom of the left panel

ratio w_B and the sound velocity c_B before the recombination are given as:

$$\begin{aligned} w_B &= \frac{P_\gamma}{\epsilon_\gamma + \epsilon_B} = \frac{\frac{1}{3}\Omega_\gamma (1+z)^4}{\Omega_\gamma (1+z)^4 + \Omega_B * (1+z)^3} = \frac{1}{3}\frac{\Omega_\gamma (1+z)}{\Omega_\gamma (1+z) + \Omega_B} \\ c_B^2 &= \frac{dP/dz}{d\epsilon/dz} = \frac{1}{3}\frac{4\Omega_\gamma (1+z)}{4\Omega_\gamma (1+z) + 3\Omega_B} \end{aligned}$$

After the recombination we use $w_B = c_B = 0$ since baryons no longer interact with photons and gas pressure is negligible. For dark matter $w_X = c_X = 0$ always. The gravity term in the perturbation evolution equation becomes (in our convention $\delta\epsilon = (\epsilon + P)\delta$ for both components and $\delta P = c_S^2 \delta\epsilon$):

$$\frac{4\pi G}{c^2}(\delta\epsilon + 3\delta P) = \frac{4\pi G}{c^2}\left((\epsilon_\gamma + \epsilon_B)(1+3c_B^2)(1+w_B)\delta_B + \epsilon_X (1+3c_X^2)(1+w_X)\delta_X\right)$$

As the gas energy density we use the sum of baryons rest energy and photons energy density. Prior to the recombination this approach is selfconsistent since both components interact and the calculation of c_B, w_B takes it into account. After the recombination the photons should be excluded, but they contribute only a little, decreasing part to the energy density.

Now we generalize our evolution equation for δ taking into account the presence of another component. Only the term related to gravitational interactions changes:

$$\begin{aligned} \ddot{\delta}_B + 2\frac{\dot{a}}{a}\dot{\delta}_B &+ \left[\frac{k^2 c_B^2 c^2}{a^2}\delta_B - \frac{4\pi G}{c^2}\left((\epsilon_\gamma + \epsilon_B)(1+3c_B^2)(1+w_B)\delta_B + \epsilon_X(1+3c_X^2)(1+w_X)\delta_X\right)\right] = 0 \\ \ddot{\delta}_X + 2\frac{\dot{a}}{a}\dot{\delta}_X &+ \left[\frac{k^2 c_X^2 c^2}{a^2}\delta_X - \frac{4\pi G}{c^2}\left((\epsilon_\gamma + \epsilon_B)(1+3c_B^2)(1+w_B)\delta_B + \epsilon_X(1+3c_X^2)(1+w_X)\delta_X\right)\right] = 0 \end{aligned}$$

The equations are written in symmetric form. (One could investigate the case of two fluids with different sound velocities.) We are interested in cold dark matter with $c_X = w_X = 0$ and

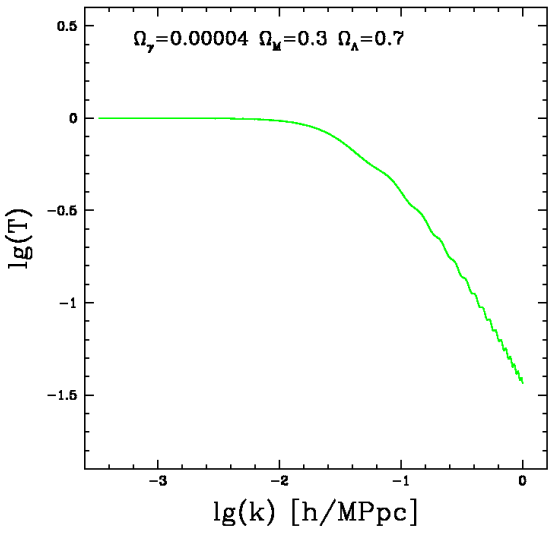

Figure 4.3: Transmission factor for the two-fluid approximation.

$\Omega_B < \Omega_X$ so after the *equality* dark matter dominates and oscillations of baryonic part are unlikely to change the sign of *square bracket* in the second equation, which implies presence of the growing mode for δ_X.

Our calculations show that the amplitudes of the density perturbation change by many orders of magnitude between the start and final and the amplification depends on the wave-length. Assuming that we use the same initial amplitudes for all wavelengths we may define the amplification $Amp(k)$ and transmission $T(k)$ factors as:

$$Amp(k) = \frac{\delta_k(z=0)}{\delta_k(z=z_{start})}$$
$$T(k) = \frac{Amp(k)}{Amp(0)} = \frac{\delta_k(z=0)}{\delta_0(z=0)}$$

The transmission factor defines the relative amplification. As seen on Fig. 4.3, for very long (always superhorizon) waves the total amplification is almost constant, but for shorter wavelengths (which undergo phase of oscillations of baryonic component) the amplification factor (and the transmission factor) decrease with increasin wavevector. Thus the Universe as an amplifier of small density perturbations filters out perturbations on short scales.

4.6 Spectrum of perturbations; Harrison - Zeldovich primary spectrum

We assume that the matter density perturbations on its linear stage are regular functions which can be Fourier-transformed. In comoving coordinates one has:

$$\delta(\vec{x}) = \int d_3k \delta_{\vec{k}} \exp(-i\vec{k}\vec{x}) \tag{4.3}$$

By the definition $\langle\delta(\vec{x})\rangle = 0$, but the square mean is positive. Using Fourier transformation we may find its value:

$$\begin{aligned}
&\frac{1}{V}\int_V d_3x|\delta^2(\vec{x})| = \\
&\frac{1}{V}\int_V d_3x \int d_3k'\delta_{\vec{k}'}\exp(-i\vec{k}'\vec{x}) \int d_3k''\delta^*_{\vec{k}''}\exp(+i\vec{k}''\vec{x}) \\
&\rightarrow \int d_3k'\delta_{\vec{k}'}\int d_3k''\delta^*_{\vec{k}''}\delta_{\mathrm{Dirac}}(\vec{k}'-\vec{k}'') \\
&= \int d_3k|\delta^2_{\vec{k}}| \approx 4\pi\int\frac{dk}{k}\ k^3|\delta^2_k|
\end{aligned}$$

where with the volume $V \rightarrow \infty$ the integration in $\vec{x}$ space produces Dirac's delta and the result becomes a single integral in $\vec{k}$ space. Using the argument of the Universe isotropy we get $\delta^2(\vec{k}) = \delta^2(|\vec{k}|)$ which changes the 3D integral into 1D integration. we replace $k^2dk \equiv k^3d\ln k$ which gives the final form of the expression. It is customary to call the function integrated over $\ln k$ *power spectrum of density fluctuations*. It shows the contributions to the amplitude square mean from different logarithmic intervals of the wave-vector. To be explicit:

$$P_\delta(k) \equiv k^3|\delta^2(k)| \tag{4.4}$$

To start any considerations of the growth of structure in the Universe one must know the primary spectrum of perturbations. In the early Universe there is no natural length scale, so the only function one my think of is the power function:

$$\delta^2(k) \sim k^n$$

With analogy to density power spectrum one may introduce the spectrum of potential perturbations:

$$P_{\delta\Phi}(k) \equiv k^3|\delta\Phi^2(k)| \tag{4.5}$$

Using Poisson equation one gets:

$$\begin{aligned}
\triangle\delta\Phi_{\vec{k}} &= -\ k^2\delta\Phi_{\vec{k}} = 4\pi G\rho_0\delta_{\vec{k}} \\
P_{\delta\Phi}(k) &\sim k^3\frac{|\delta^2_k|}{k^4} = \frac{|\delta^2_k|}{k}
\end{aligned}$$

To avoid problems with $k \rightarrow 0$ or $k \rightarrow \infty$ one has to choose $n = 1$:

$$\frac{|\delta^2_k|}{k} \sim k^0 \qquad |\delta^2_k| \sim k^1 \qquad n = 1 \tag{4.6}$$

This is so called Harrison - Zeldivich primary spectrum of fluctuations:

$$P_\delta(k) \equiv k^3|\delta^2(k)| \sim k^4$$

- apparently the short wave perturbations dominate .

4.7 Initial conditions for nonlinear calculations

The typical matter density in a galaxy is $\sim 10^6$ times above the average today so matter density fluctuatons are no longer *small* and cannot be treated in such an approximation. Instead some nonlinear or numerical approach is needed. One may assume that the linear calculations of the growth of small density, velocity, and gravity fluctuations can proceed until *switch* to nonlinear approach at $z_{sw} \sim 10^2$. These are quite simple since each plane wave component is indepemdent of all other and may be described using a set of few ordinary differential equations. Such calculations transform the primary spectrum of fluctuations into its form at z_{sw}:

$$k^3\delta_k^2(z_{sw}) = k^3\delta_k^2(\text{prim}) * T^2(k)$$

where $T(k)$ is the transmission factor. The spectrum defines only *rms* amplitude of fluctuations as a function of the wave number. (NOT amplitudes for every $\vec{k}$ of the length k !). The primary spectrum is usually of the Harrison - Zeldovich form. Some people modify it to get a better agreement with measurements of CMB anisotropy.

Important: the anisotropy of CMB is formed on the sphere of last scattering at *recombination* and only slightly modified afterwards by interactions with matter and gravitational field fluctuations (next chapters). The linear approach is still valid at last sphere, so there is relatively easy to calculate the sequence:

$$P_\delta(k) \quad \Rightarrow \quad \left(\frac{\delta T}{T}\right)_{prim} \quad \Rightarrow \quad C^2(l)$$

where the last symbol is the CMB anisotropy power spectrum.

The next step for numerical calculations is to define the initial fluctuations to start. Typically cosmological simulations use a *simulation cube* of large size (order: 50 - 500 Mpc on side). The size depends on the further applications. Some authors perform calculations using different volumes in a way zooming in the larger cube and treating its part with better spatial resolution.

All (?) simulations are based on the concept of particles and cells which follows long tradition of N-body simulations. So there is a huge number of particles which interact gravitationally with each other. At the beginning their distribution in space is almost uniform and their velocities are small. The problem with unknown matter distribution outside the cube is solved by the *periodic boundary conditions*. For a cube of side L one assumes:

$$\delta(x + jL, y + mL, z + nL) = \delta(x, y, z)$$
$$k_{min} = \frac{2\pi}{L} \qquad k_{max} \approx N^{1/3} k_{min}$$

where j, m, and n are integers. (Such conditions apply to all variables). The discrete Fourier transformations are used at many steps of calculations. It is obvious that the longest Fourier wave which fits into the cube is of the length of its side, which defines k_{min} above. The typical distance between particles in the cube is $L^3/N)^{1/3}$ (side of a cube of the volume per particle), which defines the resolution and k_{max}. Thus the Fourier series are finite. That must introduce some numerical noise, one hopes not too much of it.

Back to initial conditions. Since the spectrum of fluctuations is defined in the Fourier space, we have:

$$\delta(x, y, z) = \sum_{jmn} \delta_{jmn} e^{2\pi i(jx+my+nz)/L}$$
$$|\vec{k}(j, m, n)| = \frac{2\pi}{L}\sqrt{j^2 + m^2 + n^2}$$

The spectrum defines only the rms amplitude of each mode. It is usually assumed that fluctuations are Gaussian, so for a given wave vector one has:

$$\begin{aligned} \delta_{\vec{k}} =& X * \exp(2\pi i Y)\sqrt{\langle \delta_k^2 \rangle} \\ p(X) =& \frac{1}{\sqrt{2\pi}} \exp\left(-\frac{1}{2}X^2\right) \\ p(Y) =& 1 \qquad 0 \leq Y \leq 1 \end{aligned}$$

In other words each particular set of initial conditions is a realisation of a random process. In a sense amplitudes are being drawn from a normal distribution and phases from a uniform one. Since density fluctuations are real the condition:

$$\delta(-\vec{k}) = \delta^*(\vec{k})$$

applies. This limits the drawing to 1/2 of the Fourier space volume or to $j \geq 0$.

The Gaussianity is commonly used. The question whether some signs of non-Gaussianity are present in observations is sometimes asked, but it is rather a sofisticated problem.

N-body codes. Since dark matter is not interacting directly, its particles can be treated as point masses interacting only via gravity. A N-body code is doing just that. Of course it is impossible to treat dark matter on microscopic level. Instead in a code one uses *particles* which represent chunks of dark mass (in reality each 10^6 - 10^8 $M_\odot$ depending on L and N). As a result the code follows the changes in dark matter distribution with limited resolution: one can learn something about assembly of objects containing several tens of dark *particles*, but nothing about details of its structure below the level of single particle mass. Since dark matter contains 5 times more mass than baryonic component it becomes the main component which drives gravitational instability. The baryonic component is usually followed with hydrodynamical codes.

Drawing $\delta_{\vec{k}}$ gives $\delta(x, y, z)$; $1 + \delta(x, y, z)$ is proportional to full density and may be interpreted as probability distribution for finding a particle in any location. Accompanying velocity field gives velocities to particles, depending on their locations.

So: continuous density distribution $(1 + \delta(x, y, z))$ is represented by a finite number of particles which can map the density field only

with limited resolution. The same applies to velocity: it is given only at positions of *particles*.

Some schemes of numerical approach (based on the dscription of *Millennium Simulation*): see *Lectures*.

Chapter 5

Cosmic Microwave Background

5.1 CMB temperature fluctuations and gravitational instability

Harmonics, power spectrum To check which angular scales are important one may represent CMB temperature map by a series of spherical harmonics $Y_m^l(\theta,\phi)$. Spherical harmonics are the orthogonal basis of functions on the sphere and each regular function can be represented by an infinite series:

$$\frac{\Delta T}{T}(\theta,\phi) = \frac{T(\theta,\phi) - \langle T\rangle}{\langle T\rangle}$$
$$\frac{\Delta T}{T}(\theta,\phi) = \sum_{l=1}^{\infty}\sum_{m=-l}^{l} a_{lm} Y_m^l(\theta,\phi)$$

Harmonics:

$$Y_m^l(\theta,\phi) = \sqrt{\frac{(2l+1)(l-m)!}{4\pi(l+m)!}}\; e^{im\phi}\; P_l^m(\cos\theta)$$
$$\int_0^{\pi}\int_0^{2\pi} Y_m^l (Y_{m'}^{l'})^* d\phi \sin\theta d\theta = \delta^{ll'}\delta_{mm'}$$

Harmonics are normalized. Rotation of the coordinate frame transforms harmonics of given l parameter between themselves, so a_{lm} in one frame are linear combinations of $a_{lm'}$ in another. Imagine a function f which is a weighted sum of harmonics with the same l. Integral of f^2 must not depend on coordinates so the sum of squares of coefficients is independent of the coordinate system. It serves as a *anisotropy power spectrum*:

$$C_l = \frac{1}{2l+1}\sum_{m=-l}^{l} |a_{lm}|^2$$

Metric perturbations In the linear approximation one may choose to use the metric of the perturbed flat universe model in the form:

$$ds^2 = c^2dt^2 - a^2(t)(\delta_{\alpha\beta} - h_{\alpha\beta})dx^\alpha dx^\beta$$

where $\alpha, \beta \in \{1, 2, 3\}$ and summation convention applies. $h_{\alpha\beta}$ are small ($\ll 1$) corrections.

Metric and energy-momentum tensor perturbations can be classified as *scalar* (density perturbations), *vector* (vortices: $\nabla \times \vec{v} \neq 0$) , and *tensor* (density and velocity of the fluid unchanged). Ina a flat model, using Cartesian coordinates one has for a flat wave along x^3 the following forms of $h_{\alpha\beta}$. (next slide)

Scalar:

$$\begin{pmatrix} \frac{1}{3}h - \frac{1}{2}H & 0 & 0 \\ 0 & \frac{1}{3}h - \frac{1}{2}H & 0 \\ 0 & 0 & \frac{1}{3}h + H \end{pmatrix}$$

Vector:

$$\begin{pmatrix} 0 & 0 & h^{\perp} \\ 0 & 0 & 0 \\ h^{\perp} & 0 & 0 \end{pmatrix}$$

Tensor:

$$\begin{pmatrix} h^{+} & h^{x} & 0 \\ h^{x} & -h^{+} & 0 \\ 0 & 0 & 0 \end{pmatrix}$$

Scalar perturbations

For a scalar plane wave with a wave-vector k_α, the metric corrections can be expressed as:

$$h_{\alpha\beta} = \left(\frac{1}{3}(h(t) + H(t))\delta_{\alpha\beta} - H(t)\frac{k_\alpha k_\beta}{k^2} \right) e^{ik_\gamma x^\gamma}$$

After the recombination, ina model filled with cold matter (both dark matter and baryons are cold then) one has:

$$h = 2\delta \qquad \dot{h} + \dot{H} = 0$$

where δ is the matter density perturbation

Vector perturbations

For vector perturbations one has:

$$\begin{aligned} \ddot{h}^{\perp} + 2\frac{\dot{a}}{a}\dot{h}^{\perp} &= 0 \quad \delta_M = 0 \\ \frac{ik}{a}\dot{h}^{\perp} &= 6\left(\frac{\dot{a}}{a}\right)^2 \frac{\delta v^{\perp}}{c} \end{aligned}$$

These kind of perturbations represent *vorticities*. Conservation of angular momentum ($a * \delta v^{\perp} =$ const) results in decrease of the velocity. The upper equation implies $a^2 * \dot{h}^{\perp} =$ const, so the metric perturbation also cannot grow.

Tensor perturbations

For tensor perturbations one has (for both polarizations):

$$\ddot{h}^x + 2\frac{\dot{a}}{a}\dot{h}^x + \frac{k^2}{a^2}h^x = 0 \quad \delta_M = 0 \qquad \delta v^\alpha = 0$$

On scales much larger than the horizon $k^2/a^2 \approx 0$ so $a^2\dot{h}^x =$ const. In the early Universe one has $\dot{h}^x \sim a^{-2} \sim t^{-1}$ so h^x can only grow logarithmically. $h^x =$ const is also a solution. When perturbation enters the horion it starts to oscillate. (The matter is unperturbed, so there are no Newtonian potential perturbations, which might result in instability.)

Tensor perturbations are not capable of inducing a macroscopic motion of gas, but can perturb the motion of collision-less particles. These *gravitational waves* may influence the photons at and just after recombination, inducing so called B-modes in the pattern of CMB polarization on the sky.

Primary perturbations, free streaming of photons We neglect photon scattering and nonlinear perturbations to the metric. In an unperturbed model the product of the momentum and scale factor $P \equiv p(t)a(t)$, remains constant for any free streaming particle. We expect its derivative in a perturbed model to be small. Calculations for a photon propagating along $\vec{n}$ show:

$$\frac{dP}{dt} = \frac{1}{2}\frac{dh_{\alpha\beta}}{dt} n^\alpha n^\beta \ P$$

We are interested in photon propagation after the recombination, in a nonrelativistic model filled with cold matter. For a photon at angle θ relative to wave-vector ($\cos\theta \equiv \mu = n^\alpha k_\alpha / k$) one has:

$$\frac{1}{P}\frac{dP}{dt} = \left(\frac{1}{6}(\dot{h} + \dot{H}) - \frac{1}{2}\dot{H}\mu^2\right) e^{ik\mu\chi} = \frac{1}{2}\dot{h}\mu^2 e^{ik\mu\chi}$$

where $\chi = \sqrt{x^2 + y^2 + z^2}$ and we have used the equality $\dot{h} + \dot{H} = 0$.

Photon propagation Using the conformal time η instead of t we get:

$$\begin{aligned} cdt =& a(t)d\eta \quad \Leftrightarrow \quad \frac{d}{dt} = \frac{c}{a}\frac{d}{d\eta} \\ \eta =& \int_0^t \frac{cdt'}{a(t')} \quad \Rightarrow \quad \chi = \eta_0 - \eta \\ \frac{1}{P}\frac{dP}{d\eta} =& \frac{1}{2}\frac{dh}{d\eta}\mu^2 e^{ik\mu(\eta_0 - \eta)} \end{aligned}$$

In a flat model with $\Omega_M = 1$, we would have $\eta \propto t^{1/3}$, and as a consequence the growing mode of density perturbation $\delta \propto \eta^2$ so the integral would be analytic.

Temperature fluctuations The temperature of radiation is proportional to the averaged energy of photons, so the relative perturbations of the temperature, energy and momentum are equal to each other:

$$\frac{\Delta T}{T}(k,\mu) = \frac{\Delta P}{P}(k,\mu)$$

A single flat wave perturbation causes the following dependence of the temperature fluctuations on the direction:

$$\begin{aligned} \left(\frac{\Delta T}{T}\right)_{obs}(k,\mu) &= \left(\frac{\Delta T}{T}\right)_{rec}(k,\mu) + \left(\frac{\Delta T}{T}\right)_{grav}(k,\mu) \\ \left(\frac{\Delta T}{T}\right)_{grav}(k,\mu) &= \int_{\eta_r}^{\eta_0} \frac{1}{2}\frac{dh}{d\eta}\mu^2 e^{ik\mu(\eta_0 - \eta)} d\eta \end{aligned}$$

Initial temperature perturbations; potential fluctuations

During the recombination photons were in contact with baryons (electrons to be precise), so the concentrations of both kinds of particles were proportional to each other and the sphere of last scattering was moving with baryons. Density perturbation (baryons + dark matter) cause gravitational potential perturbations. Photons from potential holes ($\delta\Phi < 0$) undergo gravitational

redshift ($\delta T/T = \delta\Phi/c^2$), but the field also delays their propagation, so the photons coming from holes must have been radiated relatively earlier. Quantatively:

$$\nabla^2\delta\Phi = 4\pi G\rho_0\delta \qquad -\frac{k^2}{a^2}\delta\Phi = 4\pi G\rho_0\delta$$

$$\delta\Phi \sim a^2\rho_0\delta \sim t^1 * t^{-2} * t^1 \sim t^0 \qquad \delta\Phi \sim a^2\rho_0\delta \sim t^{4/3} * t^{-2} * t^{2/3} \sim t^0$$

in an early ($P = \epsilon/3$) and late ($P = 0$) stage of evolution. Time in a potential hole goes slower than at "infinity":

$$t' = (1 + \frac{\delta\Phi}{c^2})t \qquad \delta t = t' - t = \frac{\delta\Phi}{c^2}t$$

Recombination takes place when $P \approx 0$ and when $T \sim t^{-2/3}$ so:

$$\frac{\delta T}{T} = -\frac{2}{3}\frac{\delta t}{t} = -\frac{2}{3}\frac{\delta\Phi}{c^2}$$

and finally:

$$\frac{\delta T}{T} = \frac{\delta\Phi}{c^2} - \frac{2}{3}\frac{\delta\Phi}{c^2} = \frac{1}{3}\frac{\delta\Phi}{c^2}$$

Temperature fluctuations during the recombination The baryon density and velocity also have their impact:

$$\frac{\delta n_\gamma}{n_\gamma} = \frac{\delta n_B}{n_B} = \delta_B \qquad \frac{\delta n_\gamma}{n_\gamma} = 3\frac{\delta T_\gamma}{T_\gamma}$$

$$\left(\frac{\Delta T}{T}\right)_{rec} = \frac{1}{3}\delta_B - \frac{v_B}{c}\mu + \frac{1}{3}\frac{\delta\Phi}{c^2}$$

At the recombination potential perturbations are defined by the dark matter + baryon density fluctuations (dark dominating) $\delta_M \sim -k^2\delta\Phi/c^2$. For baryons one has $\delta_B \sim kv_B/c$. (See Fig. 5.1).

Comparison of amplitudes at recombination Velocity and density perturbations:

$$\begin{aligned} \dot\delta_B &= -\nabla\delta\vec v_B \\ \dot\delta_B(k) &= -\frac{i\vec k}{a}\delta\vec v_B \\ \Rightarrow \left|\frac{\delta v_b}{c}\right| &= \left|\frac{a}{kc}\dot\delta_B\right| \end{aligned}$$

where we use the fact that acoustic waves are longitudinal so the velocity vector is parallel to the wave vector. (Observers looking along the wave-vector may observe the full velocity amplidude times the phase factor. Looking sideways: full amplitude times the directional cosine times the phase factor dependening also on the direction). In numerical calculations we assume Harrison - Zeldovich primary spectrum $\delta_{prim}(k) \sim \sqrt{k}$

Potential and density perturbations:

$$\left|\frac{\delta\Phi}{c^2}\right| = \frac{a(z)^2}{k^2c^2}\ 4\pi G\Omega_M(1+z)^3\frac{3H_0^2}{8\pi G}\ \delta_M = \frac{3\Omega_M(1+z_{rec})}{2k^2}\left(\frac{a_0}{c/H_0}\right)^2\delta_M$$

Potential perturbations dominate if:

$$k < \sqrt{\frac{3}{2}\Omega_M(1+z_{rec})} * \frac{1}{3000} \approx 0.00742\frac{h}{1\text{Mpc}} \equiv 22.3\frac{1}{c/H_0}$$

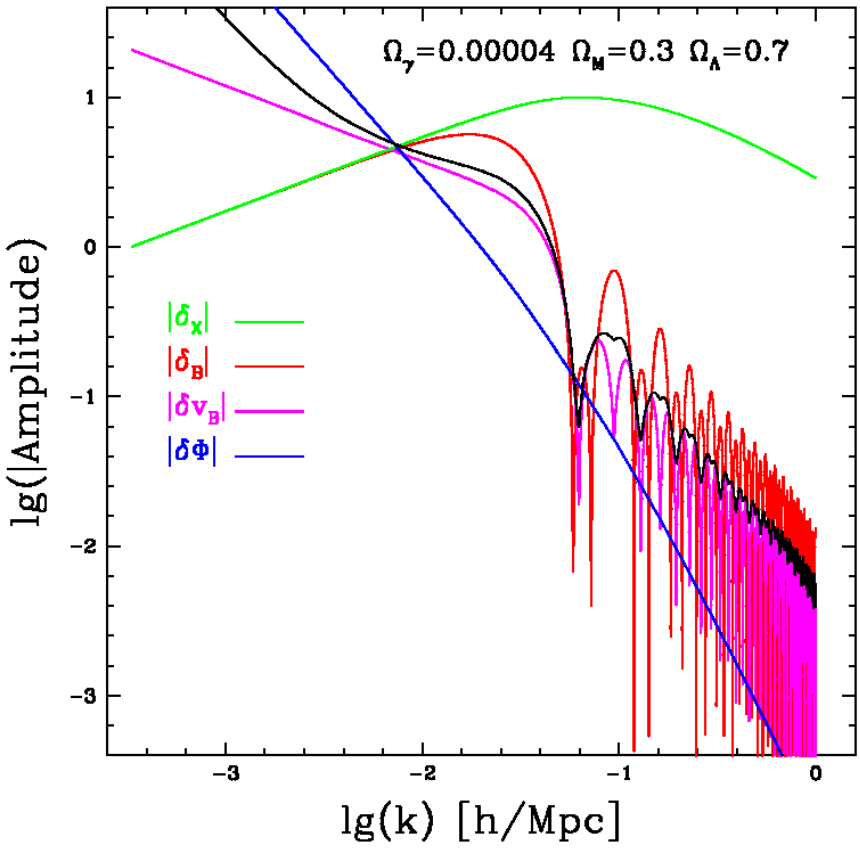

Figure 5.1: Comparison of the amplitudes of various modes at recombination

where we choose either $a_0 = 1$ MPc$/h$ or $a_0 = c/H_0$. In Fig. 5.1 we draw in black:

$$\frac{\delta T}{T} \sim \sqrt{\left(\frac{\delta\Phi}{3c^2}\right)^2 + \left(\frac{\delta v_B}{c}\right)^2 + \left(\frac{\delta_B}{3}\right)^2}$$

The units are arbitrary, so the black line does not give the expected value of CMB temperature fluctuations (which depends also on the direction of observations and the phase of plane wave at the observer location) but illustrates roughly its dependence on k.

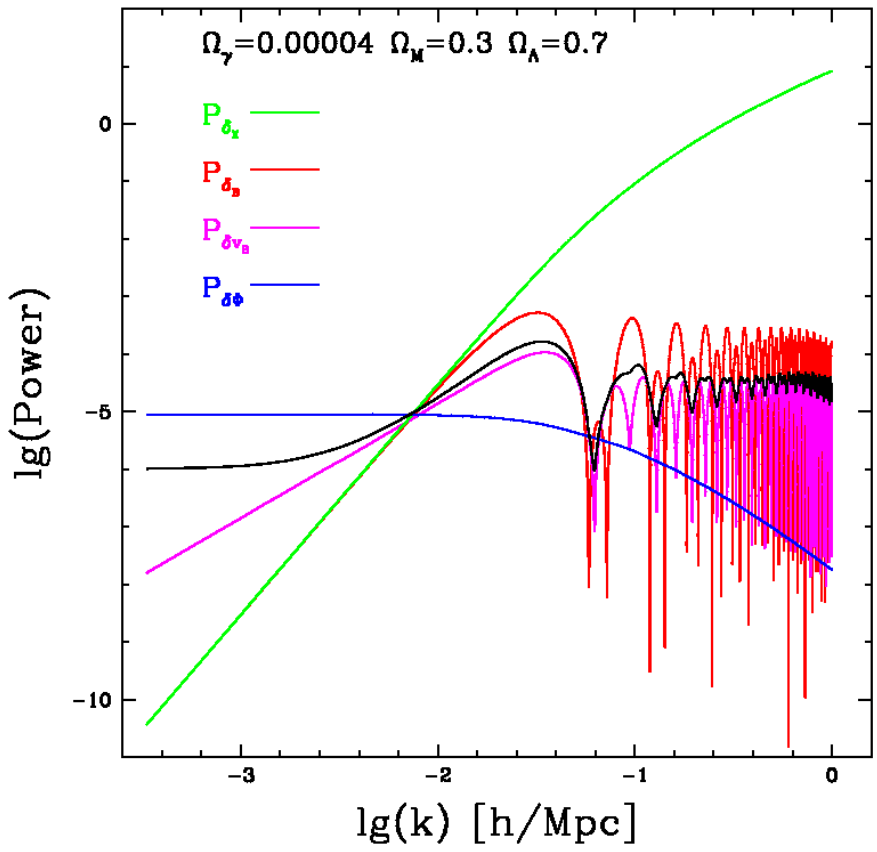

Figure 5.2: Comparison of the power spectra of various modes $P(k) = k^3|\delta_k|^2$

Comparison of power spectra at recombination

In Fig. 5.2 we show shapes of power spectra of the density, velocity and potential perturbations at recombination. Each power spectrum is defined as:

$$P_\delta(k) = k^3 * |\delta(k)|^2$$

The black line this time shows:

$$P(k) = \frac{1}{9}P_{\delta\Phi}(k) + P_{\delta v_B}(k) + \frac{1}{9}P_{\delta_B}(k)$$

which roughly gives the shape of the k-dependence of the sum of various components perturbing CMB temperature.

5.2 CMB anisotropy spectrum

Temperature fluctuations

The last scattering sphere (LSS) in our coordinates has the radius $\chi_r = \eta_0 - \eta_r$. A single plane wave perturbation introduces position dependent temperature fluctuation on LSS where $\mu \equiv \cos\theta$ is the cosine of the angle between the direction of observation and the wave-vector. The propagation of photons between LSS and the observer through the perturbed space-time introduces another kind of fluctuations dubbed *gravitational* here:

$$\left(\frac{\Delta T}{T}\right)_{rec}(k,\mu) = \left(\frac{1}{3}\delta_B - \frac{v_B}{c}\mu + \frac{1}{3}\frac{\delta\Phi}{c^2}\right)e^{ik\mu\chi_r}$$
$$\left(\frac{\Delta T}{T}\right)_{grav}(k,\mu) = \int_{\eta_r}^{\eta_0}\frac{1}{2}\frac{dh}{d\eta}\mu^2 e^{ik\mu(\eta_0-\eta)}d\eta$$
$$\left(\frac{\Delta T}{T}\right)_{obs}(k,\mu) = \left(\frac{\Delta T}{T}\right)_{rec}(k,\mu) + \left(\frac{\Delta T}{T}\right)_{grav}(k,\mu)$$

The effect of propagation introduces so called secondary fluctuations to the CMB. We shall skip it now concentrating on the primary fluctuations as inprinted in LSS.

For a single plane wave one can choose the z axis along the wave-vector, which implies the cylindrical symmetry relative to this axis. The decomposition into spherical harmonics contains then only the $m = 0$ terms:

$$a_{l0} = \sqrt{\frac{2l+1}{2}}\int_{-1}^{1} d\mu P_l(\mu)\left(\frac{\Delta T}{T}\right)(k,\mu)$$

where a_{l0} is the coefficent of the expansion into spherical harmonics series calculated as the integral over the sphere of $\Delta T/T$ with Y_{l0}.

Potential perturbations effect

For a single component of potential perturbations one has:

$$\begin{aligned} a_{l0}^{\Phi}(k) =& \sqrt{\frac{2l+1}{2}}\int_{-1}^{1} d\mu P_l(\mu)\frac{\delta\Phi_k}{3c^2}e^{ik\mu\chi_r} \\ =& \frac{2}{i^l}\sqrt{\frac{2l+1}{2}}\frac{\delta\Phi_k}{3c^2}\; j_l(k\chi_r) \end{aligned}$$

where $j_l()$ is a spherical Bessel function of the order l. Summation over plane waves gives:

$$\begin{aligned} C_l^{\Phi} =& \frac{4\pi}{2l+1}\int_0^{\infty}\frac{dk}{k}k^3|a_{l0}^{\Phi}(k)|^2 \\ =& \frac{8\pi}{9}\int_0^{\infty}\frac{dk}{k}k^3\left|\frac{\delta\Phi_k}{c^2}\right|^2 j_l^2(k\chi_r) \end{aligned}$$

The spectrum of potential perturbation under the integral should be flat according to Harrison - Zeldovich argument.

$$k^3\left|\frac{\delta\Phi_k}{c^2}\right|^2 \sim k^0$$

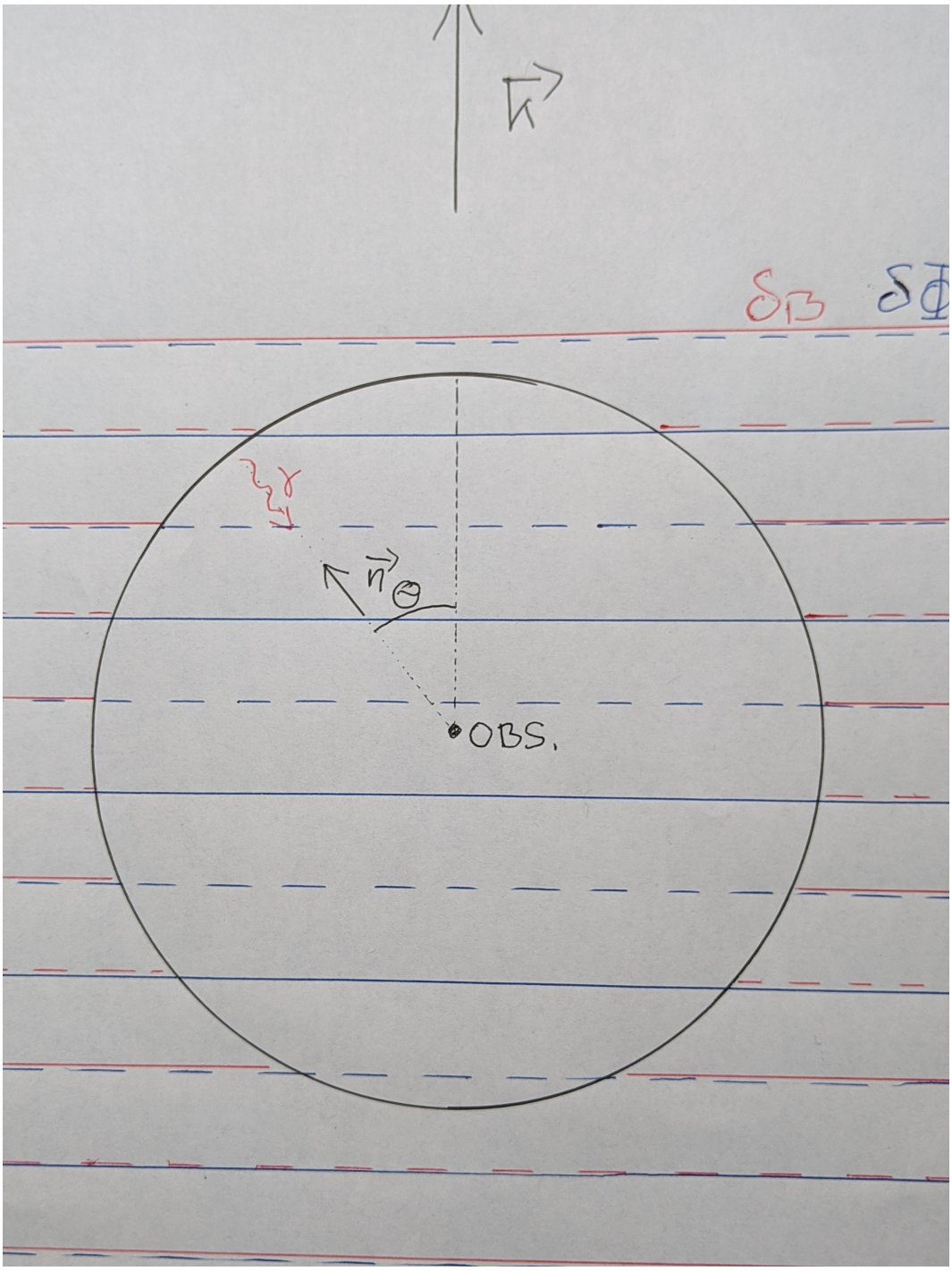

Figure 5.3: Last scattering sphere (LSS) and a "long" plane wave. Solid lines show the maxima of perturbations, dashed lines the minima. Red is used for baryon density fluctuations, blue for potential perturbations (where density has maximum, potential has minimum). Inside the sphere (between the sphere and the observer, or after the recombination) the red is absent since photons decoupled from plasma on LSS. Blue is present to denote metric perturbations which can still influence the photons.

to avoid singularity at $k \to 0$ or $k \to \infty$. The growth of perturbations in an expanding model conserves the spectrum shape for long waves and there is a cut at shorter wave-lengths, which does not affect multipoles with low l:

$$C_l^\Phi \sim \int_0^\infty \frac{dk}{k} j_l^2(k\chi_r) = \int_0^\infty \frac{dx}{x} j_l^2(x) \sim \frac{1}{l(l+1)}$$

Density perturbations effect

For a single component one has:

$$\begin{aligned} a_{l0}^\rho(k) =& \sqrt{\frac{2l+1}{2}} \int_{-1}^1 d\mu P_l(\mu) \delta_B(k) e^{ik\mu\chi_r} \\ =& \frac{2}{i^l} \sqrt{\frac{2l+1}{2}} \delta_B(k)\ j_l(k\chi_r) \end{aligned}$$

Integrating we obtain:

$$\begin{aligned} C_l^\rho =& \frac{4\pi}{2l+1} \int_0^\infty \frac{dk}{k} k^3 |a_{l0}^\rho(k)|^2 \\ =& \frac{8\pi}{9} \int_0^\infty \frac{dk}{k} k^3 \left|\delta_B(k)\right|^2 j_l^2(k\chi_r) \end{aligned}$$

This time there is density fluctuation spectrum under the integral:

$$k^3 \left|\delta_B(k)\right|^2 = \left[k^3 \left|\delta_B(k)\right|^2\right]_{\text{init}}\ T_B^2(k) \sim k^4\ T_B^2(k)$$

where $T_B(k)$ is the transmission factor. This is rather a complicated function of k (see Fig. 5.2) so a numerical integration is needed.

Velocity perturbation effect

For a single component one has;

$$\begin{aligned} a_{l0}^v(k) =& \sqrt{\frac{2l+1}{2}} \int_{-1}^1 d\mu P_l(\mu) \frac{v_B}{c}(k) \mu e^{ik\mu\chi_r} \\ =& 2\sqrt{\frac{2l+1}{2}} \frac{v_B}{c}(k)\ \left(\frac{l+1}{2l+1} j_{l+1}(k\chi_r) - \frac{l}{2l+1} j_{l-1}(k\chi_r) \right) \end{aligned}$$

The formula is more complicated, since there is dependence on the direction on the sky, not only on the velocity amplitude and $\mu P_l(\mu)$ (not $P_l(\mu)$ alone) is integrated with the exponential function.

$$\begin{aligned} C_l^v =& \frac{4\pi}{2l+1} \int_0^\infty \frac{dk}{k} k^3 |a_{l0}^v(k)|^2 \\ \propto& \int_0^\infty \frac{dk}{k} k^1 \left|\delta_B(k)\right|^2 \left(\frac{l+1}{2l+1} j_{l+1}(k\chi_r) - \frac{l}{2l+1} j_{l-1}(k\chi_r) \right)^2 \end{aligned}$$

where we have used the approximation $v_B \sim \delta_B/k$. This is not always valid and in practice one should use the velocity perturbation with greater reliability (i.e. numerically calculated).

CMB anisotropy spectrum

Using our results for two-fluid instability we make our own calculation of CMB anisotropy. Spectra of perturbations at the epoch of recombination $P_{\delta_B}(k)$, $P_{\delta v_B}(k)$, and $P_{\delta\Phi}(k)$ are the results

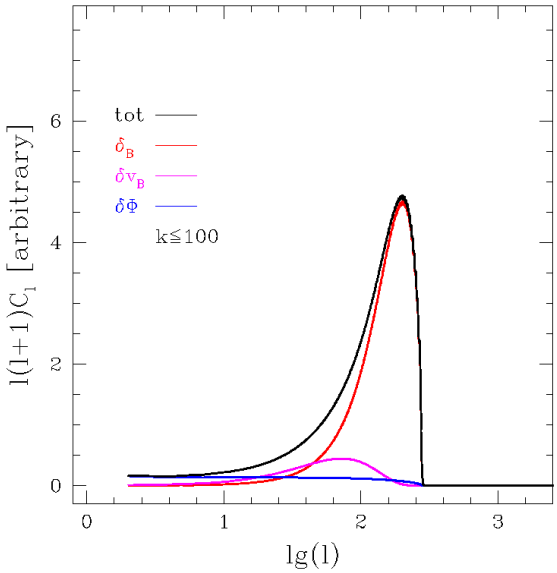
tot
δ_B
δv_B
$\delta\Phi$
k≦100
l(l+1)C$_l$ [arbitrary]
lg(l)

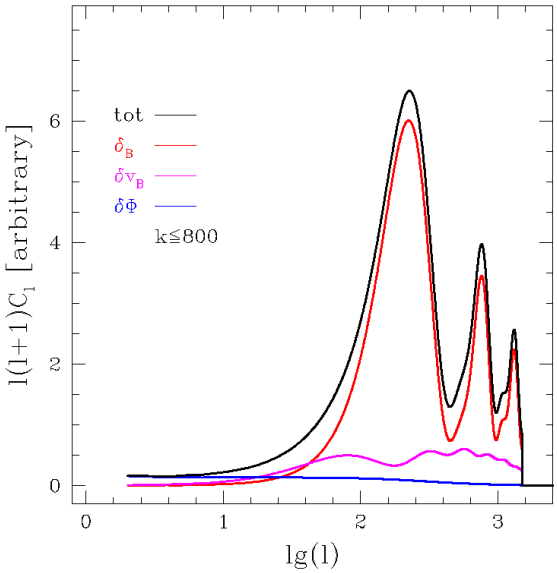
tot
δ_B
δv_B
$\delta\Phi$
k≦800
l(l+1)C$_l$ [arbitrary]
lg(l)

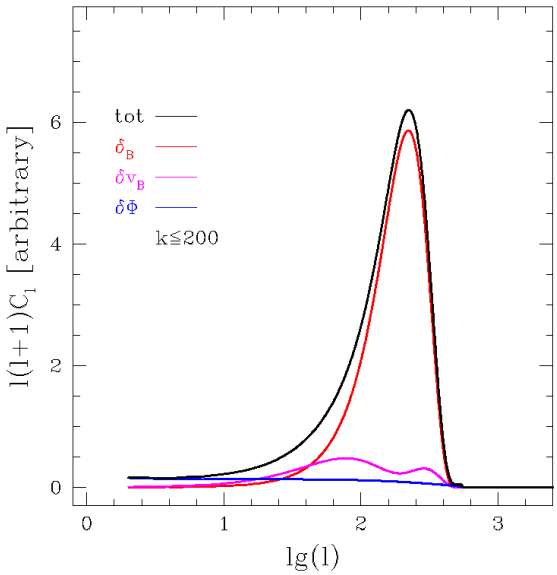
tot
δ_B
δv_B
$\delta\Phi$
k≦200
l(l+1)C$_l$ [arbitrary]
lg(l)

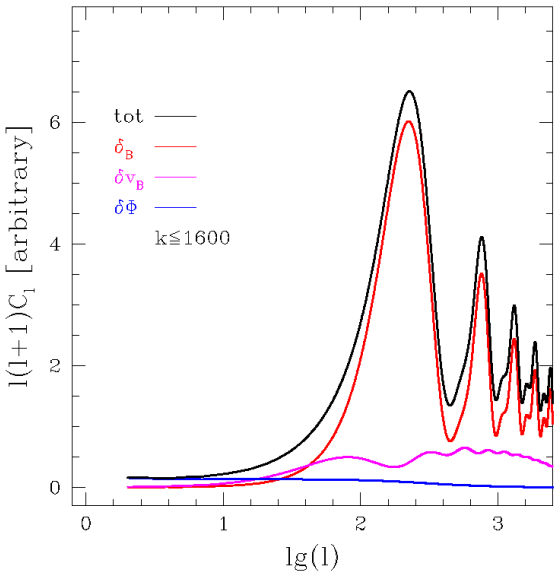
tot
δ_B
δv_B
$\delta\Phi$
k≦1600
l(l+1)C$_l$ [arbitrary]
lg(l)

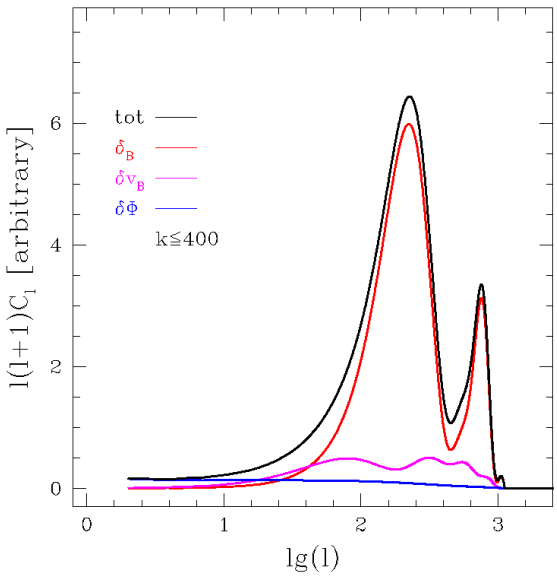
tot
δ_B
δv_B
$\delta\Phi$
k≦400
l(l+1)C$_l$ [arbitrary]
lg(l)

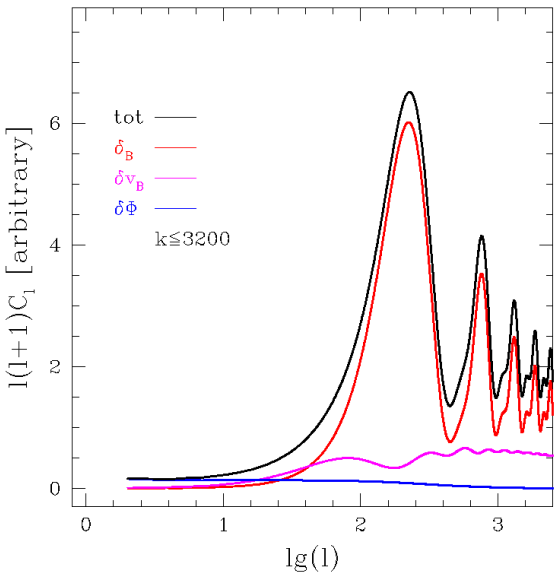
tot
δ_B
δv_B
$\delta\Phi$
k≦3200
l(l+1)C$_l$ [arbitrary]
lg(l)

of our caculations. Spherical Bessel functions are calculated with the help of *Numerical Recipes*. The coordinate distance to recombination for a flat model with $\Omega_M = 0.3$ and $\Omega_\Lambda = 0.7$ is

$$\chi_r = \int_0^{z_{rec}} \frac{dz}{h(z)} = 2.775$$

which translates into comoving distance $c/H_0 * \chi_r$. (In a flat $\Omega_M = 1$ model $\chi_r = 3$, a close value.) So here c/H_0 is a length unit and wave number $k = 1$ corresponds to the wavelength $\lambda = 2\pi c/H_0$ (and $\lambda(k) = 2\pi c/H_0/k$. Instability results cover $k = 1, 2, 3, ..., 6000$. Above $k \approx 3500$ *Recipes* suggest using asymptotic formulae for Bessels...

The figures below show the CMB anisotropy spectrum based on growing number of plane waves taken into account, $(k \leq 100, 200, ..., 3200)$. One can see that short waves are necessary to model high order multipoles. Also: with $k \leq 3200$ we reach $l \leq 3000$ and there is not much difference between using $k \leq 1600$ and $k \leq 3200$.

Calculations are qualitatively good (domination of potential pert. for low l, position of the 1st peak, presence of other peaks ...)

The ratio of peaks heights is wrong (2nd and 3rd should be comparable).

These are preliminary results of calculations with known numerical limitations. There is no guarantee this will be overcome. Others have already produced their nice plots ...

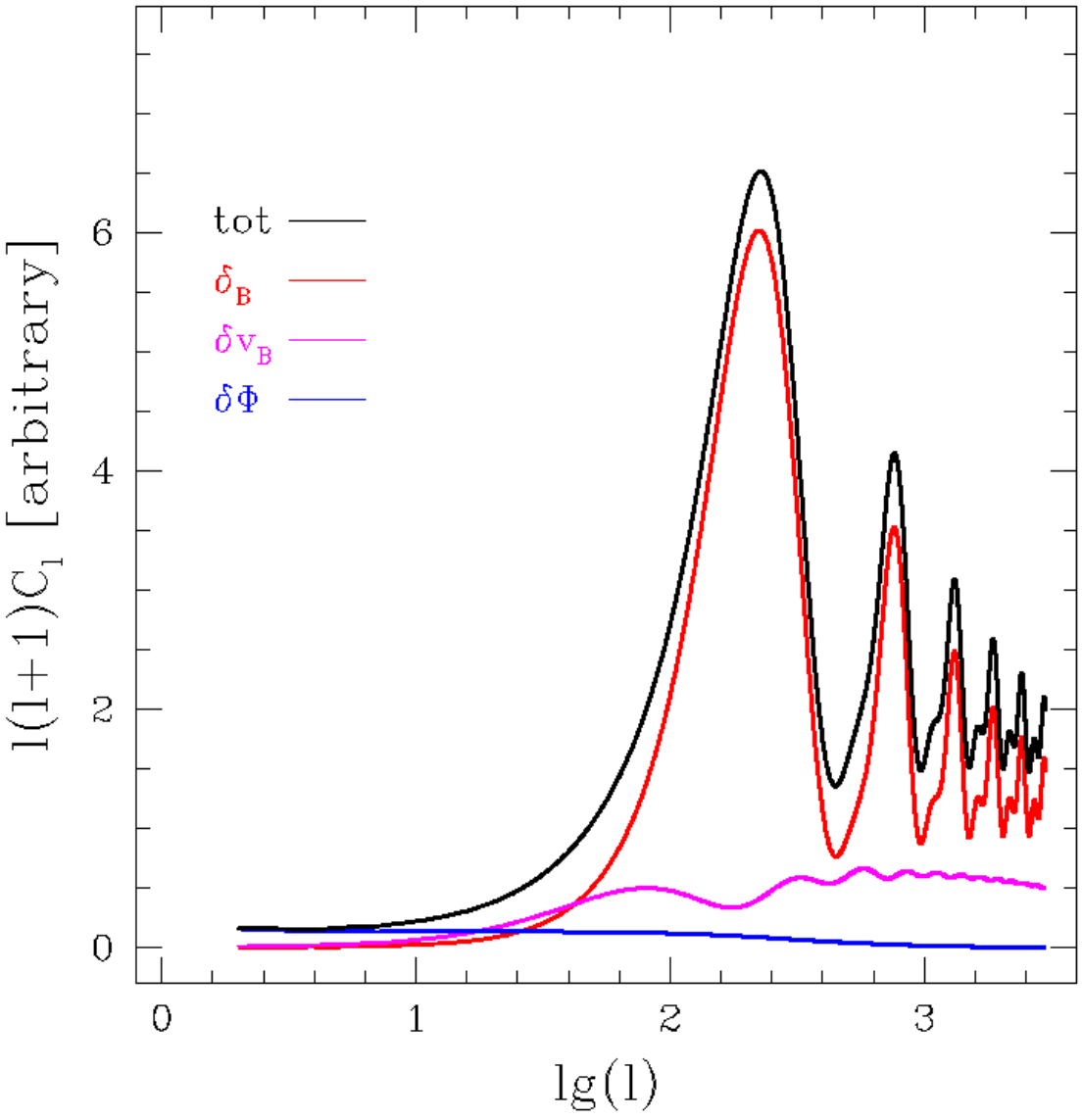

Figure 5.4: CMB anisotropy power spectrum based on the calculations of two-fluid instability. The domination of potential perturbations as a source of anisotropy is seen up to $l \approx 20$, where the blue line ($\delta\Phi$) crosses the magenta line (δv_B). For $l \geq 40$ the domination of density perturbations is present, after the magenta and the red line (δ_B) cross. (Should this occur for larger l ? Are the velocity perturbations somehow suppressed ?

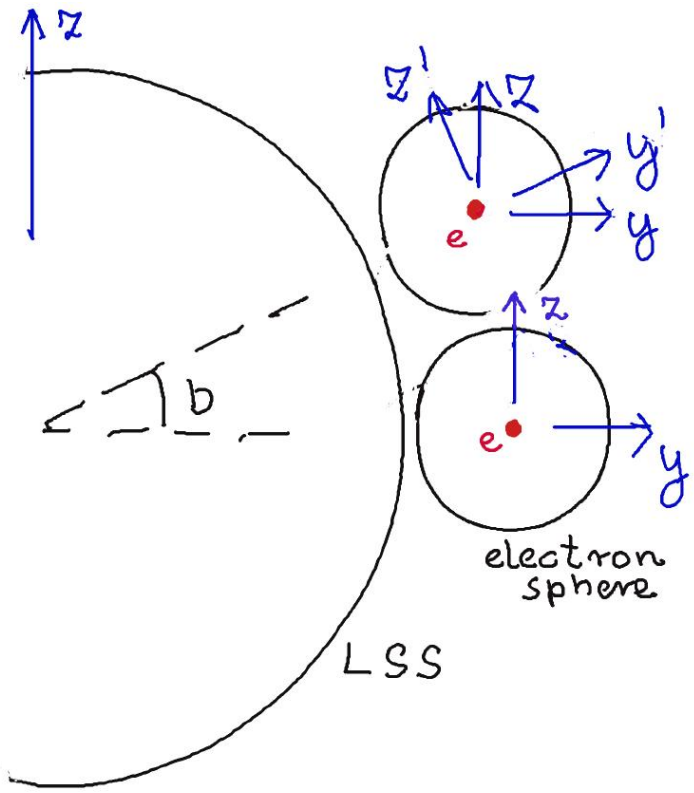

Figure 5.5: *Electron sphere*

5.3 CMB polarization

At the last scattering surface (LSS) photons are scattered, not emitted. The angular distribution of scattered photons depends on their polarization ⇒ photons scattered toward an observer may be partially polarized.

Considering the radiation as electromagnetic (EM) waves is the simplest way to get some intuition. On the celestial sphere directions E, W, N, and S are well defined and all are perpendicular to the line of sight (LOS). Suppose there is a scattering region at LSS on our LOS and there is a single unpolarized EM wave coming to the region from E. EM waves are transversal, so the excited electrons move in the plane defined by LOS and N-S. There is no electron motion in E-W direction. As a consequence the scattered wave along LOS is completely polarized in N-S direction. Of course EM waves scattered in other direction are only partially polarized with details depending on the geometry.

In reality radiation is coming to any region on LSS near some LOS from all possible directions, in the first approximation from a sphere of optical depth unity, $\tau_e = 1$. Below we consider this approximation in detail.

Electron in LSS Photons which are scattered by an electron in LSS and then go to the observer, earlier travel the distance $\sim \Delta r$ corresponding to the unit optical depth ($\Leftrightarrow \; n_e \Delta r \sigma_e = 1$). To be more accurate: the intensity of the radiation coming from given direction is an integral along LOS taking into account contributions from all optical depths:

$$I = \int_0^\infty I(\tau) \exp(-\tau) d\tau$$

In the presence of perturbations the intensity varies along LOS. In our approximations we make 2nd order Taylor expansions, so

$$\begin{aligned} I(\tau) &= I_0 + I'\tau + \frac{1}{2}I''\tau^2 \\ I &= \int_0^\infty I(\tau)\exp(-\tau)d\tau = I_0 + I' + I'' \end{aligned}$$

Taking into account only the linear term we see that $I = I(\tau = 1)$, which is equivalent to the assumption that all photons come from the sphere of $\tau = 1$ surrounding the electron. With the quadratic term alone we have $I = I(\tau = \sqrt{2})$, which makes the radius of the sphere $\sqrt{2}$ times larger. We shall use the name *electron sphere* for a region of $\tau \approx 1$ surrounding an electron, compare Fig. 5.5.

The critical density today corresponds to $\sim 12h^2$ baryons/m^3. Taking into account density of baryon matter $\Omega_B = 0.022/h^2$ and primordial abundances ($X = 0.75$, $Y = 0.25$) we get the present averaged electron density $n_0 = 0.45h^2$ electrons/m^3. The distance corresponding to $\tau = 1$ at recombination is:

$$\begin{aligned} n_0(1 + z_{rec})^3\sigma_e\Delta r = 1 \quad &\Rightarrow \quad \Delta r \approx 2.8\times 10^{19}h^{-2}\text{ m} \approx 0.9h^{-2}\text{ kpc} \\ \Delta r_0 = (1+z_{rec})\Delta r \approx 1h^{-2}\text{Mpc} \quad &\Rightarrow \quad \Delta\chi = \frac{\Delta r_0}{c/H_0} = \frac{1}{3000h} \approx 0.000476 \end{aligned}$$

We calculate the comoving size of the electron sphere (Δr_0) and the corresponding coordinate size, where we use c/H_0 as a unit of length today and $H_0 = 70$ km/s/Mpc ($h = 0.7$). In approximations below we treat $k\Delta\chi$ as small quantity, which correspond to $k < 2100$. For shorter wavelengths corresponding to higher wave numbers some of our approximations below do not hold.

5.3.1 Scalar perturbations

For a single scalar wave one can define an effective temperature fluctuation as:

$$\begin{aligned} T &= T_0\left(1 + \frac{1}{3}\delta_B(k) - \frac{v(k)\cos\theta}{c} + \frac{1}{3}\frac{\delta\Phi(k)}{c^2}\right) \\ &= T_0 + \Delta_1 T(k)\cos(kz+\alpha_0) + \Delta_2 T(k)\cos\theta\sin(kz+\alpha_0) \\ \Delta_1 T(k) &= \left(\frac{1}{3}\delta_B(k) + \frac{1}{3}\frac{\delta\Phi(k)}{c^2}\right)T_0 \qquad \Delta_2 T(k) = -\frac{v(k)}{c}T_0 \end{aligned}$$

where baryon density, velocity, and potential perturbations are taken into account. Wave vector is directed along the z-axis, the electron is in the origin of the coordinate system, α_0 is the wave phase at $z = 0$, and θ is the spherical coordinate on the sphere. We take into account the $\pi/2$ shift of the velocity perturbation phase. If the surface of the electron sphere were a black body, it would emit radiation with intensity $I = \sigma T^4/\pi$. The surface is only a thought experiment, but the radiation at its location is a blackbody of given temperature, so the formula for I is correct. Few conventions and facts:

$$\begin{aligned} z &= \chi\cos\theta \quad \tau = \frac{\chi}{\Delta\chi} \;\Rightarrow\; kz = k\Delta\chi\cos\theta * \tau \equiv a\tau \\ \int_0^\infty &\cos(a\tau)exp(-\tau)d\tau = \frac{1}{1+a^2} \qquad \int_0^\infty \sin(a\tau)exp(-\tau)d\tau = \frac{a}{1+a^2} \end{aligned}$$

The intensity of the radiation exciting the photon may be written as (where at the beginning we avoid approximations):

$$\begin{aligned} I(\theta) &= I_0 + (\Delta_1 I \cos\alpha_0 + \Delta_2 I \sin\alpha_0 \cos\theta) \int_0^\infty \cos(a\tau)\exp(-\tau)d\tau \\ &+ (-\Delta_1 I \sin\alpha_0 + \Delta_2 I \cos\alpha_0 \cos\theta) \int_0^\infty \sin(a\tau)\exp(-\tau)d\tau \\ &= I_0 + \frac{\Delta_1 I \cos\alpha_0 + \Delta_2 I \sin\alpha_0 \cos\theta}{1 + k^2\Delta\chi^2\cos^2\theta} \\ &+ \frac{(-\Delta_1 I \sin\alpha_0 + \Delta_2 I \cos\alpha_0 \cos\theta) k\Delta\chi \cos\theta}{1 + k^2\Delta\chi^2\cos^2\theta} \end{aligned}$$

As we shall learn below, only the part of $I(\theta)$ which is even in $\cos\theta$ will give nonvanishing contribution to expressions of interest averaged over the sphere. Omitting odd terms and isotropic part, which plays no role in polarization, we have

$$I(\theta) = \frac{\Delta_1 I + \Delta_2 I k\Delta\chi\cos^2\theta}{1 + k^2\Delta\chi^2\cos^2\theta}\cos\alpha_0$$

The Cartesian coordinate system (x, y, z) in part seen on Fig. 5.5 has the x-axis along the E-W direction (perpendicular to the figure plane). The coordinate system (θ, ϕ) on the electron sphere has standard relation to the Cartesian one.

The intensity of radiation coming from the different directions on the electron sphere depends on one coordinate $I = I(\theta)$ and is unpolarized (both polarization have the same intensity). Radiation coming from a given direction can excite electron motion in the perpendicular plane. For EM waves coming from (θ, ϕ) and having polarization along ϕ direction (or along parallels on the electron sphere) the resulting excitations are:

$$E_x^2(\theta,\phi) \sim I(\theta)\sin^2\phi \qquad E_y^2(\theta,\phi) \sim I(\theta)\cos^2\phi \qquad E_z^2(\theta,\phi) = 0$$

Where E_x^2 (E_y^2) symbolize the square of the electric field along x (y) axis in an emitted by the electron EM wave. The incident radiation is incoherent so we add intensities of contributions from diffrent directions (and intensities are proportional to E^2), not amplitudes. For EM waves with polarization along θ direction (along the meridians on the electron sphere) we have:

$$E_x^2(\theta,\phi) \sim I(\theta)\cos^2\theta\cos^2\phi \qquad E_y^2(\theta,\phi) \sim I(\theta)\cos^2\theta\sin^2\phi \qquad E_z^2(\theta,\phi) \sim I(\theta)\sin^2\theta$$

We take into account EM waves from the whole electron sphere. Averaging over ϕ we get

$$\begin{aligned} < E_x^2 >_\phi &= < I(\theta)(\sin^2\phi + \cos^2\theta\cos^2\phi) >_\phi = \frac{1}{2} I(\theta)(1 + \cos^2\theta) \\ < E_y^2 >_\phi &= < E_x^2 >_\phi \\ < E_z^2 >_\phi &= < I(\theta)\sin^2\theta >_\phi = I(\theta)\sin^2\theta \\ Q(\theta) &= E_x^2 - E_z^2 = I(\theta)\left(\frac{3}{2}\cos^2\theta - \frac{1}{2}\right) \end{aligned}$$

where we have introduced $Q(\theta)$, which, after averaging over the electron sphere, becomes the

Stokes polarization parameter for the emission along y-axis. Averaging gives:

$$\begin{aligned}
\langle Q(\theta)\rangle_\theta &= \int_0^{\pi/2} \sin\theta d\theta Q(\theta) \\
&= \Delta_1 I \cos\alpha_0 f_1(k\Delta\chi) + \Delta_2 I \cos\alpha_0 f_2(k\Delta\chi) \\
f_1(k\Delta\chi) &= \frac{3}{2}C_2(k\Delta\chi) - \frac{1}{2}C_0(k\Delta\chi) \qquad f_2(k\Delta\chi) = \left(\frac{3}{2}C_4(k\Delta\chi) - \frac{1}{2}C_2(k\Delta\chi)\right) k\Delta\chi \\
C_n(k\Delta\chi) &= \int_0^{\pi/2} \sin\theta d\theta \frac{\cos^n\theta}{1+k^2\Delta\chi^2\cos^2\theta}
\end{aligned}$$

The integrals C_n are analytic (include arctg$(k\Delta\chi)$). For low k ($\Rightarrow\ k\Delta\chi \ll 1$) $f_1(k\Delta\chi) \sim k^2\Delta\chi^2$ while $f_2(k\Delta\chi) \sim k\Delta\chi$ so for low k the velocity perturbations are relatively more important.

We have calculated the polarization as seen along the y-axis, perpendicular to the wave-vector. Now we shall calculate the polarization as seen by observer from different direction (axis y' on Fig. 5.5). Again using the argument "add intensities not amplitudes" we have:

$$\begin{aligned}
E_{z'}^2 &= E_z^2\cos^2 b + E_y^2\sin^2 b \ \ (\text{and } E_{y'}^2 = E_y^2\cos^2 b + E_z^2\sin^2 b \ \ E_{x'}^2 = E_x^2) \\
E_{x'}^2 - E_{z'}^2 &= E_x^2 - E_z^2\cos^2 b - E_y^2\sin^2 b = (E_x^2 - E_z^2)\cos^2 b \ \Rightarrow \\
Q(b) &= Q(0)\cos^2 b
\end{aligned}$$

The relation between Stokes parameters measured at different angles is solely due to the projection. When looking at different positions on LSS the modulation by the perturbation phase is also present. Going back to the first group of equations in this subsection we have:

$$Q_k(\mu) = (\Delta_1 I f_1(k\Delta\chi)\cos(k\chi_r\mu + \alpha_0) + \Delta_2 f_2(k\Delta\chi)\sin(k\chi_r\mu + \alpha_0))\,(1-\mu^2)$$

where we use $\mu = \cos\Theta$, where Θ is a spherical coordinate on LSS sphere. This gives the polarization pattern on LSS due to a single plane component. Expansion into spherical harmonics gives the coefficients:

$$\begin{aligned}
b_{l0}(k) &= \Delta_1 I f_1(k\Delta\chi)\cdot\sqrt{\frac{2l+1}{2}}\int_{-1}^{+1} d\mu P_l(\mu)(1-\mu^2)\cos(k\chi_r\mu+\alpha_0) \\
&+ \Delta_2 I f_2(k\Delta\chi)\cdot\sqrt{\frac{2l+1}{2}}\int_{-1}^{+1} d\mu P_l(\mu)(1-\mu^2)\sin(k\chi_r\mu+\alpha_0)
\end{aligned}$$

For odd values of l the first integral vanishes, for even l values - the second, so the contributions from the potential/density perturbations and from the velocity perturbations add separately. For simplicity one may use complex number notation:

$$\begin{aligned}
b^1_{l0}(k) &= \Delta_1 I f_1(k\Delta\chi)\cdot\sqrt{\frac{2l+1}{2}}\int_{-1}^{+1} d\mu P_l(\mu)(1-\mu^2)\exp(ik\chi_r\mu+i\alpha_0) \\
b^2_{l0}(k) &= -i\Delta_2 I f_2(k\Delta\chi)\cdot\sqrt{\frac{2l+1}{2}}\int_{-1}^{+1} d\mu P_l(\mu)(1-\mu^2)\exp(ik\chi_r\mu+i\alpha_0)
\end{aligned}$$

having in mind the real part of te expressions and then forgetting about it. The integrals with $P_l(\mu)$ produce spherical Bessel functions of the order l ($j_l(k\chi_r)$). With an extra μ^2 factor we get a combination of j_l and $j_{l\pm2}$:

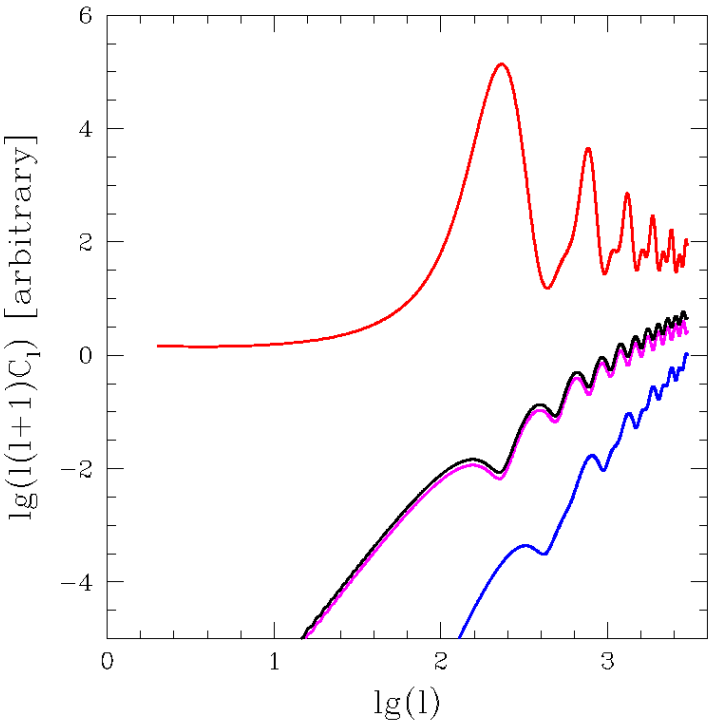

Figure 5.6: Red: temperature anisotropy power spectrum (C_l^{TT}) Black: polarizatio anisotropy (C_l^{EE}) in different scale. Magenta: velocity perturbations contribution to polarization, blue: potential + density perturbation contribution.

$$\begin{aligned} F_l(k\chi_r) &= -\frac{2}{i^{l+2}}\frac{(l+2)(l+1)}{(2l+3)(2l+1)}j_{l+2}(k\chi_r) + \frac{2}{i^l}\frac{2l^2+2l-2}{(2l+3)(2l-1)}j_l(k\chi_r) - \frac{2}{i^{l-2}}\frac{l(l-1)}{(2l+1)(2l-1)}j_{l-2}(k\chi_r) \\ &= \frac{2}{i^l}\left(\frac{(l+2)(l+1)}{(2l+3)(2l+1)}j_{l+2}(k\chi_r) + \frac{2l^2+2l-2}{(2l+3)(2l-1)}j_l(k\chi_r) + \frac{l(l-1)}{(2l+1)(2l-1)}j_{l-2}(k\chi_r)\right) \end{aligned}$$

Finally we calculate the polarization power spectrum adding contributions from all plane wave components:

$$\begin{aligned} C_l &= \frac{4\pi}{2l+1}\int_{-\infty}^{+\infty} d\ln k\ k^3|b_{l0}(k)|^2 \\ &= \pi\int_{-\infty}^{+\infty} d\ln k\ k^3(|\Delta_1 I(k)f_1(k\Delta\chi)|^2 + |\Delta_2 I(k)f_2(k\Delta\chi)|^2)F_l(k\chi_r)F_l^*(k\chi_r) \end{aligned}$$

Again two kinds of perturbations which are shifted in phase by $\pi/2$ add separately in quadrature. The shape of the polarization anisotropy power spectrum (with two contributions and their sum shown separately) is plotted in Fig. 5.6.

5.3.2 Vector perturbations

We use the same coordinate system in the electron sphere, with z-axis along the wave-vector. The velocity perturbations have the direction of the x axis. $\vec{n}$ is a unit vector at the electron sphere center in the direction of (θ, ϕ) on its surface. The temperature on the sphere as seen from the

electron position is:

$$\begin{aligned}
\vec{v} &= (\delta v \sin(\alpha_0 + kz), 0, 0) \qquad \vec{n} = (\sin\theta\cos\phi, \sin\theta\sin\phi, \cos\theta) \\
T(\theta,\phi) &= T_0(1 - \vec{v}\cdot\vec{n}/c) \\
I(\theta,\phi) &= I_0 + \Delta I \sin(\alpha_0 + kz)\sin\theta\cos\phi \\
&= I_0 + \Delta I\,(\cos\alpha_0 \sin(kz) + \sin\alpha_0\cos(kz))\sin\theta\cos\phi
\end{aligned}$$

where $|\Delta I/I_0| = 4|\Delta T/T_0| = 4|\delta v/c|$. Now we average the intensity over optical thickness, as in the case of scalar perturbations. We get the intensity as seen by the electron.

$$\begin{aligned}
I(\theta,\phi) = I_0 &+ \Delta I \cos\alpha_0 \frac{k\Delta\chi\cos\theta}{1 + k^2\Delta\chi^2\cos^2\theta}\sin\theta\cos\phi \\
&+ \Delta I \sin\alpha_0 \frac{1}{1 + k^2\Delta\chi^2\cos^2\theta}\sin\theta\cos\phi
\end{aligned}$$

As before we estimate the electron ability to emit radiation polarized along different axes. The intensity of emitted radiation is proportional to the square of electric field in the EM wave. We use amplitudes in calculations, but only the quantities of E^2 dimension have interpretation. We introduce $E_0(\theta,\phi)$, such that $I(\theta,\phi) \propto E_0^2(\theta,\phi)$. We shall omit arguments of E_0 below for compactness.

Following similar procedure in the case of scalar perturbation we show the electron "ability" to emit EM waves of given polarization, when irradiated by $I(\theta.\phi)$. For the incident radiation with polarization along ϕ (parallels) we have:

$$E_x \sim -E_0\sin\phi \qquad E_y = +E_0\cos\phi \qquad E_z = 0$$

and similarly for the incident radiation polarized along θ (meridians):

$$E_x \sim E_0\cos\theta\cos\phi \qquad E_y \sim E_0\cos\theta\sin\phi \qquad E_z \sim E_0\sin\theta$$

The perturbation of the incident radiation on the sphere is proportional to $\cos\phi$. Averaging over ϕ gives $\langle E_x^2\rangle = \langle E_y^2\rangle = \langle E_z^2\rangle = 0$. Thus $Q \sim E_x^2 - E_z^2 = 0$. Rotating the axes by 45 deg we have:

$$\begin{aligned}
E_a &= \frac{1}{\sqrt{2}}(E_x + E_z) \qquad E_b = \frac{1}{\sqrt{2}}(-E_x + E_z) \\
V &\sim \left\langle E_a^2 - E_b^2\right\rangle = \langle 2E_xE_z\rangle \sim \langle(-\sin\phi + \cos\theta\cos\phi)\sin\theta\cdot I(\theta,\phi)\rangle \\
&\sim \int_0^{2\pi} d\phi \int_0^{\pi} \sin\theta d\theta \cos\theta\cos\phi\sin\theta\cdot\frac{k\Delta\chi\cos\theta\sin\theta\cos\phi}{1 + k^2\Delta\chi^2\cos^2\theta} \\
&\sim k\Delta\chi\int_0^{\pi}\sin\theta d\theta\,\frac{\cos^2\theta(1-\cos^2\theta)}{1 + k^2\Delta\chi^2\cos^2\theta}
\end{aligned}$$

where we preserve only nonvanishing terms. V is another Stokes parameter measuring polarization relative to axes rotated by 45 deg.

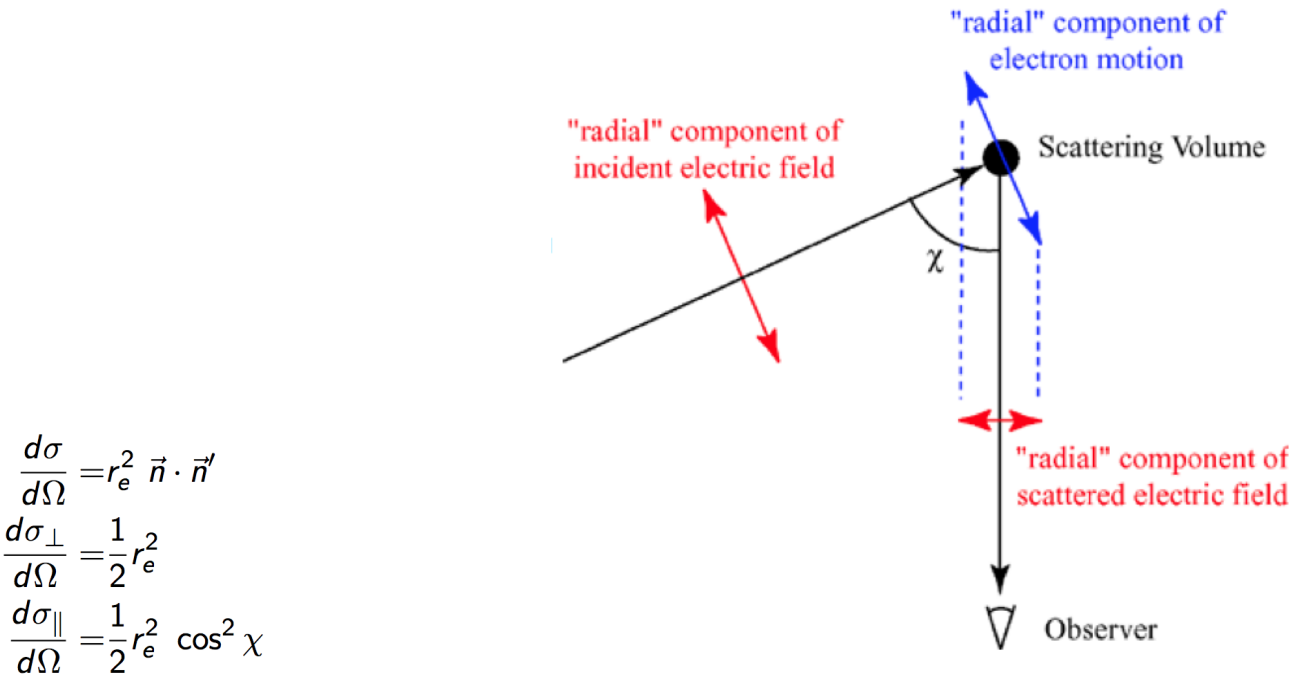

Figure 5.7: Thomson scattering. Left: differential crossection. Right: scattering of an EM wave with electric vector parallel to the scattering plane (Wikipedia).

5.3.3 Polarization: using algebraic approach

The observer's sphere (the sky) is parametrized by (Θ, λ), which are two spherical coordinates, the first measuring angle from the z-axis in Cartesian frame, and the second is a kind of longitude with x-axis along $\lambda = 0$. We define three unit vectors:

$$\vec{m}_1 = (\sin\Theta\cos\lambda, \sin\Theta\sin\lambda, \cos\Theta) \quad \vec{m}_2 = (-\sin\lambda, \cos\lambda, 0) \quad \vec{m}_3 = (-\cos\Theta\cos\lambda, -\cos\Theta\sin\lambda, \sin\Theta)$$

The first is directed toward a position on the sky, the second along the parallel at this position, the third along the meridian at this position. Suppose an electron at this position has scattered a photon toward the observer. We parametrize the electron sphere by the angle $\theta \equiv \pi - \chi$, where χ is the scattering angle as on Fig. 5.7. Another angle ϕ defines the orientation of the scattering plane. The photon moves in the direction $-\vec{n}$ before the scattering and in the direction $-\vec{m}_1$ after, where

$$\vec{n} = \vec{m}_1\cos\theta + \vec{m}_2\sin\theta\cos\phi + \vec{m}_3\sin\theta\sin\phi$$

Thomson scattering For a single scattering one has:

$$I'_\perp \sim \frac{1}{2}r_e^2 \qquad I'_\parallel \sim \frac{1}{2}r_e^2\cos^2\theta \qquad Q' = I'_\parallel - I'_\perp \sim -\frac{1}{2}r_e^2(1-\cos^2\theta)$$

where we use differential crossections for two polarizations of Thomson scattering. Parallel and perpendicular means "relative to the scattering plane". The Stokes parameter Q' (as measured in the frame defined by scattering geometry) is given above, and the Stokes parameter $V' = 0$ because intensities of polarizations at axes rotated by ± 45 deg relative to "perpendicular" are the same. The scaterring plane is at angle ϕ to $\vec{m}_2$. Measuring Stokes parameters relative to $\vec{m}_2$ and

$$
\begin{aligned}
I &\equiv |E_x|^2 + |E_y|^2 \\
I &= |E_a|^2 + |E_b|^2 \\
I &= |E_l|^2 + |E_r|^2 \\
Q &\equiv |E_x|^2 - |E_y|^2 \\
U &\equiv |E_a|^2 - |E_b|^2 \\
V &\equiv |E_l|^2 - |E_r|^2
\end{aligned}
$$

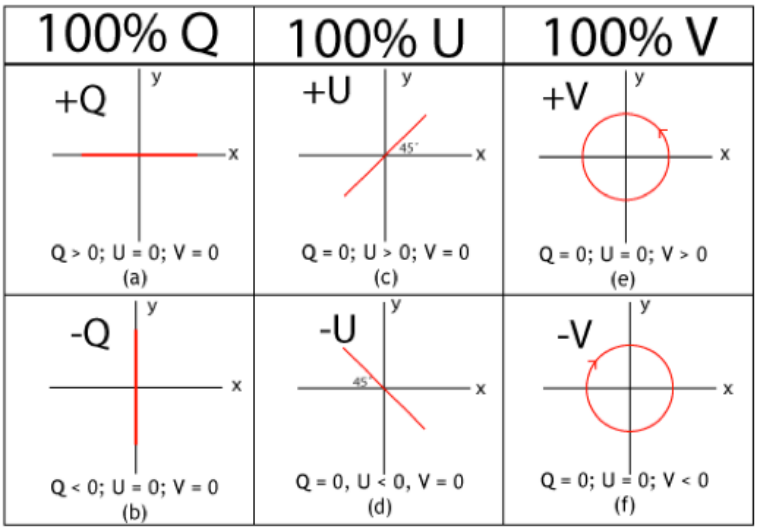

Figure 5.8: Stokes parameters, definitions, illustrations.

$\vec{m}_3$ gives:

$$
\begin{aligned}
Q &= Q' \cos 2\phi - U' \sin 2\phi = Q' \cos 2\phi \\
U &= Q' \sin 2\phi + U' \cos 2\phi = Q' \sin 2\phi
\end{aligned}
$$

The above formulae describe a single scattering on a single electron. There are many electrons in LSS and there are many photons illuminating each of them. The polarization seen at some particular direction on LSS is an effect of averaging of the single electron polarizations taking into account photons arriving from all directions on its electron sphere. The incident and scattered radiation are incoherent so we add intensities, not amplitudes. For an incident radiation with constant intensity on the electron sphere the polarizations of scattered photons would perfectly cancel out and the scattered radiation would be unpolarized. Only if there are some perturbations of the intensity on the electron sphere, one can expect some net effect, NOT necessarilly for any kind of perturbation (see below).

Scalar perturbations Following previous description of scalar perturbations we have:

$$\Delta I(\vec{n}) = \Delta_1 I \cos(\alpha_0 + kz) + \Delta_2 I \vec{n} \cdot \vec{e}_z \sin(\alpha_0 + kz)$$

where $\vec{n} \cdot \vec{e}_z \equiv n_z$ replaces $\cos\theta$ used before. We expect that when averaging with $I(\vec{n})$ only its part even in n_z will not vanish automatically. This is:

$$\Delta I(\vec{n}) \approx \Delta_1 I \cos\alpha (1 - k^2 \Delta\chi^2 n_z^2) + \Delta_2 I \cos\alpha_0 k \Delta\chi n_z^2$$

Evaluating n_z^2:

$$n_z^2 = (\cos\Theta\cos\theta + \sin\Theta\sin\theta\sin\phi)^2 = \cos^2\Theta\cos^2\theta + 2\cos\Theta\sin\Theta\cos\theta\sin\theta\sin\phi + \sin^2\Theta\sin^2\theta\sin^2\phi$$

We see that only the last term $\sim \sin^2\phi$ and only when averaged with $\cos 2\phi$ gives non-vanishing result. Thus the Stokes parameter $U = Q' \sin 2\phi$ is automatically zero. Averaging:

$$\left\langle n_z^2 (1 - \cos^2\theta)\cos 2\phi \right\rangle = \sin^2\Theta \left\langle \sin^2\phi \cos 2\phi \right\rangle \left\langle (1 - \cos^2\theta)\sin^2\theta \right\rangle = -\frac{4}{15}\sin^2\Theta$$

Finally:

$$Q(\vec{n}) = \frac{4}{15}\sin^2\Theta(\Delta_1 k^2\Delta\chi^2\cos(\alpha_0 + k\chi_r\cos\Theta) + \Delta_2 k\Delta\chi\sin(\alpha_0 + k\chi_r\cos\Theta))$$

which is our previous result approximated to second order in $k\Delta\chi$ with the replacement $\mu \equiv \cos\Theta$.
Vector perturbations For a vector perturbation with the velocity along y-axis one has:

$$\Delta I(\theta,\phi) \sim -\vec{n}\cdot\frac{\delta\vec{v}}{c}\sin(\alpha_0 + kz) \approx \Delta I\ \vec{n}\cdot\vec{e}_y\sin(\alpha_0 + k\Delta\chi\vec{n}\cdot\vec{e}_z)$$

where we have omitted the optical depth averaging and neglected the terms quadratic in $k\Delta\chi$. Thus for the long waves we have:

$$\begin{aligned}\Delta I(\theta,\phi) &= \Delta I\ \vec{n}\cdot\vec{e}_x\left((\sin(k\Delta\chi\vec{n}\cdot\vec{e}_z)\cos\alpha_0 + \cos(k\Delta\chi\vec{n}\cdot\vec{e}_z)\sin\alpha_0\right)\\ &\approx \Delta I\cos\alpha_0\ k\Delta\chi\ \vec{n}\cdot\vec{e}_y\ \vec{n}\cdot\vec{e}_z\end{aligned}$$

where we again neglect 2nd order terms in $k\Delta\chi$. The product $n_y n_z$ is rather a complicated expression but only some of the terms will be of interest.

We have to average the above expressions over the electron sphere with $\Delta I(\theta,\phi)$. Neglecting irrelevant terms in $n_y n_z$ and omiting the phase dependence on z we have :

$$\begin{aligned}Q(\Theta,\lambda) &\sim -\cos\Theta\sin\Theta\sin\lambda\left\langle\sin^2\theta\sin^2\phi(1-\cos^2\theta)\cos 2\phi\right\rangle\\ &= \cos\Theta\sin\Theta\sin\lambda\left\langle\frac{1}{4}(1-\cos^2\theta)^2\right\rangle = \frac{2}{15}\cos\Theta\sin\Theta\sin\lambda\\ U(\Theta,\lambda) &\sim \sin\Theta\cos\lambda\left\langle\sin^2\theta\sin\phi\cos\phi(1-\cos^2\theta)\sin 2\phi\right\rangle\\ &= \sin\Theta\cos\lambda\left\langle\frac{1}{4}(1-\cos^2\theta)^2\right\rangle = \frac{2}{15}\sin\Theta\cos\lambda\end{aligned}$$

Finally:

$$Q(\Theta,\lambda) \sim \frac{2}{15}\cos\Theta\sin\Theta\sin\lambda\sin(\alpha_0 + k\chi_r\cos\Theta) \qquad U(\Theta,\lambda) \sim \frac{2}{15}\sin\Theta\cos\lambda\sin(\alpha_0 + k\chi_r\cos\Theta)$$

Tensor perturbations We consider one of two possible GW polarizations where oscillations take place along our x and y axes (shifted in phase by π) and the wave-vector is along z-axis. The motion of test particles under the influence of gravitational wave resembles shear (shrinking in one direction and stretching in perpendicular one) so the velocity may be written as:

$$\delta\vec{v} \sim h_{GW}\omega(x\vec{e}_x - y\vec{e}_y)$$

where h_{GW} is the dimensionless amplitude of the GW ($\delta x = h_{GW}x$) and $\omega = 2\pi f = 2\pi c/\lambda_{GW}$ - its angular frequency. For the velocity amplitude on the electron sphere we get:

$$\lambda_{GW} = \frac{2\pi c/H_0}{k} \ \Rightarrow\ \omega = kH_0 \qquad \frac{\delta v}{c} = \frac{\omega h_{GW}\Delta\chi c/H_0}{c} = h_{GW}k\Delta\chi$$

For an electron it is important what is the velocity of a point on the electron sphere at the direction $\vec{n}$. The comoving radius of the sphere is $\Delta\chi$ so in comoving coordinates one has $\vec{r} = \vec{n}\Delta\chi$, $x = \vec{r}\cdot\vec{e}_x = n_x\Delta\chi$, and $y = \vec{r}\cdot\vec{e}_y = n_y\Delta\chi$. and for the perturbation of the radiation intensity on the sphere one has:

$$\Delta I(\theta,\phi) \sim -\vec{n}\cdot\frac{\delta\vec{v}}{c} \sim \vec{n}\cdot(n_x\Delta\chi\vec{e}_x - n_y\Delta\chi\vec{e}_y) = (n_x^2 - n_y^2)\Delta\chi$$

where the dependence on angles in electron sphere (θ, ϕ) as well as on observer's direction of observations (Θ, λ) is implicit since $\vec{n} = \vec{n}(\Theta, \lambda, \theta, \phi)$.

The polarization of radiation from any direction is given by averaging over the electron sphere of the polarization of a single photon, which has two modes ($Q \sim (\cos^2\theta - 1)\cos 2\phi$, $U \sim (\cos^2\theta - 1)\sin 2\phi$). Of many terms of $n_x^2 - n_y^2$ expression we choose only these proportional to $\cos^2\phi$ or $\sin^2\phi$ (for $\cos 2\phi$ averaging) or to $\sin\phi\cos\phi$ (for $\sin 2\phi$ averaging). Terms of interest:

$$\begin{aligned} a_1 &= (m_{2x}^2 - m_{2y}^2)\sin^2\theta\cos^2\phi \\ a_2 &= (m_{3x}^2 - m_{3y}^2)\sin^2\theta\sin^2\phi \\ b &= 2(m_{2x}m_{3x} - m_{2y}m_{3y})\sin^2\theta\sin\phi\cos\phi \end{aligned}$$

Averaging gives:

$$\begin{aligned} Q &= \int_0^\pi \sin\theta d\theta \int_0^{2\pi} (a_1 + a_2)(\cos^2\theta - 1)\cos 2\phi \sim \frac{4}{15}(1 + \cos^2\Theta)\cos 2\lambda \\ U &= \int_0^\pi \sin\theta d\theta \int_0^{2\pi} b(\cos^2\theta - 1)\sin 2\phi \sim \frac{4}{15}(2\cos\Theta)\sin 2\lambda \end{aligned}$$

Now we include the phase modulation of the result, its dependence on the GW stress (h_{GW}) and on the electron sphere radius ($\Delta\chi$) and GW frequency

$$\begin{aligned} Q &\sim h_{GW}k\Delta\chi * (1 + \cos^2\Theta)\cos 2\lambda * \sin(\alpha_0 + k\chi_r\cos\Theta) \\ U &\sim h_{GW}k\Delta\chi * 2\cos\Theta\sin 2\lambda * \sin(\alpha_0 + k\chi_r\cos\Theta) \end{aligned}$$

The above result is up to some factor (at least 4/15). The definition of the electron sphere is applicable, since velocity $\sim$ distance $\sim$ optical depth. But (as in general) only for the long waves ($k\Delta\chi \ll 1$) the calculations are selfconsistent. Otherwise the phase shift of the GW within the electron sphere would spoil the results.

Chapter 6

21 cm cosmology

The lecture does not require comments

Chapter 7

Inflation

The lecture does not require comments